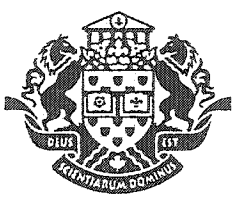

Université d'Ottawa · University of Ottawa

Université d'Ottawa · University of Ottawa

FACULTÉ DES ÉTUDES SUPÉRIEURES ET POSTDOCTORALES

FACULTY OF GRADUATE AND POSTDOCTORAL STUDIES

Shahram ZAMANI ZAVIEH

AUTEUR DE LA THÈSE - AUTHOR OF THESIS

M. A. Sc. (Civil Engineering)

GRADE - DEGREE

Department of Civil Engineering

FACULTÉ, ÉCOLE, DÉPARTEMENT - FACULTY, SCHOOL, DEPARTMENT

TITRE DE LA THÈSE - TITLE OF THE THESIS

Punching Shear Strength of Edge Column Connections of Rectangular Flat Plates

N. J. Gardner

DIRECTEUR DE LA THÈSE - THESIS SUPERVISOR

CO-DIRECTEUR DE LA THÈSE - THESIS CO-SUPERVISOR

EXAMINATEURS DE LA THÈSE - THESIS EXAMINERS

M. S. Cheung

B. Martin-Pérez

H. Tanaka

J.-M. De Koninck, Ph.D.

LE DOYEN DE LA FACULTÉ DES ÉTUDES SUPÉRIEURES ET POSTDOCTORALES

SIGNATURE

DEAN OF THE FACULTY OF GRADUATE AND POSTDOCTORAL STUDIES

Punching Shear Strength of Edge Column Connections of Rectangular Flat Plates

SHAHRAM ZAMANI ZAVIEH

Thesis submitted to the
Faculty of Graduate and Postdoctoral Studies
in partial fulfillment of the requirements
for the degree of Master of Science in Civil Engineering

Department of Civil Engineering
The Ottawa-Carleton Institute for Civil Engineering
University of Ottawa

Your file Votre référence
ISBN: 0-612-90363-X
Our file Notre référence
ISBN: 0-612-90363-X

DEDICATION

A truly heartfelt and special thanks goes to my best friends, confident, and shoulder who has always been the deriving force behind my perseverance and excitement in every thing I do; My parents.

ACKNOWLEDGEMENTS

This research was made possible with the help of many individuals. I want to acknowledge my supervisor Prof. Dr. N.J. Gardner, for his continuous guidance, untiring advice, encouragement and support all the way along this journey. I also want to thank technical staff of the Civil Engineering Department of the University of Ottawa, especially Mr. Majid Muslim, Mr. Robert Moore and Mr. Madan Makasare, for their help during the experimental work.

Several individual also provided help during casting of slab. I would like to thank my friends and the structural graduate students for their help during casting of the slab. I would like to express my deep appreciation to my father, Javad Zamani Zavieh, and my mother, Farideh Khoshroo, for their unlimited love and support on my whole life. I am very grateful to my three brothers for their love.

Abstract

Edge column slab connections of continuous flat plate structures, under combined shear and moment transfer, can be susceptible to failure by punching shear. Most of the available literature has been developed for square flat slab systems. A 2 bay by 2 bay, rectangular flat plate, panel aspect ratio 2:1, was fabricated and loaded to failure under a simulated uniformly distributed load. Because the slab panel aspect ratio was 2:1 the reinforcement/unit width in the longer direction was approximately twice that in the shorter direction. The edge and corner columns were supported so that the reactions and reactive moments could be measured. All edge columns were rectangular in section. The interior column, no moment transfer, punching shear strength was less than inferred from previous research. Based upon the strain gauge results neither the long or short direction flexural reinforcements yielded. The fact that the interior column was rectangular in section was a complication.

Comparison of the measured reactions to those calculated by finite element analysis, FEM, and a modified direct design method, RDDM shows that both methods predict the reactions with acceptable accuracy. Consequently it is concluded that the Direct Design Method limitation on a minimum of three spans in each direction can be removed provided the interior column moment is increased.

Only the ACI 318-99, BS 8110-85 and Gardner 97 prediction equations were considered. The punching shear capacities of the edge column slab connections were conservatively predicted by the ACI 318-99 equations with a mean predicted/experimental value of 0.6. The very simplistic BS 8110-85 expressions predicted a mean predicted/experimental ratio of 0.7. Gardner's prediction using a simple multiplier was very close to reality for edge column connections where there are unbalanced moments for simple structures with a mean predicted/experimental ratio of 0.95.

For corner column connections the main cracks, which cause the failure, are not diagonal as assumed in the Canadian code CSA A23.3-94. The current research shows in most cracks occur around the column-slab connection rather than diagonal.

TABLE OF CONTENTS

LIST OF TABLES

LIST OF FIGURES

NOTATION

A = area of slab critical section located at $d/2$ from column faces

α_s = is 40 for interior columns, 30 for edge columns and 20 for corner columns

b = side square loaded area (BS 8110-85)

b_0 = perimeter of the critical section located d/2 from face of the column or loaded area

β_c = the ratio of long side to short side of the column, concentrated load or reaction area ($\beta_c \leq 2$)

β_m = positive moment resistance per unit width provided by the bottom reinforcement parallel to the slab edge passing through the column

c = side of equivalent square for circular loaded area (BS 8110-85)

c = dimension of square column of same cross sectional area as the actual column(Gardner)

c_1 = the length of the column face perpendicular to the bending axis

c_2 = the length of column face parallel to the bending axis

c_{AB} = distance from the centroid of critical shear section to the inner side of critical section

c_{AC} = distance from the centroid of critical shear section to the side AC

c_{BD} = distance from the centroid of critical shear section to the side BD

c_{CD} = distance from the centroid of critical shear section to the side CD

d = effective slab depth

d' = concrete cover

e = load eccentricity

e_s = eccentricity of the loads acting at the centroid of critical shear section

e_1 = distances from the centroid of the critical section to the face of the critical section.

e_2 = distances from the centroid of the critical section to the face of the critical section.

E_s = Modulus elasticity of steel

E_{cm} = average measured modulus elasticity of concrete

ε_{om} = measured average concrete strain at maximum stress

ε_y = yield strain of steel

f'_c = specified compressive strength of concrete cylinders

f_{ck} = characteristic compressive strength of concrete cylinders

f_{cm} = measured average compressive strength of concrete cylinders

$f_{cm,28}$ = measured average compressive strength of concrete cylinders at 28 days

f_{ct} = calculated compressive strength of concrete cylinders at time t

f_{cu} = compressive strength of concrete cube (= $1.25\, f_{ck}$)

f_y = nominal yield strength of steel

γ_f = a fraction of unbalanced moment transferred by flexure

γ_m = a partial safety factor in BS 8110-85 (= *1.25*)

γ_v = a fraction of unbalanced moment transferred by shear

γ_{vx} = a fraction of unbalanced moment about principal axis X transferred by shear

γ_{vy} = a fraction of unbalanced moment about principal axis Y transferred by shear

h = slab thickness

I_x = moment area of the assumed critical section about principal axis X

I_y = moment area of the assumed critical section about principal axis Y

J = property of assumed critical section analogous to the polar inertia

J_x = polar moment inertia about X axis

J_y = polar moment inertia about Y axis

λ = concrete density factor (*1* for normal weight, *0.85* for semi light weight)

M = unbalanced moment at centroid of critical shear section

M_{col} = moment capacity of connections at column centroid

M_f = flexural moment provide by the top reinforcement perpendicular to slab edge passing through the column

M_{flex} = flexural capacity of connections

M_{neg} = moment capacity near the support

M_o = total factored static moment

M_s = applied moment at the centroid of critical shear section

M_t = design factored moment transferred to the column (BS 8110-85)

M_u = ultimate failure moment

M_{ux} = unbalanced moment about a principal axis X

M_{uy} = unbalanced moment about a principal axis Y

ln =clear span

l_1 =length of span in direction that moments are being determined, measured center-to-center of supports

l_2 =length of span transverse to l_1, measured center-to-center of supports.

ρ = average reinforcement ratio calculated for a width equal to (c + 3d) or (b + 3d) (BS 8110-85)

ρ_x = reinforcement ratio calculated for a width equal to (c + 3d) or (b + 3d) (BS 8110-85)

ρ_y = reinforcement ratio calculated for a width equal to (c + 3d) or (b + 3d) (BS 8110-85)

ϕ = a safety factor of ACI 318-99 (= *0.85* for shear)

ϕ_c = concrete partial safety factor of CSA A23.3-94 (= *0.6*)

Φ = diameter of steel

u = length of the critical section taken at *1.5d* from the column faces (BS 8110-85)

u_o = perimeter of square column section or the same cross sectional area

v = shear stress resistance

v_A = shear stress at critical shear section at point *A*

v_B = shear stress at critical shear section at point *B*

v_c = shear stress provided by concrete

v_D = shear stress at critical shear section at point *D*

v_{max} = maximum shear stress allowed by the codes (ACI 318-99 or CSA A 23.3-94)

v_n = nominal shear stress

v_u = shear stress at failure

V = column axial load

V_c = shear stress at critical shear section

V_{col} = shear capacity of connection measured at column centroid

V_{eff} = design effective shear force

V_t = design shear force (BS 8110-85)

w = equivalent load on the strip per unit length

x = length of the side of perimeter parallel to the axis of bending (BS 8110-85)

X_{eg} = distance from column centroid to the centroid of critical shear section (Sherif's approach)

z = moment arm of concrete section taken as *0.9d*

Chapter 1

Introduction

1.1 General

Flat slabs have significant advantages over traditional beam and column structures. Construction using flat slabs without beams is faster and cheaper than other structural systems because the formwork is less complex and more easily suited to repetition. For the owner the benefit of flat slab structures is that the occupier does not need to worry about restrictions about partition locations and, as necessary, can change the internal partition layouts to suit new clients. Eliminating beams and girders can reduce the overall building height that reduces cost of architectural cladding and mechanical services. Minimizing the slab thickness will save concrete and the reduced building weight will reduce the size of vertical elements and foundations. However two characteristics of flat slab structures have to be taken into consideration; the possibilities of a punching shear failure and excessive deflections causing serviceability problems. Punching shear occurs without warning and often leads to progressive collapse with large loss of life. Early age flexural cracking and excessive deflections can cause serviceability problems such as partitions cracking, doors not fitting, file cabinets not staying closed etc..

One of the problems of flat slabs is modeling punching shear. Most codes use empirical equations developed from experimental results. Most of the experimental results in current literature are based upon isolated slab–column specimens. The problem of this type of specimen is that the boundary conditions of these specimens are different from real slabs which are continuous.

1.2 Punching shear failures examples

Punching shear is a brittle failure that happens suddenly without any warning. When one slab column connection fails, load will transfer to other columns which collapse in turn and the failed slab falls on the slab below, which in turn is overloaded and the sequence continues until the whole structure collapses. Because of lack of warning before collapse, punching shear failures often cause loss of life.
There are many examples that are reported as punching shear failures.

The almost complete Coco Beach, Florida, Harbour Cay Condominium collapsed during the afternoon of March 27, 1981. Punching shear failure of the fifth floor triggered a progressive failure of the entire structure. The building was a residential, five-story reinforced concrete flat plate structure. Each floor slab collapsed vertically breaking away from the columns and landing on the next lower floor all the way to the ground level. Eleven workers died and twenty three were injured while they were working on the fifth floor slab. Based on the investigations of U.S Federal Agencies and independent engineering firms, low punching shear capacity was the most probable cause of the tragic event. Investigations showed that punching shear calculations were omitted in the design stage of the flat slabs and the slab thickness was less than the minimum slab thickness required by the American Concrete Institute Code for the given spans and column sizes. By using a slab thickness of 203 mm instead of the 280 mm specified, the punching shear capacities of the flat slabs were reduced, and in construction the wrong size chairs were used reducing the effective depth of the slab and the shear resisting capacity was reduced significantly. There was insufficient shoring to support the top three floors and the flying forms on the fifth floor.

Two thirds of the 2000 Commonwealth Avenue, Boston, 16 storey high rise apartment building collapsed during construction on 25th of January 1971. When the workers took break from placing concrete for the mechanical room floor slab, there was a failure in the floor slab. Punching shear was noticed around one of the edge column connections. Casting had started at the west edge and proceeded to the east. After hearing a warning, most of the workers managed to cross over to the west side of the building. The roof slab began to form a belly shape and then collapsed onto the sixteenth floor. Progressive collapse occurred twenty minutes after the roof collapsed. The weight of the roof caused the 16th floor to collapse on to the 15th and so on down to the ground. Four workers lost their lives in this collapse. At the time of collapse, construction was almost complete. Many factors, including improper design, flaws during construction and premature removal of formwork contributed to the collapse. Punching shear occurred because the concrete strength was well below the required 21 MPa, inadequate shoring under the roof slab and construction equipment and two boilers were stored on the roof.

In the afternoon of June 29, 1995, the five storey Sampoong Department Store building collapsed in Seoul, South Korea causing almost 500 deaths, 900 injured and about 216 million US dollars in lost properties. The Sampoong department store was inaugurated on the 7th of July 1990 in Seocho-Ku, in the middle of an apartment development area. The heavy water tank built on the top of the fifth floor was not considered in the design and was the most probable cause of this tragic event. The punching shear capacities of the flat slabs were reduced by using 18 MPa strength concrete instead of the specified 21 MPa and the thickness was 360 mm instead of 410

mm. Failure initiated at the 5th floor and progressed to the ground. Because the building was already in service the fatalities and disasters were very high.

Punching shear can also occur in bridge decks. On October 17th 1989 a Richter magnitude 7.1 earthquake shook some parts of California. The epicenter was located near Loma Prieta in the Santa Cruz Mountains about 16 km northeast of Santa Cruz along a segment of the San Andreas Fault. Approximately 2.5 minutes after the main jolt, an earthquake of 5.2 occurred followed by thousands of aftershocks. As a result of the main shock and the aftershocks, the concrete T-beam type bridge on State Highway 1, crossing Struve Slough 1.6 km south of Watsonville, failed. Punching shear failure occurred on portions of the slab. Support piles punched through the bridge deck as the transverse girders below the deck separated

1.3 Previous research at University of Ottawa

Five 2 bay by 2 bay, large scale reinforced and prestressed concrete flat slabs have been fabricated and tested to investigate punching shear at the University of Ottawa.

A 2 bay by 2 bay square reinforced concrete flat plate, bay dimensions 2944 x 2944 mm, 140 mm thick was tested by Shao (1993). A uniformly distributed load was simulated by 40 point loads spaced at 914 mm in each direction. Forty steel rods, spaced at 914 mm, passed through the holes of the structure lab floor. A steel box section connected the rods in pairs. A hydraulic jack, reacting against the lower surface of the strong floor was mounted at mid-span of each steel box section. All the jacks were connected to a single hydraulic pump.

The slab had four equal panels, four edge columns, four corner columns and one middle column. Because the four edge columns and four corner columns could rotate

freely, most of the applied load transferred to middle column and the middle column connection collapsed at a uniformly distributed load of $W_u = 34.4 KN/m^2$. The slab was unloaded and the interior column was shored. Because the interior connection was shored load was transferred to the edge and corner columns. Then the edge columns started to collapse at the same load $W_u = 34.4 KN/m^2$.

Rezai in 1998 constructed and tested a prestressed concrete flat slab. The slab was a two bays by two bays square slab with 5.69m length and 90 nominal thickness that was supported on six 200 mm square columns and three 200 mm diameter circular columns. The design of the slab was according to ACI 318-89 section 13.7. The slab was prestressed with 20 cables in each direction. All the tendons were uniformly distributed in one direction and banded in the perpendicular direction. Forty point loads were applied to the slab. The system of loading was the same as used by Shao. The 44 MPa compression strength of the concrete was higher than the 30 MPa specified. In this research one of the edge columns failed first. After shoring the edge column the middle column connection failed. The middle and edge column connections failed at 31 kN/m^2.

To investigate experimentally the punching shear behavior of edge column connections in unbonded, post tensioned concrete flat slabs, a two bays by two bays prestressed concrete slab with the same dimensions as Shao's slab was constructed by Sharifi (1998). The slab was post-tensioned with different tendon distributions in the edge column regions.

To measure precompression in the concrete, vibrating wire gauges were cast at mid-depth of the slab. The thickness of the slab was 90 mm. The system of loading was

like Shao's. The rotations of edge and corner columns were restrained by threaded rods reacting against a steel frame.

Most of the edge columns failed at an applied load of 23-26 kN/m^2. The middle column and one of the edge columns failed at an applied load of 29.2 kN/m^2. All the corner columns survived an applied load of 32.1 kN/m^2.

To investigate the interaction of moment and shear force on edge columns, Sudarsana (2001) constructed a two bay by two bay slab similar to Shao's slab. This time the objective was to determine edge connection moment shear interaction by loading each edge column separately under different combinations of moment shear force. During the tests of one connection the other columns were fixed to the structure lab's strong floor. One of the edge columns was subjected to vertical concentrated load only. A second edge column was subjected to moment only. The other two edge columns were subjected to both moment and vertical load. All the corner columns were subjected to moment and vertical load. Because the slab was designed to collapse under distributed load and the loading system was different the behavior of the slab was different from that expected.

1.4 Scope

In this research the behavior of rectangular flat slab under a uniformly distributed load is investigated. The slab was designed so that it would collapse by punching shear. Drop panels; shear reinforcement or shear ladders were not used. The bending reinforcements were over-designed to avoid bending collapse of the flat slab. The reinforcement detailing was according to modified direct design method that is based on ACI 318-99. This thesis is presented in six chapters.

Chapter 1 presents general information on flat slabs and a short history about past disasters of punching shear failures. Short descriptions of previous research at the University of Ottawa about the behavior of flat slabs are also presented. The objective and scope of the thesis are discussed.

Chapter 2 provides a brief description of different analysis methods and approaches that are used to predict punching shear behavior of flat slabs for edge, middle column and corner columns by the American code ACI 318-99, British code BS8110-85 and Gardner's approach.

Chapter 3 describes the experimental work performed by the author. Details of the slab, apparatus, procedures and instrumentation are presented.

Chapter 4 presents the test results, the failure crack pattern, slab deflections, measured column reactions and moments.

Chapter 5 discusses and analyzes the test results related to punching shear failure of the edge and middle column connections of the slab. Code predicted shear resistances of the edge and middle column are compared with the experimental results.

Chapter 6 Conclusion of the thesis and recommendations for future tests are described.

Appendix A CD is attached which contains the experimental deflections and deformations of the reinforcements and threaded rods during the tests. It also includes output files and input files of the finite element analysis.

CHAPTER 2

LITERATURE REVIEW

2.1 Introduction

Predicting the non-elastic behavior of indeterminate structures, such as continuous reinforced flat slab systems is extremely difficult. For continuous flat slab structures the equilibrium shear forces and moments transferred through the slab-column connections need to be determined. These force resultants are then converted into stresses, shear stresses in the case of punching shear, which are compared to the limiting shear strength of the section. Analyzing the experimental behaviour of a continuous slab requires consideration of methods of calculating the connection force resultants and the prediction/behavior equations for the connections.

This research is a continuation of the research by Sudarsana (2001). An extensive literature review up to 2001 can be found in his Ph.D. thesis. Only the code provisions of ACI 318-02, CSA A23.3-94, BS 8110-85/97 and the proposal of Gardner will be reviewed.

2.2 Methods of Analysis

Most of the analysis methods are directed to determine the distribution of bending moments in the structures. The methods available are elastic plate theory, yield line analysis, elastic analysis considering the slab system as a series of plane frames acting longitudinally and transversely through the structure, and the direct design method (a method that satisfies equilibrium).

2.2.1 Elastic plate analysis

The behaviour of an elastic plate of uniform thickness can be described by a fourth order differential equation.

$$\frac{\partial^4 z}{\partial x^4} + 2\frac{\partial^4 z}{\partial x^2 \partial y^2} + \frac{\partial^4 z}{\partial y^4} = -\frac{w}{D} \tag{2.1}$$

where the plate rigidity, D, is :

$$D = \frac{E.t^3}{12(1-\upsilon^2)} \tag{2.2}$$

w = uniform surface load

z = deflection

In elastic plate theory Equation 2.1 is solved to determine a solution for z that satisfies the boundary conditions, and the moments are calculated from:

$$m_x = -D(\frac{\partial^2 z}{\partial x^2} + \frac{\upsilon \partial^2 z}{\partial y^2}) \tag{2.3}$$

$$m_y = -D(\frac{\partial^2 z}{\partial y^2} + \frac{\upsilon \partial^2 z}{\partial x^2}) \tag{2.4}$$

$$m_{xy} = -D(1-\upsilon)\frac{\partial^2 z}{\partial x \partial y} \tag{2.5}$$

In practice the most common tool used to analyze slabs using elastic plate theory is a computer program based on the finite element method.

2.2.2 Yield line analysis

This method is an upper bound method that involves estimating the flexural capacity of the structure by applying trial and error to determine the crack pattern, yield

lines, and the minimum failure load. This method is very complicated for slabs with non uniform distribution of reinforcement. It is allowed in different codes, but it is not popular except for very important projects in special locations like earthquake zones. Appropriate assumptions are needed to ensure serviceability is satisfied.

2.2.3 Elastic analysis (linear analysis)

In practice most structures are analyzed using linear elastic methods. To analyze a flat slab structure by linear elastic methods three approaches can be used.

2.2.3.1 Elastic finite element analysis

This method, which is based on numerical methods was not popular not long ago but during the eighties, because of recent technology and the availability of high speed computers it became more popular among designers and consulting engineers. One of the problems of this method is the accuracy of the answer depends on the size and shape of the mesh.

2.2.3.2 Equivalent Frame method

This method, which is permitted by the American, British and Canadian codes, analysizes the slab and its columns as two-dimensional equivalent frames carrying the total load in each direction. The slab design strip is referred to as a slab-beam element and is supported by equivalent columns, which are fixed at their far ends. The stiffness of the slab-beam members and equivalent columns approximate the behavior of the three dimensional slab system. EFA (Equivalent Frame Analysis) will be used referring to this method. As the total load is used in each direction the reactions at a column calculated from the analysis of two orthogonal design strips are different; the larger value should be taken.

Defined factors are used to distribute moments between critical sections. The ACI code allows 10 percent moment redistribution between negative and positive moment areas. While CSA 23.3-94, clause 13.10.3.3, mentions that negative and positive moments can be modified by 15 percent.

2.2.3.3 Direct Design Method (ACI 318-99)

This method is widely used to determine the reinforcement of rectangular flat slab systems subject to gravity loads that meet a number of restrictive criteria namely; three panels in each direction, successive span lengths do not differ by more than 1/3 of the longer span and the factored live load does not exceed twice the factored dead load. The panel equilibrium moment is determined as:

$$M_0 = \frac{w l_2 l_n^2}{8} \tag{2.6}$$

where:

w applied load per square meter

l_2 width of the panel

l_n clear span (face to face of columns)

Portions of M_0 are considered in different locations of the span according to Table 2.1. The slab is divided into two strips: column and middle strip Figure 2.1. Table 2.1 shows how much of the distributed moments are considered for the column strips and middle strip.

Moments	End Span			Interior Span	
	(1)	(2)	(3)	(4)	(5)
	Exterior Negative	Positive	First Interior Negative	Positive	Interior Negative
Total Moment	$0.26\,M_0$	$0.52\,M_0$	$0.7\,M_0$	$0.35\,M_0$	$0.65\,M_0$
Column Strip	$0.26\,M_0$	$0.31\,M_0$	$0.53\,M_0$	$0.21\,M_0$	$0.49\,M_0$
Middle strip	0	$0.21\,M_0$	$0.17\,M_0$	$0.14\,M_0$	$0.16\,M_0$

Table 2.1: Design moment factors for flat plate

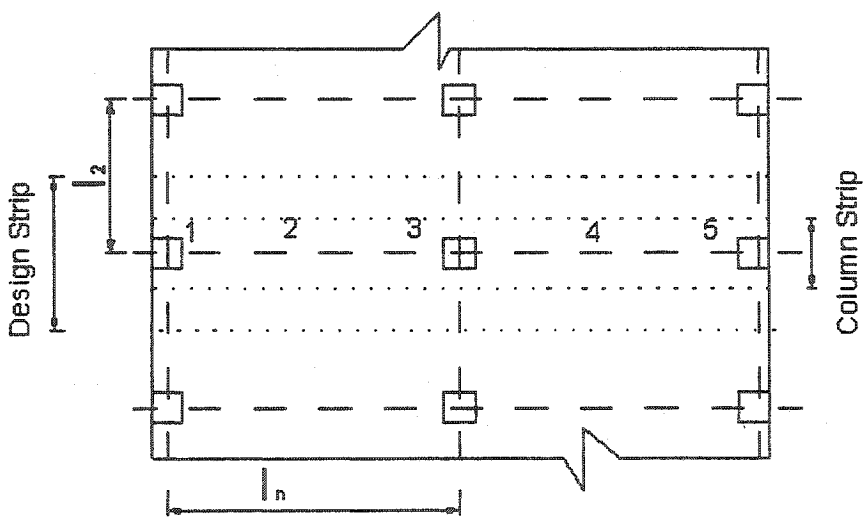

Figure 2.1 Design strips for frame analysis of slab

The moment factors for column strips in CSA 23.3-94 are a little different from ACI 318-99, but the logic is the same.

The distribution of positive and negative moment between the column strips and the middle strips in CSA 23.3-94 are a little different from ACI 318-99 but the method is same.

Sherif (1996) conducted experimental work on four full scale isolated edge column-slab connections containing shear studs and two continuous reinforced concrete slabs. Sherif concluded the direct design method, equivalent frame method and prismatic member analysis of the flexural strain at interior columns give similar results. The experimental results showed better agreement for moments transferred to column connections calculated by the direct design method than the other approaches.

2.2.3.3.1 Modified (Refined) Direct Design Method

Because the Direct Design Method is limited to a minimum of three spans in the flat slab, Gardner (1997) suggested a modified (refined) direct design method, RDDM, for two span flat slab systems using 85 percent M_0 at the interior column and 27.5 percent M_0 at an edge column. For a two bay by two bay system, the total load carried by the interior column is 30 percent of the total four panel load, 12.5 percent of the total four panel applied load is carried by an edge column, and 5 percent of the four panel applied load is carried by a corner column. Sharifi in 1996 determined from experimental measurements that the RDDM approximated his measured moments.

2.3 Punching shear phenomenon

Interior columns usually experience little unbalanced moments. Comparing punching shear in flat slab to punching in beam column may give a better idea about the mechanism of failure. The load path in a beam is two-dimensional but in a flat slab the load path is three-dimensional. When a beam is loaded the upper chord of the beam at the support is in tension and the lower chord in compression, which results in diagonal strains to the support connection. However in a slab, around the concentrated load or column, there are two types of strains, tangential strains and radial strains. Compressive force resultants in the two orthogonal directions result in much greater shear capacity in a slab compared to a beam.

2.4 Punching shear with moment transfer

Interior columns may experience unbalanced moment because of earthquake force or unequal adjacent spans. All edge and corner column connections in slabs have to transfer moments. The generally accepted method of combining shear and moment transfer is the eccentric shear method used by the ACI, CSA and others. In clause 11.12.6, ACI 318-99 mentions that load causes transfer of unbalanced moment between a slab and column, a portion of this moment being transferred by non-uniform shear stress as shown in Fig. 2.2. ACI 318 and CSA A23.3 use a shear perimeter d/2 from the column face.

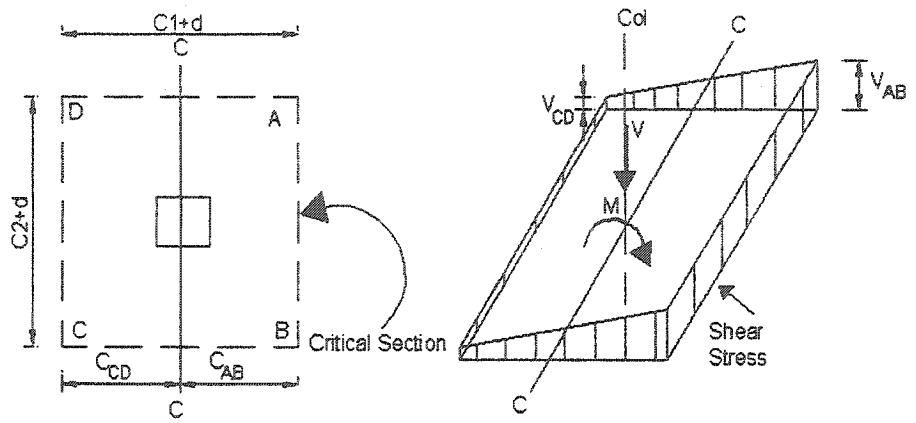

(A) Interior Column

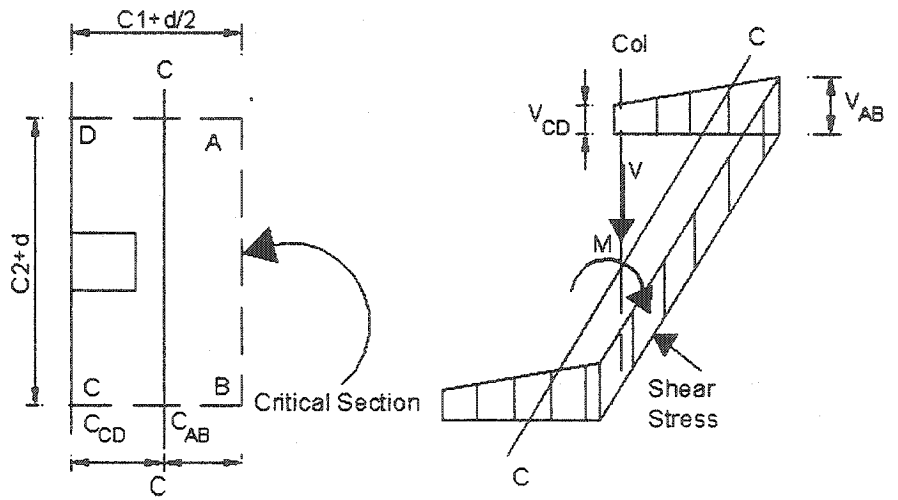

(B) Edge column

Figure 2.2: Assumed distribution of shear stress

The shear force V and unbalanced moments M are determined at the centroid of the critical section. The shear stress is the maximum of the following two equations:

$$v_{AB} = \frac{V}{A} + \frac{\gamma_v M . e_1}{J} \qquad 2.7$$

$$v_{CD} = \frac{V}{A} - \frac{\gamma_v M . e_2}{J} \qquad 2.8$$

e_1, e_2 are the distances from the centroid of the critical section to the face of the critical section.

γ_V = portion of unbalanced moment which is resisted by shear.

J = property of assumed critical section analogous to the polar moment of inertia.

A = area of critical section

These parameters can be calculated using the following formulas:

Interior Column:

$$A = 2d(c_1 + c_2 + 2d)$$

$$e = \frac{c_1 + d}{2}$$

$$J = \frac{(c_1 + d)d^3}{6} + \frac{(c_1 + d)^3 d}{6} + \frac{d(c_2 + d)(c_1 + d)^2}{2}$$

$$\gamma_v = 1 - \frac{1}{1 + \frac{2}{3}\sqrt{\frac{c_1 + d}{c_2 + d}}}$$

Edge Column:

$$A = d(2c_1 + c_2 + 2d)$$

$$e = \frac{(c_1 + \frac{d}{2})^2}{2(c_1 + c_2 + 2d)}$$

Corner Column:

$$A = d(c_1 + c_2 + d)$$

$$e = \frac{(c_1 + \frac{d}{2})^2}{2(c_1 + c_2 + d)}$$

$$\gamma_v = 1 - \frac{1}{1 + \frac{2}{3}\sqrt{\frac{c_1 + \frac{d}{2}}{c_2 + \frac{d}{2}}}}$$

$$J = \frac{(c_{1+} \frac{d}{2})d^3 + (c_1 + \frac{d}{2})^3 d}{12} + (c_2 + \frac{d}{2})de^2 + 2(c_1 + \frac{d}{2})d(\frac{c_1 + \frac{d}{2}}{2} - e)^2$$

Clause 11.12.6.1 of ACI 318-99 states 60 percent of moment should be considered transferred by flexure across the perimeter of the critical section and 40 percent by eccentricity of shear about the centroid of the critical section.

2.4.1 ACI provision for punching shear strength

The empirical equation proposed by ACI 318-99 to calculate punching shear strength includes the compressive strength of concrete, ratio of the long side of column to short side of the column, and the perimeter of the critical section. The ACI 318-99 considers the shear perimeter d/2 from the face of the column or the loaded area. The ACI uses the following equation to calculate the punching shear strength of slab-column connection in two-way reinforced flat slabs:

$$v_c = \left(2 + \frac{4}{\beta_c}\right)\frac{\sqrt{f_{ck}}}{12} \qquad (2.9)$$

$$v_c = \left(\frac{\alpha_s d}{b_o} + 2\right)\frac{\sqrt{f_{ck}}}{12} \tag{2.10}$$

$$v_c = \frac{1}{3}\sqrt{f_{ck}} \tag{2.11}$$

where:

α_s is 40 for interior columns, 30 for edge columns and 20 for corner columns

$$\beta_c = \frac{c_1}{c_2}$$

c_1 long side of the column

c_2 short side of the column

b_0 perimeter of the critical section located d/2 from face of the column or loaded area.

f_{ck}= characteristic compressive strength of concrete.

Reference 11.12.6.2 of ACI 318-99 expresses the maximum shear stress due to the factored shear force and moment shall not exceed $\phi.v_n$ for members without shear reinforcement,

$$\phi.v_n = \phi.V_c / (b_0.d) \tag{2.12}$$

v_c is defined as the least of equations 2.9, 2.10 and 2.11.

2.4.2 CSA provision for punching shear strength

Both CSA and ACI use an ultimate limit state approach to check punching shear strength of flat slabs. Both the load factor and material partial safety factors Φ for CSA23.3-94 are less than ACI 318-99. Therefore in CSA 23.3-94 a factor of 0.4 is used

instead of 0.33 in equation 2.11 in order not to be more conservative than ACI. All other terms and conditions are the same as in the ACI equation.

2.5 BS 8110-85 provision

The British code, BS 8110-85, uses a rectangular control perimeter 1.5 d from the face of the column to calculate for both circular and rectangular columns. The formula below for reinforced concrete flat slabs can derive the effective shear force:

$$\frac{V_{eff}}{b_0 d} < v_{cBS} = 0.79\left(100\rho\frac{f_{cu}}{25}\right)^{1/3}\left(\frac{400}{d}\right)^{1/4} < 5.0 < 0.8\sqrt{f_{cu}} \quad MPa \qquad (2.13)$$

where f_{cu} is the specified concrete cube strength, MPa.

$b_0 = 4\ (c + 3d)$ for circular loaded areas, mm

$b_0 = 4\ (b + 3d)$ for square loaded areas, mm

$\rho = (\rho_x + \rho_y)/2$ calculated for a width equal to $(c + 3d)$ or $(b + 3d)$

The difference in consequences of punching shear due to an applied load and punching shear around a column are recognised by BS 8110-85. To allow for moment transfer at an interior column the applied factored shear force is increased by 15 percent in braced structures with approximately equal spans.

For corner columns and edge columns with bending about an axis parallel to the free edge, the effective shear force is:

$$V_{eff} = 1.25\ V_u \qquad (2.14)$$

For edge column connections, unbalanced moment about an axis perpendicular to the free edge, the effective shear force is as follows:

$$V_{eff} = V_t(1.25 + \frac{1.5M}{Vx}) \quad (2.15)$$

or V_{eff} may be taken as 1.4 V for approximately equal spans.

2.6 Gardner's (1996) proposed equation

Gardner and Shao developed this method in 1996. They extended the logic of Shehata (1989) and Regan (1990). Gardner checked the dependence of the punching shear resistance to concrete strength and tie strength for reinforced concrete slabs using a control perimeter at the periphery of the loaded area and an expression similar to Shehata (1989). Columns with rectangular cross sections or circular were analysed as square columns of the similar cross sectional area.

By using the coefficient of variation of the equation coefficient, as a criteria of closeness to reality, an accurate analysis was done to demonstrate that a good model is composed of concrete strength and steel yield force to the power 0.333 to predict the punching shear resistance of reinforced concrete slab.

$$V_r = 0.79\,\lambda\, u\, d_{eff} \underbrace{\left[1 + \left(\frac{200}{d}\right)^{0.5}\right]}_{(a)} \underbrace{\left(\frac{h}{4c}\right)^{0.5}}_{(b)} [\rho . f_y]^{1/3} [f_{ck}^{1/3}] \quad (2.16)$$

where (a) = size effect term

(b) = strength enhancement factor

c = dimension of square column of same cross sectional area as the actual column (mm).

d_{eff} = effective slab depth to reinforcement, (mm).

f_{ck} = specified concrete cylinder strength, (MPa).

f_y = yield strength of flexural reinforcement, (MPa)

h = slab thickness, (mm).

λ = 1 for normal density concrete, 0.85 for lightweight concrete

u = perimeter of equivalent square column attached to slab, (mm)

ρ = ratio of flexural tensile reinforcement calculated over a width c+6d

To calculate combined shear and moment transfer two alternative methods were suggested by Gardner and Shao for continuous reinforced concrete flat slabs: Using the ACI eccentric shear method with a control perimeter around the loaded area or simply using the BS 8110-85 method.

For slabs subjected to vertical loads the effective shear force can be derived from the nominal shear force for edge and corner column slab connections using the simple multipliers given in equations (2.17), (2.18).

For edge connections subjected to moments perpendicular to the slab edge

$$V_{eff} = 1.5\, V_u \tag{2.17}$$

For corner column slab connections:

$$V_{eff} = 2.0\, V_u \tag{2.18}$$

Chapter 3

Experimental program

3.1 General

The primary purpose of this experimental research was to examine the punching shear behavior of edge slab-column connections of rectangular (non square) flat plates. A two bay by two bay reinforced concrete flat slab with appropriate flexural reinforcement in the short and long directions was constructed. The edge and corner columns were instrumented to measure both column reactions and moments. The overall outside dimensions of the slab were 4572mm in the short and 8228 mm in long directions respectively. The center to center column distances were 2082.8mm in the short direction and 4012.4 mm in the long direction for the corner and edge columns, and 3961.6mm for the edge and middle columns. The thickness of the slab was 140 mm (5.5"). The effective depth of the slab was 105mm. All column dimensions in the short direction were 203.2 mm (8"). The dimensions of the corner columns were 203.2×203.2mm (8" ×8"), the edge columns were 304.8×203.2mm (12" ×8") on the short sides and 254.2×203.2mm (10" ×8") on the long sides. The plan view of the slab is shown in Figure 3.1. A letter identifies each panel and a combination of a letter and number identifies each column. For example 3C means corner column 3, 2E means edge column 2 and 9M means middle column 9. To reduce the effect of scale, the dimensions of the slab were chosen as a compromise between the space available in the structural lab and to be close as possible to full scale. The thickness of the slab was 140mm, span/(35-45), to control deflection. The smaller the slab thickness, the smaller the load required to fail the slab. A uniformly

distributed load, was simulated by a total of 44 equal point loads spaced at 914 mm in two directions.

To represent the distance to the points of contra flexure the length of the column below the slab was chosen to represent the half height of a realistic column. The height from bottom of the slab to the floor was 970 mm to facilitate working and setting the instruments under the slab.

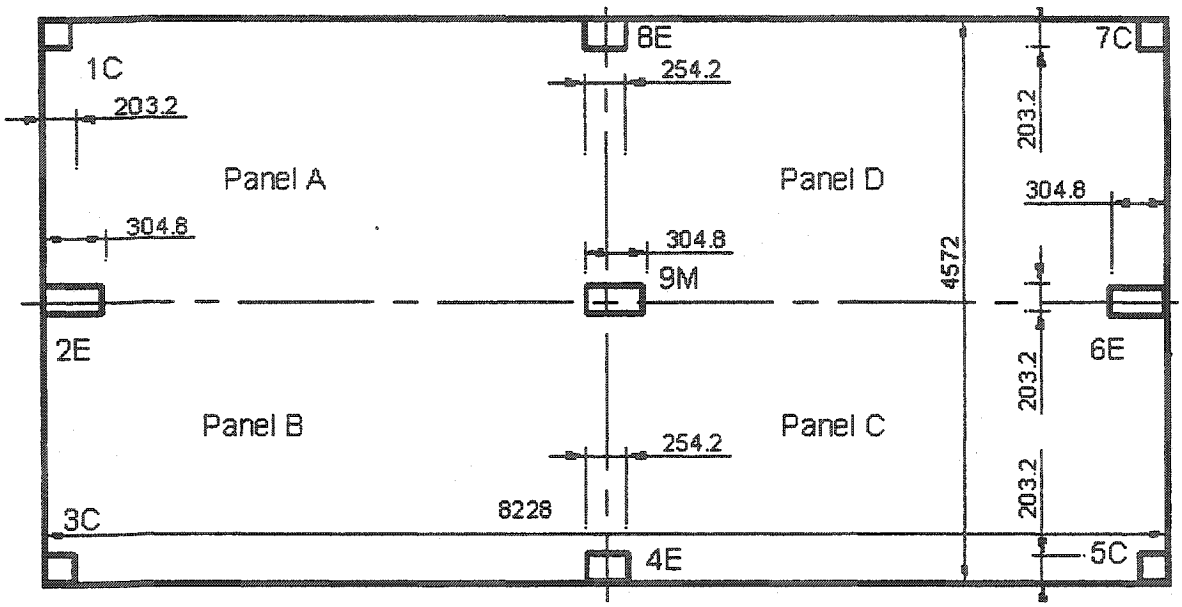

Figure 3.1 Plan view of the slab

3.2 Formwork

The slab was formed on plywood sheets. The plywood was supported on eighteen aluminum I beams 6.4m (21 ft) long, 6 beams in the short direction and 12 beams in the long direction, supported in turn on concrete blocks. The ply wood sheets were covered with polyethylene to avoid bonding between concrete and the formwork and to prevent absorption of water by the wood.

3.3 Casting and curing

A local company delivered six cubic meters of $f_c' = 30MPa$ specified strength ready-mixed concrete with maximum size of 10mm aggregate and slump of 70 mm. The columns were cast with the slab. Casting started from panel C and the columns around it using a bucket moved by crane. Casting took 4 hours. Twenty-two standard 150×300 mm cylinders, were molded to determine the value of f_c'. The slab was moist cured for 10 days under moist burlap. The formwork was removed 10 days after casting.

3.4 Material properties

Three concrete cylinders (150 diameter and 300 mm height) were crushed at 3 days, 10 days, 52 days, 88 days, 114 days and 123 days. The development of measured strength with age is shown in Figure 3.2.

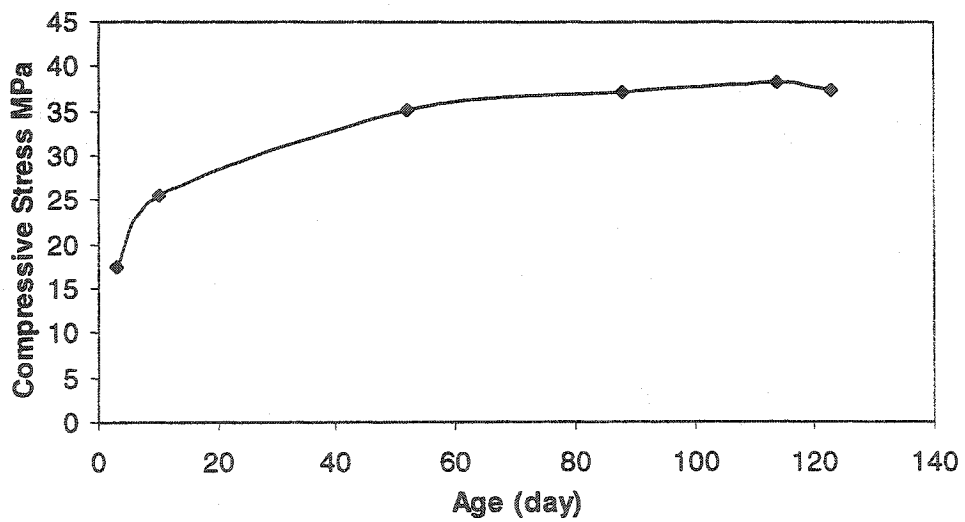

Figure 3.2 Development of concrete cylinder strength with age

The measured stress-strain behavior of the #10 reinforcing steel is shown in Figure 3.3. The failure stress was 630 MPa and yield stress was 475MPa for #10M reinforcement.

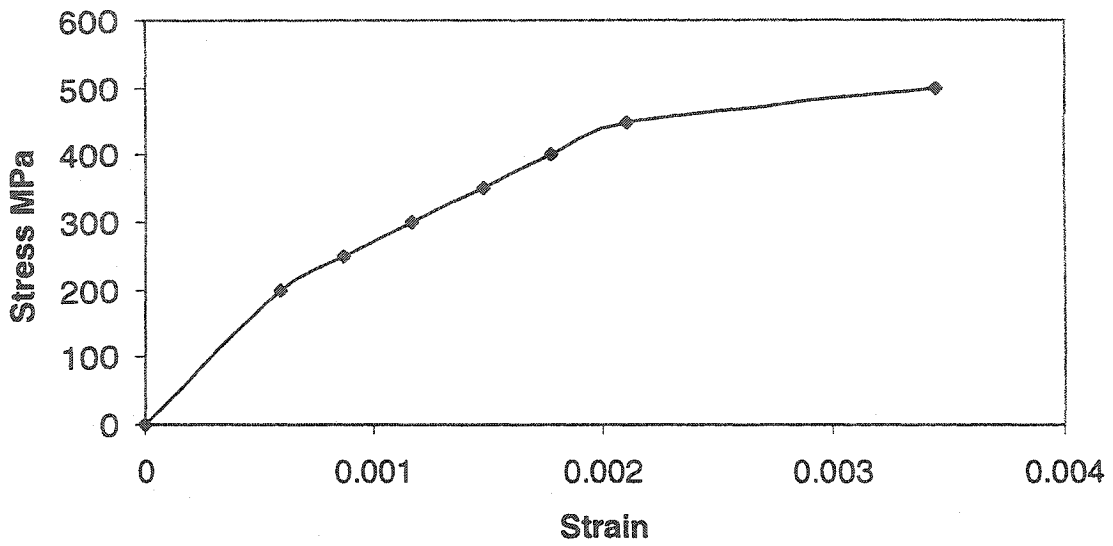

Fig 3.3: Stress-Strain relationship for #10M reinforcement

3.5 Detail of the flexural reinforcements in flat slab

The flexural reinforcement was designed using the RDDM method. Ultimate load for the slab was assumed to be 35 kN/m^2 at a concrete cylinder strength of 30 MPa. Number 10M bars were used as far as possible to maximize slab effective depth (d). In the long direction 15 M bars were used for the negative moment flexural steel to avoid bending moment failure in the flat slab. The cover was 20 mm. Figures 3.4, 3.5 and 3.6 show details of the reinforcement.

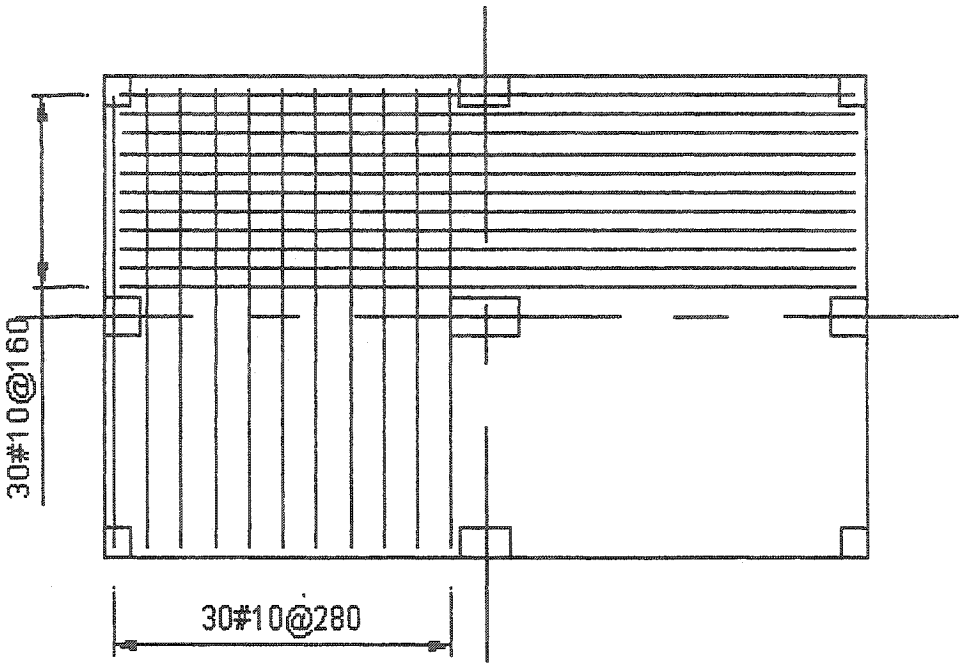

Figure 3.4: Detail of positive moment steel

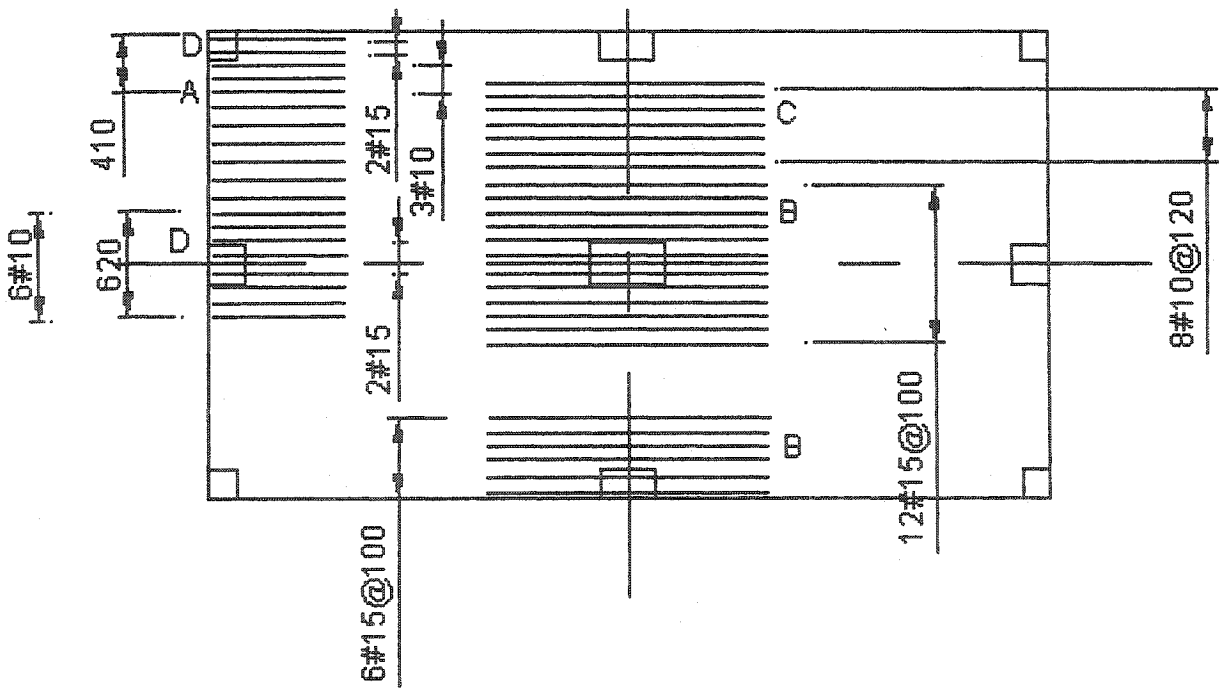

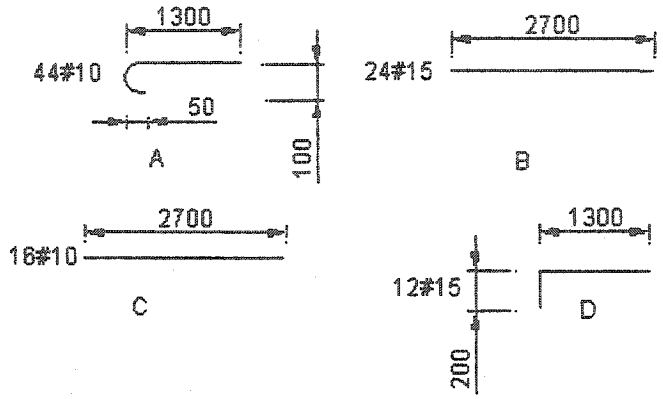

Figure 3.5: Detail of Negative moment reinforcements in long direction

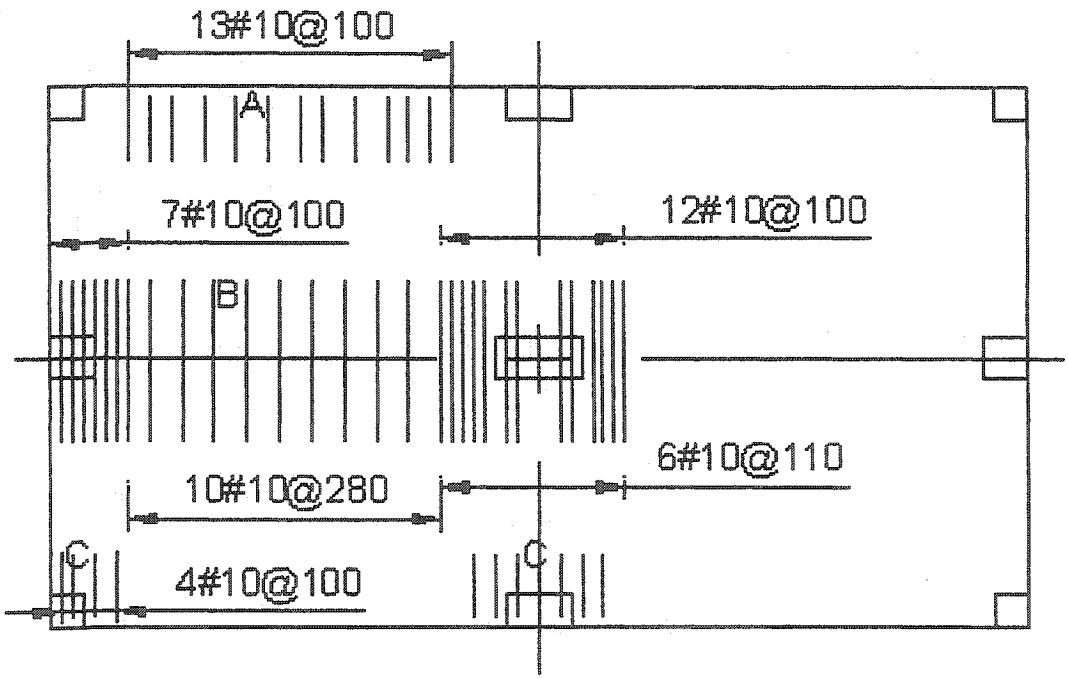

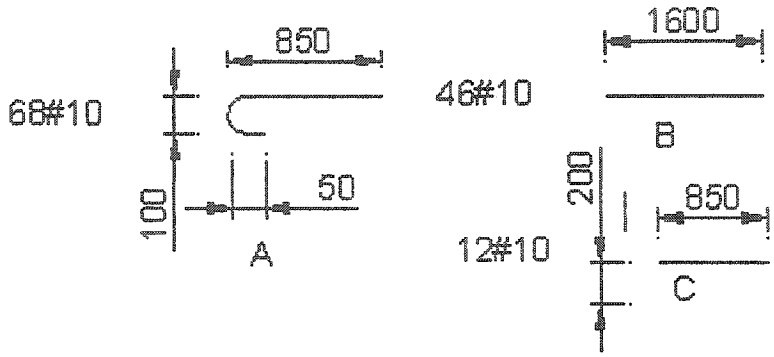

Figure 3.6 Detail of negative moment reinforcement in short direction

3.6 Details of columns

For the corner columns, steel reinforcement cages were built using 4#15 and 2#20 bars, 8#20 were used for edge and middle columns (Fig 3.7). For stirrups #10 bars were used; the specified yield strength of the bars was 400 MPa. To provide 20 mm cover the cages were located in the column formwork using side spacers.

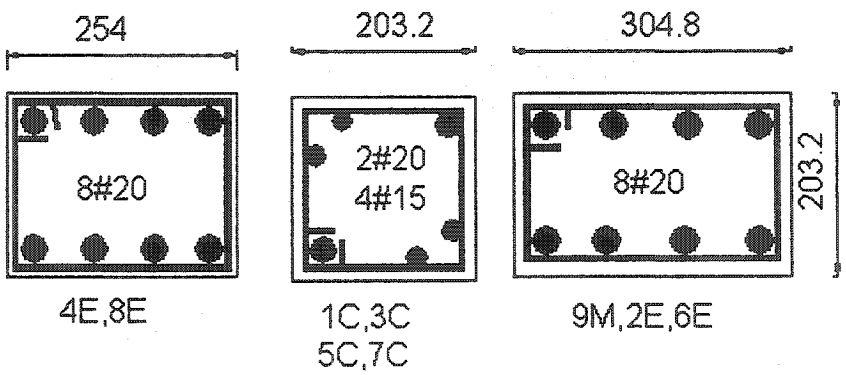

Fig 3.7 Detail of the columns

3.7 Measurement of column reactions

To measure the column vertical reactions and moments, the columns were supported by load measuring devices (load cells). The columns were supported on balls and rollers to replicate the points of contra flexure. Column rotation and horizontal displacement was prevented by two, strain gauged 19 mm threaded rods, which permitted

moments to be measured. The vertical reaction was measured by a load cell.

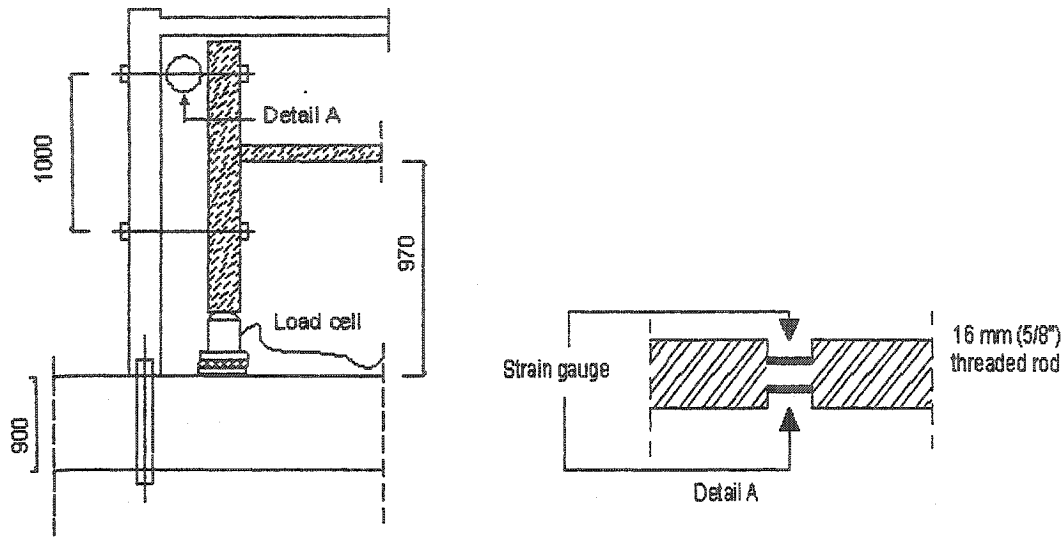

Fig 3.8: Schematic view of the steel frame

Steel columns were provided beside each edge and corner columns to provide reactions for the threaded rods. Threaded rods prevented horizontal movements of the edge and corner concrete columns, which were anchored to 8 HSS 203×203×9 steel columns. Fig 3.8 shows one of these columns that were fixed by a pre-stressing bolt to the laboratory floor. The compression threaded rod load cells, which were the lower threaded rods, of the edge columns buckled during the first test and were replaced by hollow circular tubes (OD=26.62 mm ID=18.8) before the second test because of their larger moments of inertia. The force-strain relationship for the threaded rod is shown in Figure 3.9A. The force strain relationship of the steel tubes is shown in Figure 3.9B

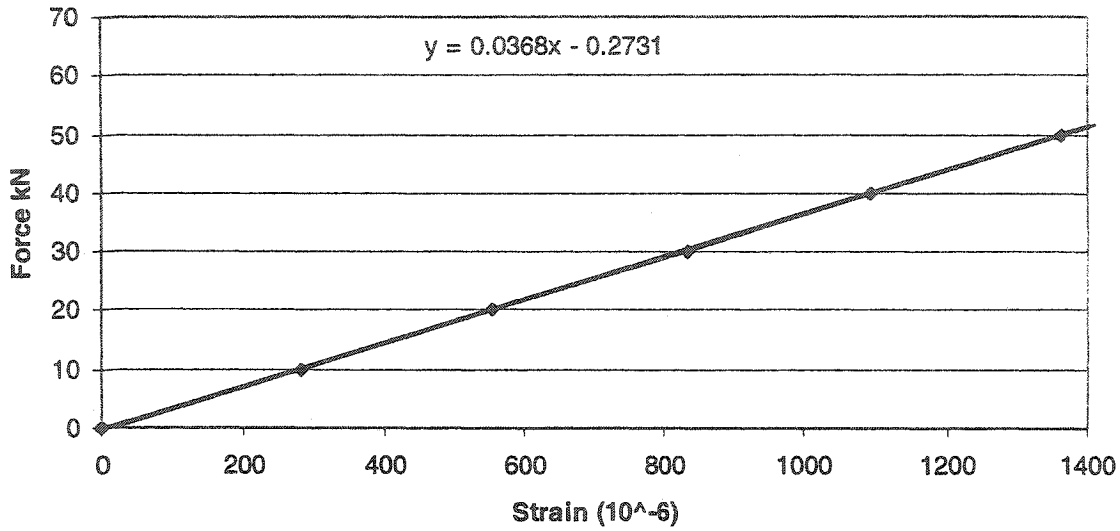

Fig 3.9A: Relationship force and strain for a 19mm threaded rod

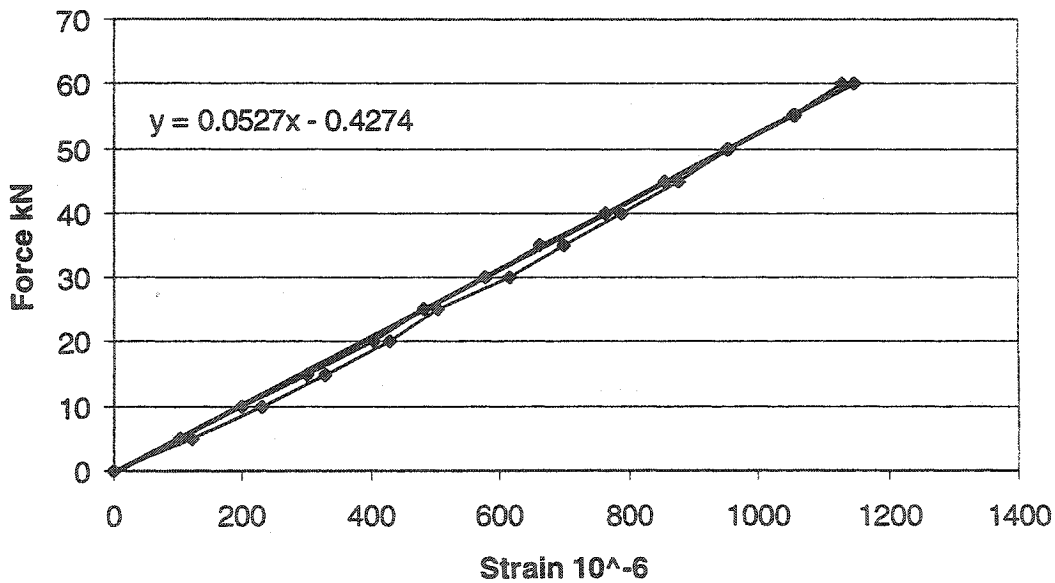

Figure 3.9B: Strain vs force for tested tubes.

3.8 Vertical reactions

Only five load cells were available to measure the axial reactive forces of the columns. A large capacity load cell was used under the middle, interior, column, two 400

kN load cells were used for the edge columns and two 125 kN load cells for the corner columns. Appropriate height stands were made to substitute for the edge and corner column load cells enabling the load cells to be moved to connections which had not failed. The stands are shown in Figures 3.10 and 3.11

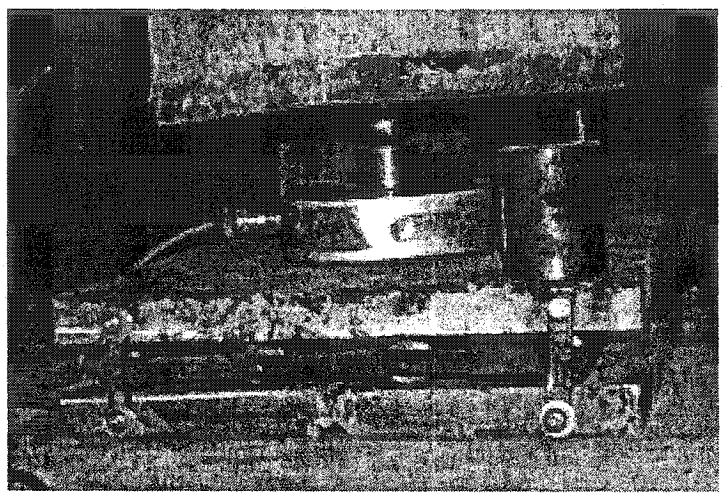

Figure 3.10: Load cell with stand for corner column

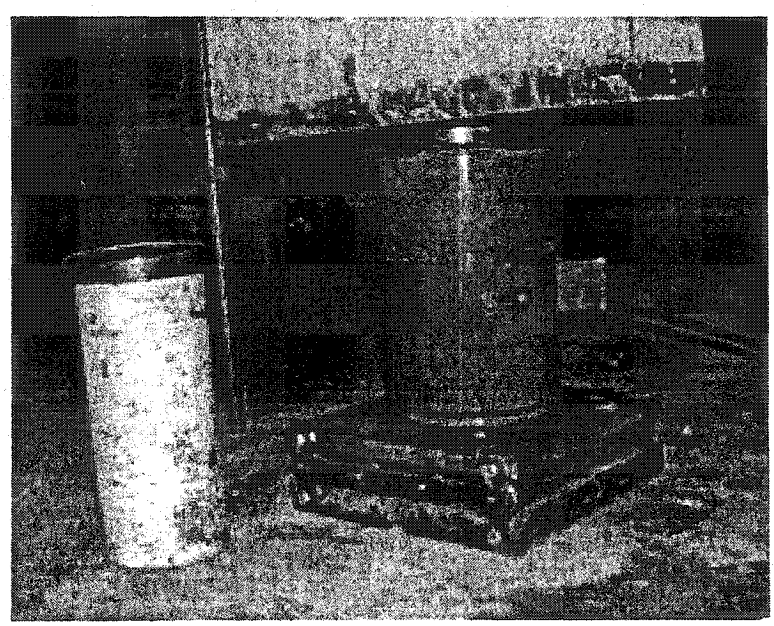

Figure 3.11: Load cell with its stand for edge column

3.9 Details of restraint frame

Figure 3.12 shows a schematic of the restraint frame. Figure 3.13 is a photograph of the slab and restraint frame.

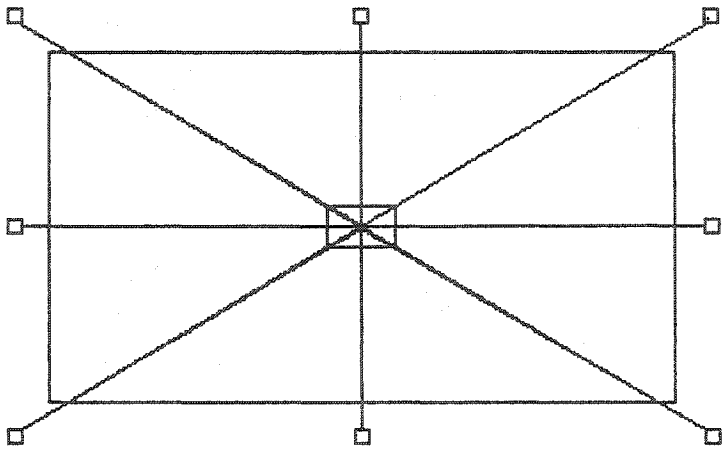

Fig 3.12: Plan View of the steel frame

The steel columns were made of HSS 203×203×9. HSS 76×76×9 steel beams were welded from the top of each 203×203×9 mm columns to the opposite column. Theses restrains are shown in Fig 3.13. They were all welded to a 12.7mm steel plate bolted to the interior column to reduce the effective length of theses restraints.

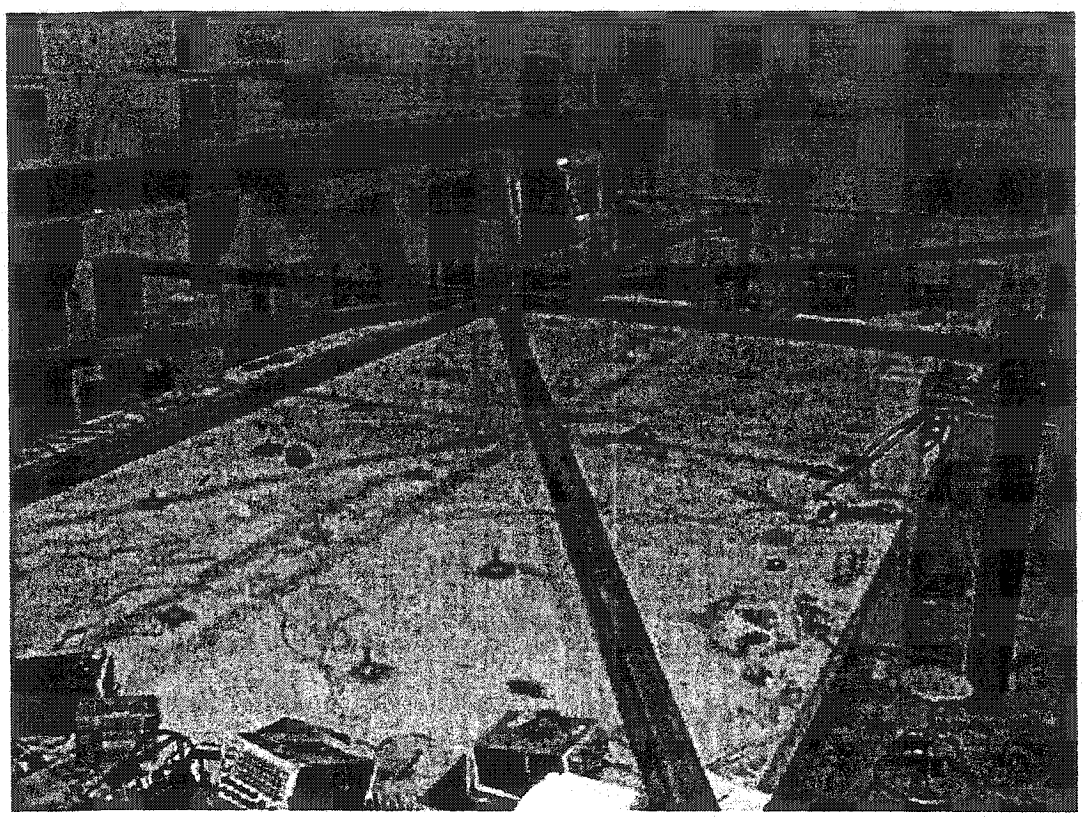

Fig 3.13: Picture of the steel frame

3.10 Load System

Forty-four rods penetrated the slab spaced 914mm (3 ft) from each other. These rods passed through the floor of the lab. A steel box-section HSS 101×101×9mm 1.2 m long beam connected each pair of rods. A hydraulic jack was located at the middle of each beam. Twenty-two hydraulic jacks, an area of 1445 mm^2 and maximum pressure of 69 MPa (10000 psi) were used. Part of the loading system under the slab floor is shown in Figure 3.14. The rods were pulled down by the reaction of the jacks against the floor. Half of the jack force would transfer to the slab by each rod. Wooden washers were used to center the rod at the middle of the hole, one underneath the floor and the other at floor level. All hoses were checked for leakage and all jacks were calibrated using a universal

testing compression machine before installation. Small section steel box beams supported the beams laterally to avoid lateral movement of the beams during loading. Fig 3.14 and 3.15 show the beams carrying the jacks and those providing the lateral support. Pressure gauge of the pump multiplied by the number of jacks used in the test and by their ram areas divided by area of the slab indicates the slab loads, unless otherwise mentioned. A finite element program used by Rezai (1993), indicated that discrepancy between a uniformly distributed load system and this loading system is less than 3%.

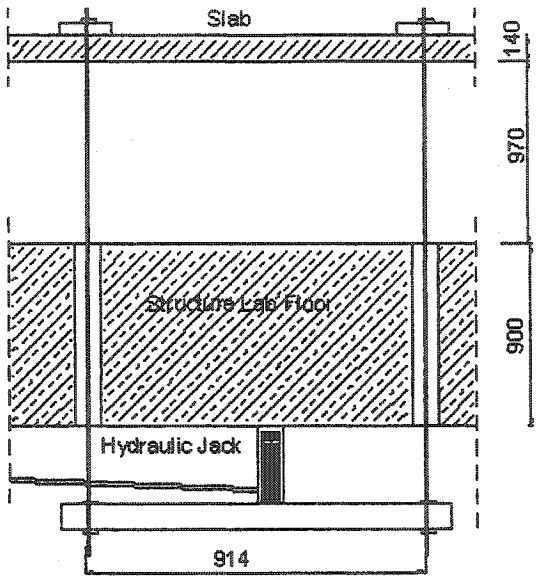

Fig 3.14: Schematic view of loading system

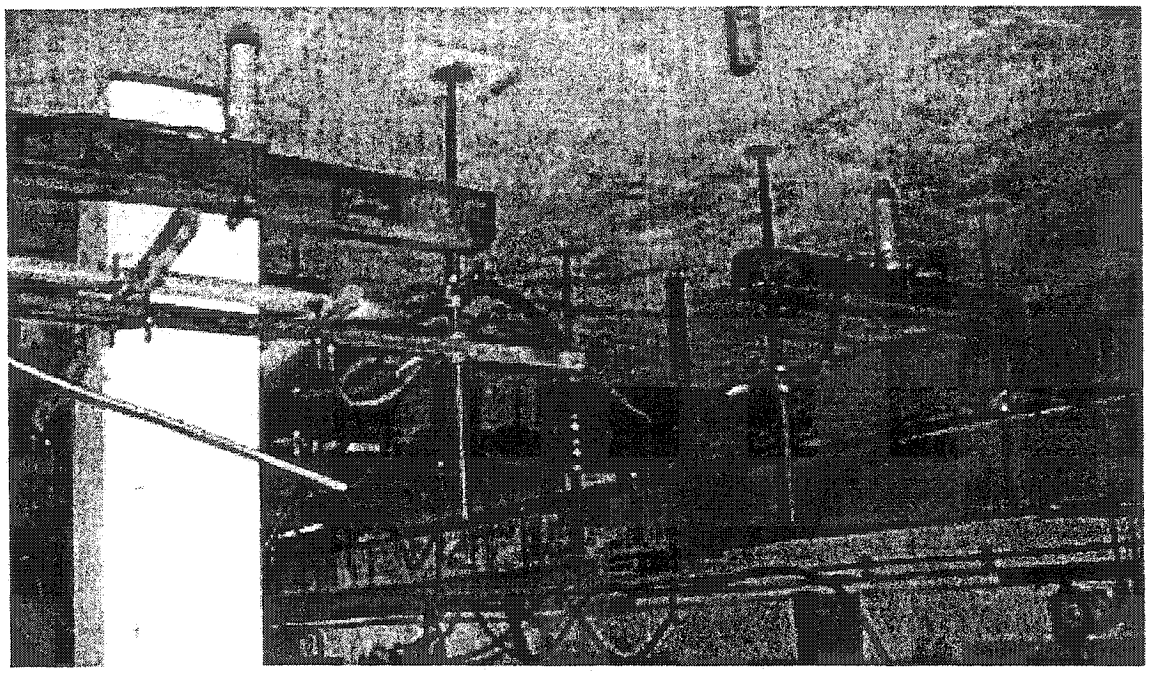

Fig 3.15: View of loading system

3.11 Detail of instrumentation

Five load cells were used under selected columns. Under columns 3C and 7C two small load cells with maximum capacity of 125 kN were used. Under edge columns 2E and 4E, two load cells with maximum capacity of 400 kN were used. To measure the load transferred to interior column 9M a large load cell of 900 kN maximum capacity was used. Two strain gauges were glued on flats machined on opposite sides of each rod to measure the force in the threaded rod as illustrated in Fig.3.8. To measure readings in these rods totally thirty-two 10 mm strain gauges were used. Tubes with larger second moments of area replaced all lower threaded rods for the second test. These strain gauges were wired to strain indicators. A total of 160 strain gauges were used to measure strain in the reinforcement. Two strain gauges were glued to opposite sides of each bar of flexural reinforcement. The strain gauges were located 25 mm from the face of the columns.

All the balance units with number of the strain gauges, which were connected to those channels with their related strains, are copied in the attached C.D. Figure 3.16 through 3.25 show the location of the strain gauges.

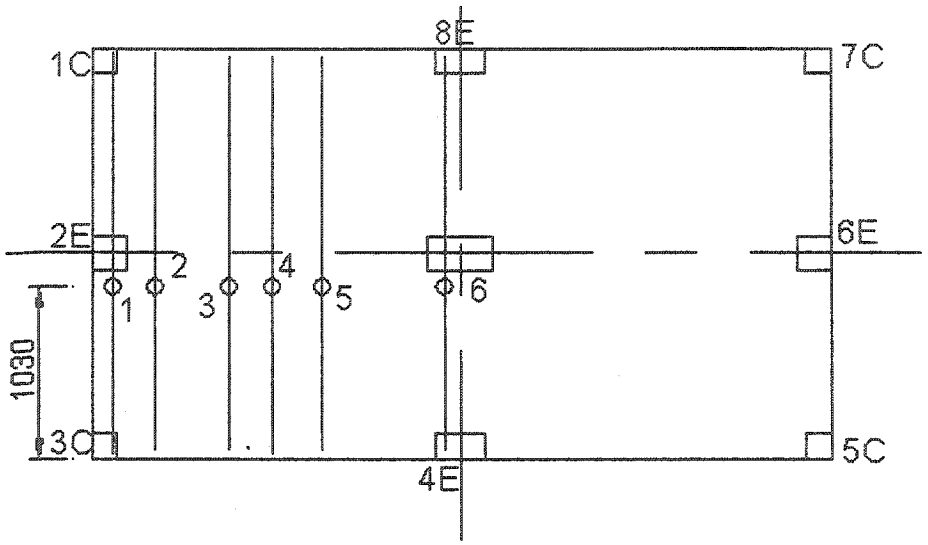

Fig 3.16: Position of strain gauges glued to positive reinforcements (short direction)

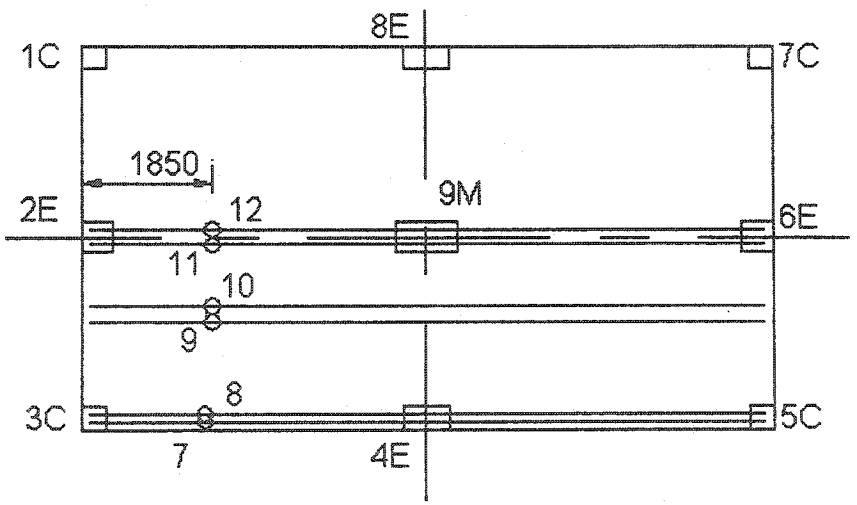

Fig 3.17 Position of strain gauges glued to positive reinforcements (long direction)

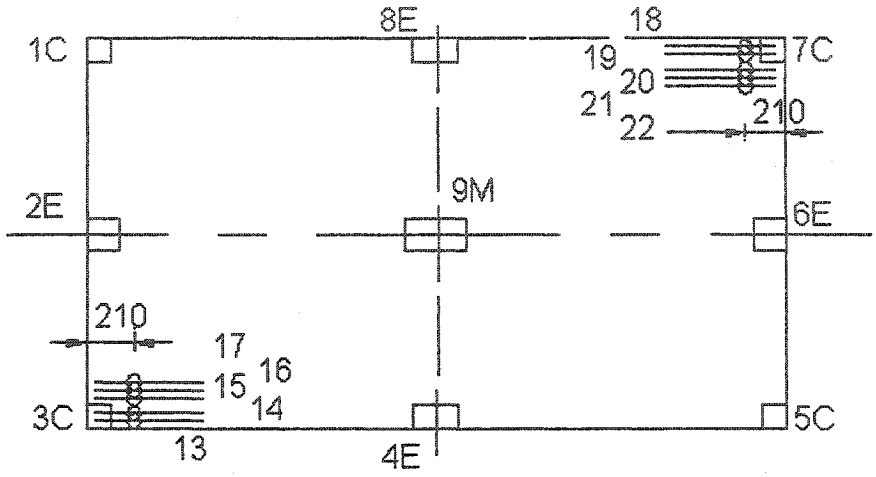

Fig 3.18 Position of strain gauges glued to negative reinforcements

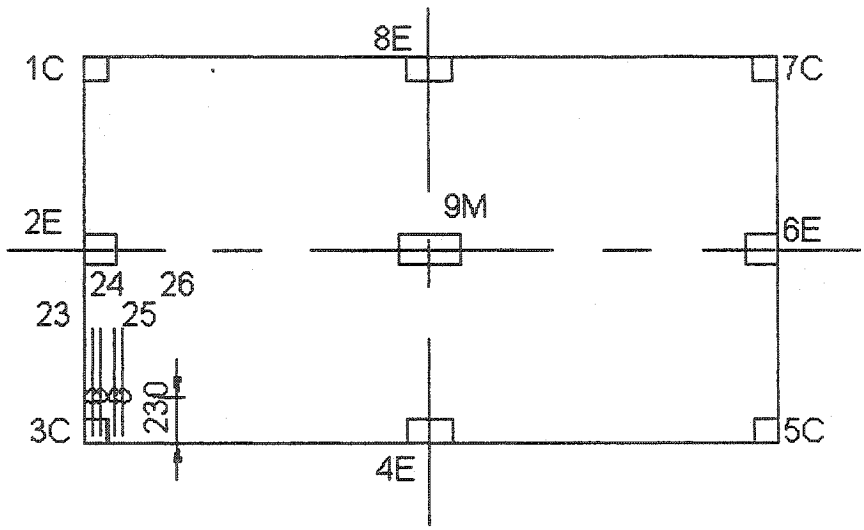

Fig 3.19: Position of strain gauges glued to negative reinforcements

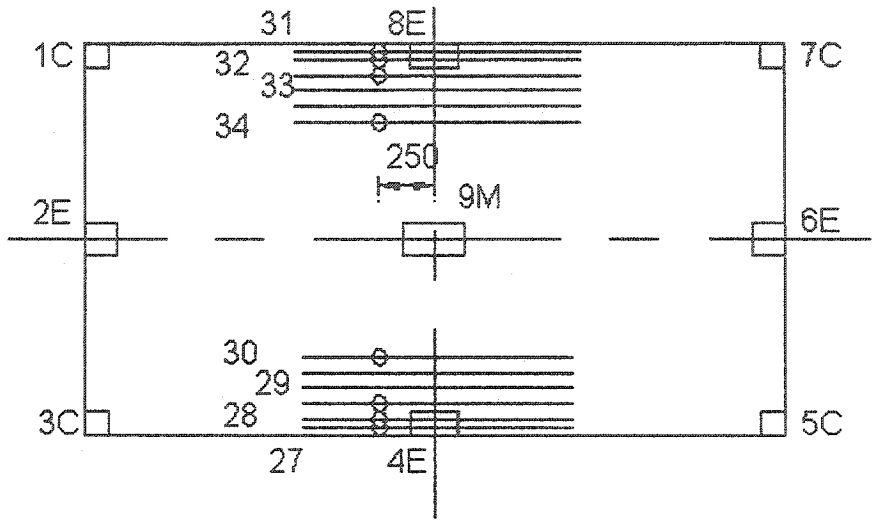

Fig 3.20: Position of strain gauges glued to negative reinforcements

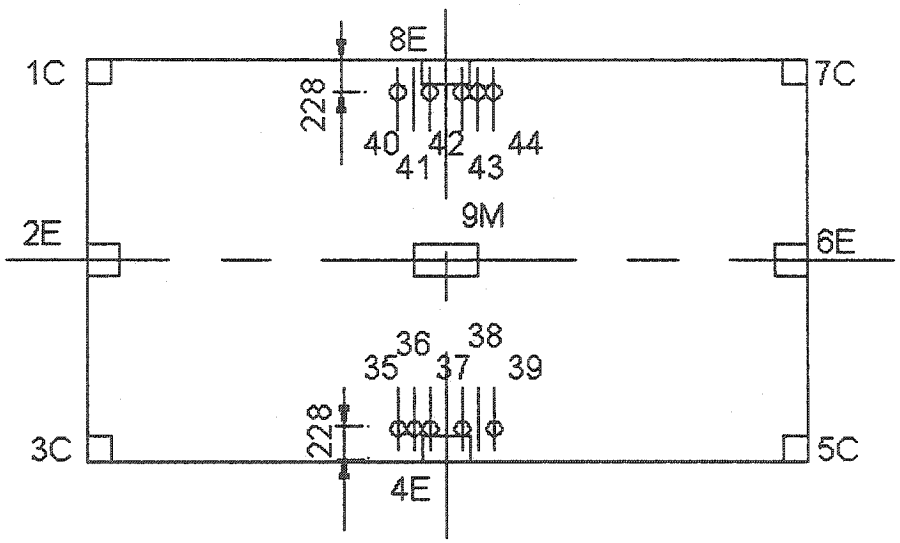

Fig 3.21: Position of strain gauges glued to negative reinforcements

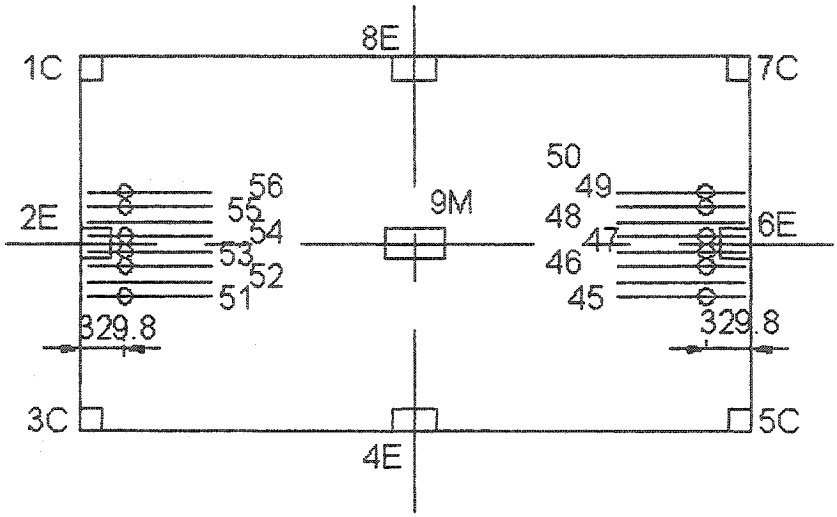

Fig 3.22: Position of strain gauges glued to negative reinforcements

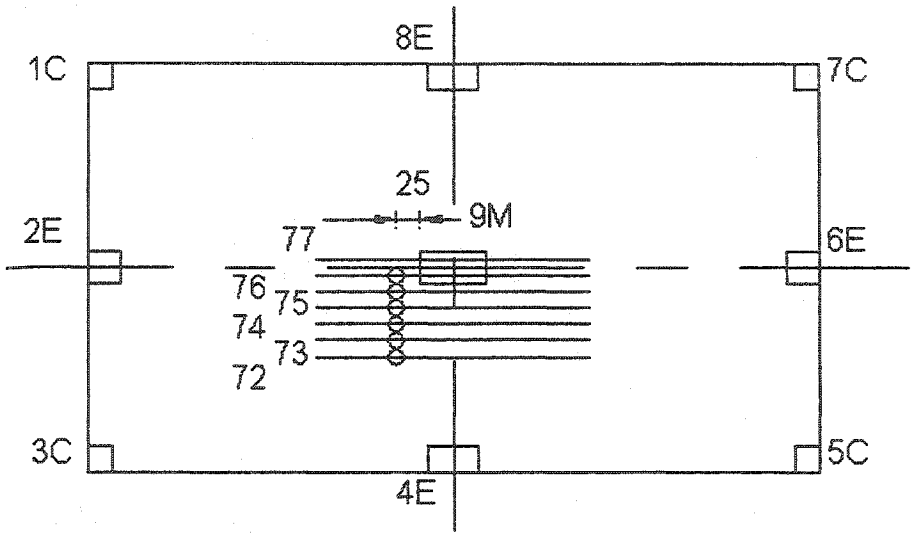

Fig 3.23: Position of strain gauges glued to negative reinforcements

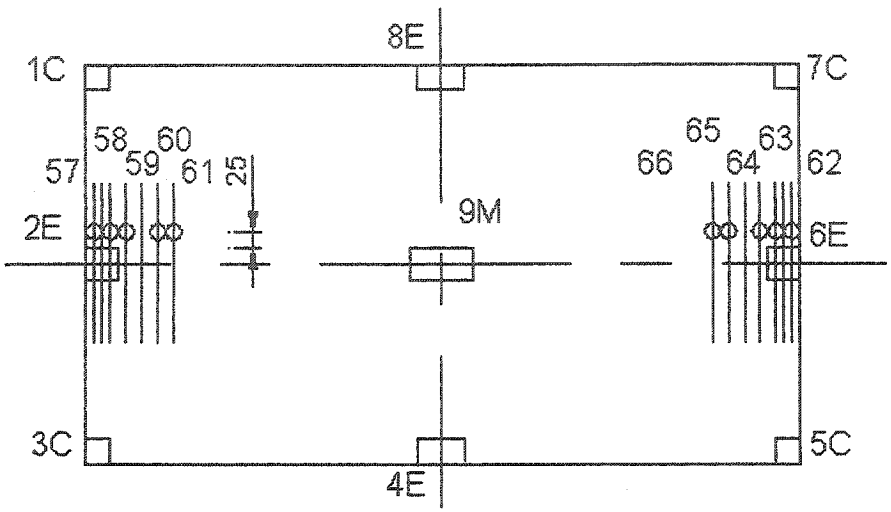

Fig 3.24: Position of strain gauges glued to negative reinforcements

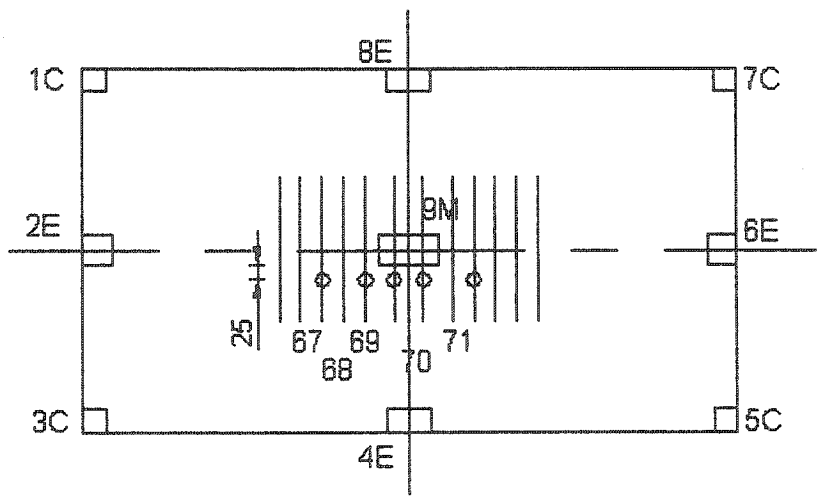

Fig 3.25: Position of strain gauges glued to negative reinforcements

To measure mid panel deflections, four dial gauges were used. The positions of these dial gauges are shown in Fig 3.26. The self-weight of the slab was not included in the readings which were taken during the test. The dial gauges were zeroed before each test. The readings were due to external applied loads.

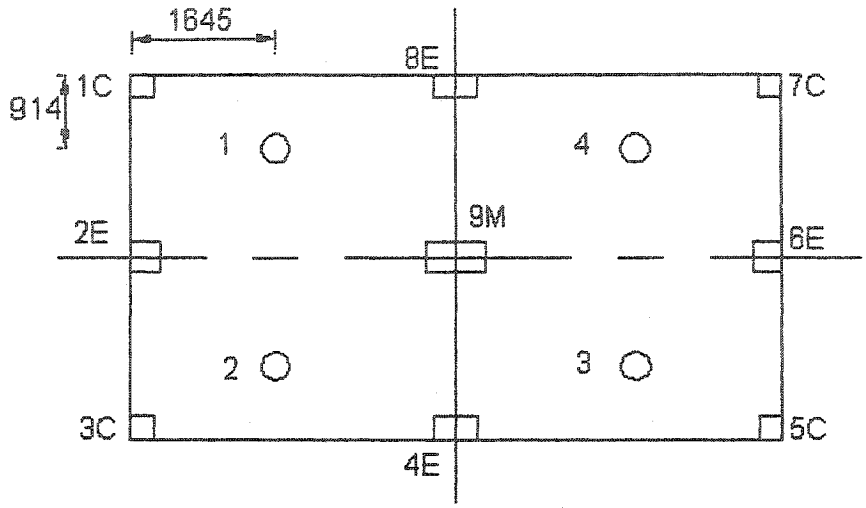

Fig 3.26: Position of dial gauges

Chapter 4

Test Results

4.1 Overview

The first step was to check the hydraulic system for leaks and that the various response devices worked. For convenience, slab loads are referred to as the line pressure in the hydraulic system. A pretest check was done by applying 14 MPa, in steps of 3.5 MPa, to the load system. The behavior of the slab was linear during this range and no cracks were noticed.

The first test to fail a connection had to be abandoned .The pressure was increased to 7 MPa, 14 MPa, 21 MPa, and the response data recorded. Unfortunately at 28 MPa the load could not be maintained and it was determined that a hose was leaking. The slab was unloaded, the hose replaced and the system pressurized with the jacks disconnected. The hydraulic hoses were reconnected to jacks.

After the hoses had been reconnected the load was monotonically increased until a connection failed. The first connection to fail was the interior column connection 9M at 42 MPa. The slab was unloaded, the failed concrete removed and replaced. The connection was shored with screw jacks to increase its shear perimeter and punching capacity. At this time the buckled lower horizontal column threaded bar restraints were replaced with tubes.

The next connection to fail was the long side edge column 8E at 45.5 MPa. The slab was unloaded and the connection and the companion long side edge connection 4E were shored with 90 mm square props. The slab was again loaded until failure occurred at

the short side edge column 2E at 50 MPa. The failed connection 2E was shored and the shores removed from connection 4E.

The slab was loaded but connection 4E failed at a pressure of 40 MPa – less than previously experienced.

Connection 4E was shored and the slab loaded until connection 6E failed at 50 MPa.

All four edge columns were now shored and the shores were removed from connection 9M exposing the repaired 9M connection and the corner connections to load. However the repaired connection failed at 27.6 MPa.

The interior connection 9M was shored and the four edge columns remained shored. The slab was loaded to fail a corner connection. At a system pressure of 58 MPa the test was halted. The loading system was not designed to exert loads greater than those due to 58 MPa. For calculation purposes it is assumed that the failure capacity of the corner connections is greater than 58 MPa.

In this chapter the following topics are discussed:

1. Collapse load for each column connection.
2. Crack pattern for each column connection
3. Strain in flexural reinforcement at failed connection
4. Slab deflections (measured by dial gauges)

Bending cracks occurred before collapse of the slab column connections. The bending cracks started in the short direction, perpendicular to the direction of the larger moment, and increased in width as the test progressed. There was very little cracking in the long direction. The cracks are shown in Figure 4.1.

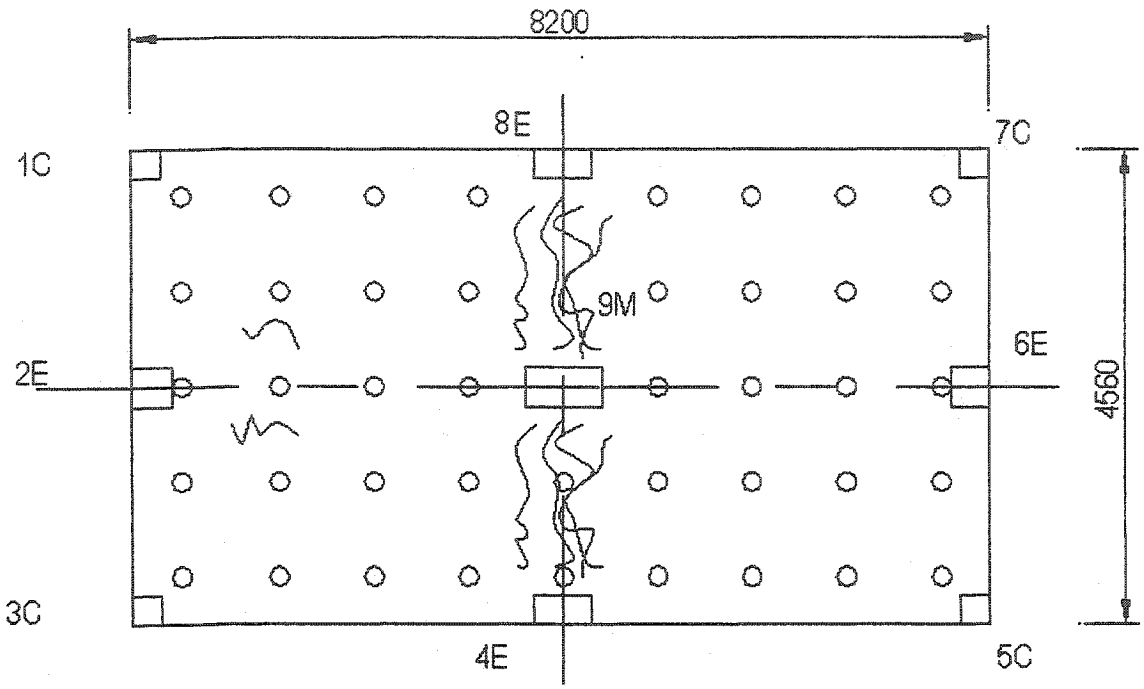

Fig 4.1: Negative bending cracks before punching shear

4.2 Failure of Connection 9M

Unexpectedly the first column connection to collapse was the middle column connection 9M. The test proceeded normally as the jack pressure was increased with cracks developing in the flexural tension regions, reinforcement strains and slab deflections increasing. It was observed that at a jack pressure of 41.4 MPa (6000 psi) the lower horizontal column compression restraints had buckled. This is shown in Figure 4.2. After buckling of the compression threaded rods at column connections 2E and 6E, the middle column connection 9M started to collapse. Without increasing the load the interior column connection failed.

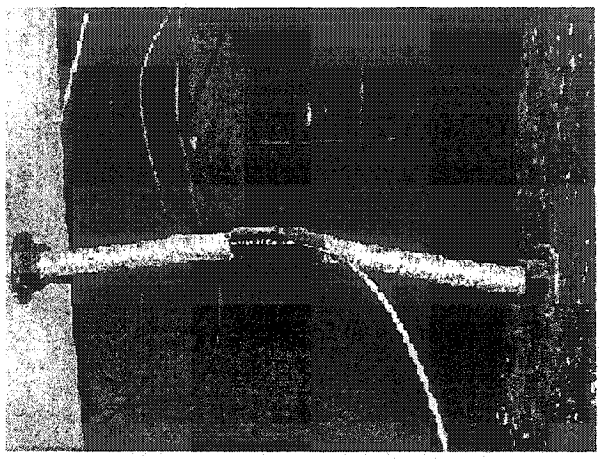

Figure 4.2: Buckling of the compression threaded rods of 2E and 6E columns

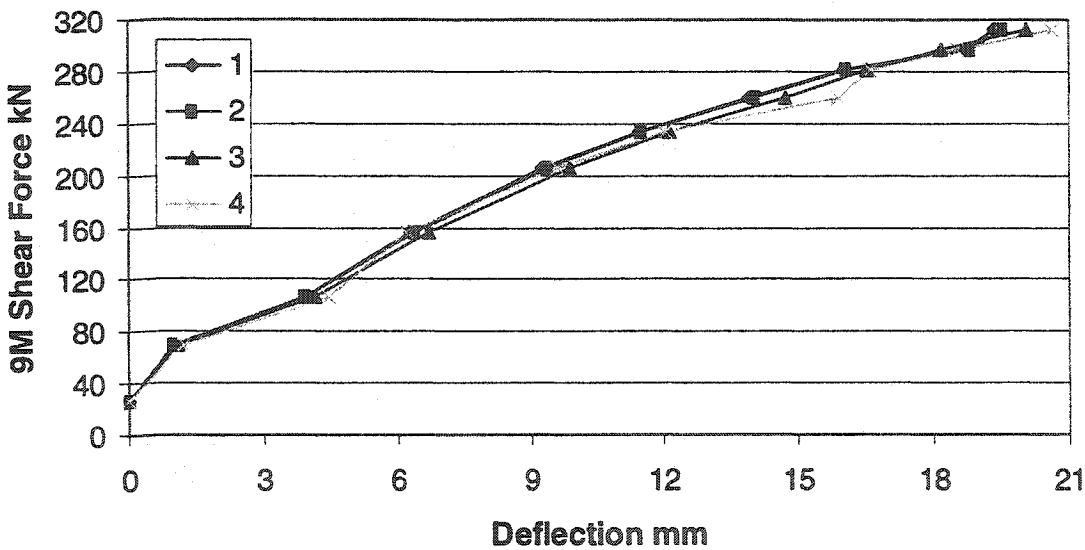

Fig 4.3: Deflection of the slab according to dial gauges.

The measured mid-panel deflections are shown in Figure 4.3. It can be observed the deflections of the four panels of the slab were almost identical. The shear force is the force read from the load cell under column 9M.

Column reactions were measured for columns 3C, 7C, 9M, 2E and 4E. The relationships between jack line pressure and the measured vertical reactions are shown in Figure 4.4. It can be seen from Figure 4.4 the slab behaved symmetrically.

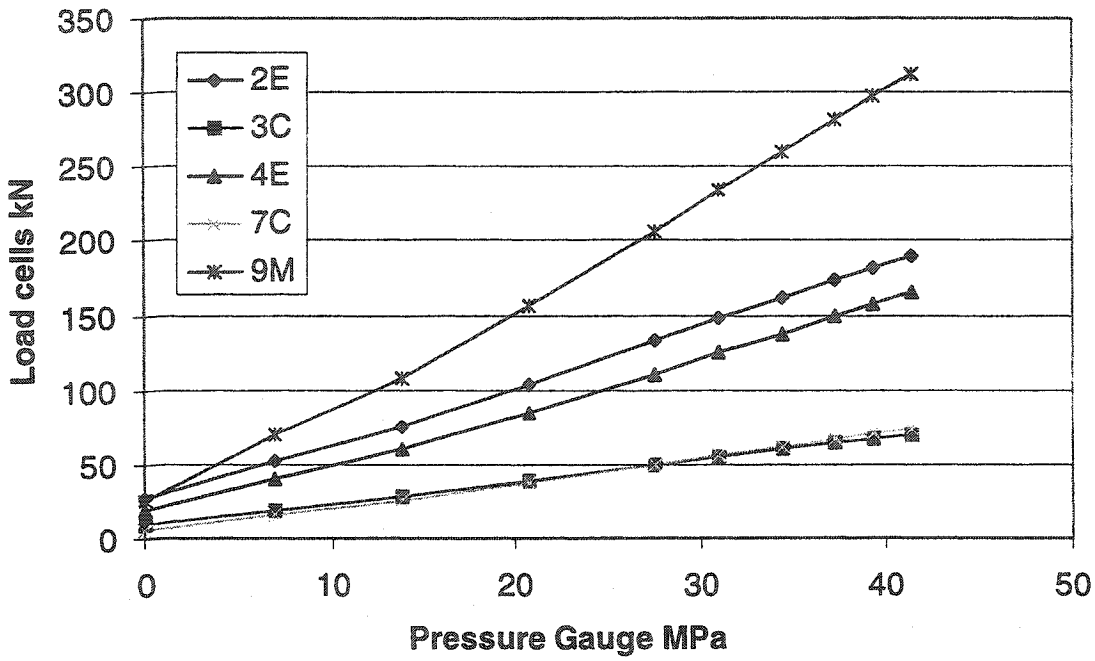

Fig 4.4: Relationship of the pressure in hydraulic pump and measured column loads.

To check that all the systems worked properly the following simple calculation for vertical equilibrium was done:

Total jack force = 22 jacks × 41.36 MPa ×1445 mm ^{2} = 1314 kN

Self weight of slab = 132.6 kN

Total force: 132.6 +1314=1446.6 kN

Total force according to load cells assuming symmetry:

$7C = 73.64kN, 3C = 70.58kN,\ 2E = 189.41kN$, 4E=165.33kN , $9M = 312.76kN$

Total reaction: 1310.6 kN

As the difference is almost 136 kN, almost 10% of total loading. Responses are plotted against the appropriate connection force. The edge and corner columns were

restrained against rotation by strain gauged threaded rods. Figures 4.5, 4.6, 4.7 and 4.8 give the measured force in the threaded rods.

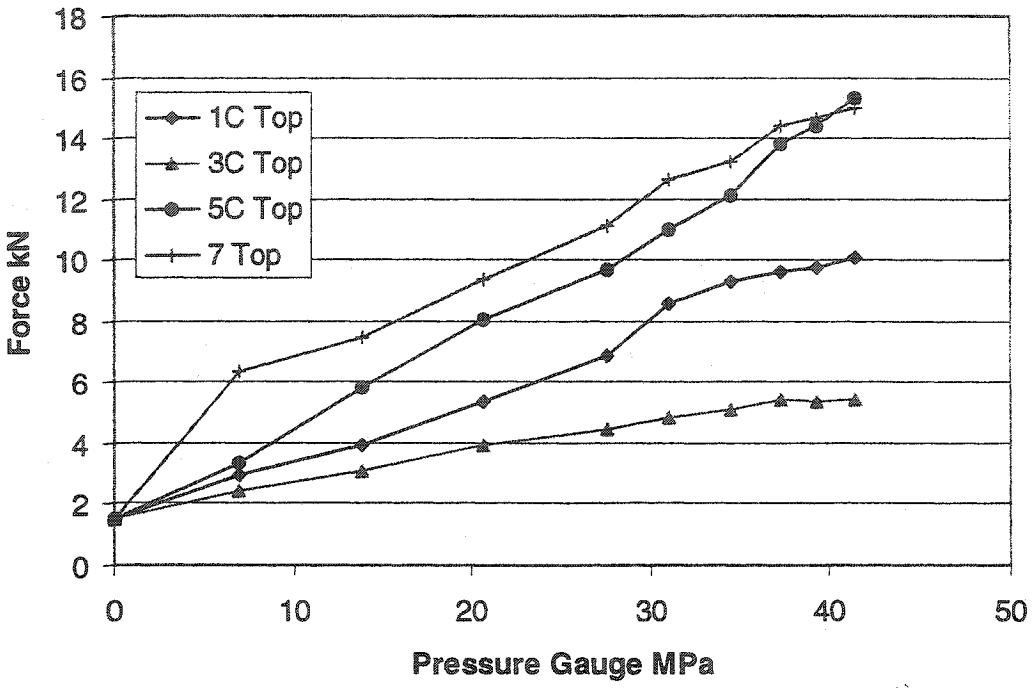

Fig. 4.5: Forces of tension rods versus pressure gauge at corner columns

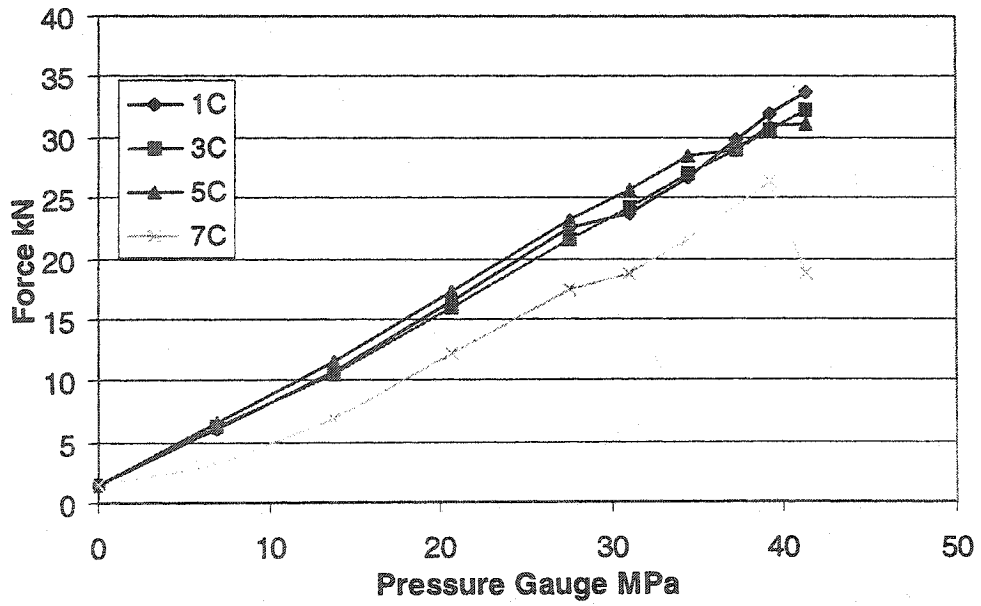

Fig 4.6 Forces of compression rods versus pressure gauge at corner columns

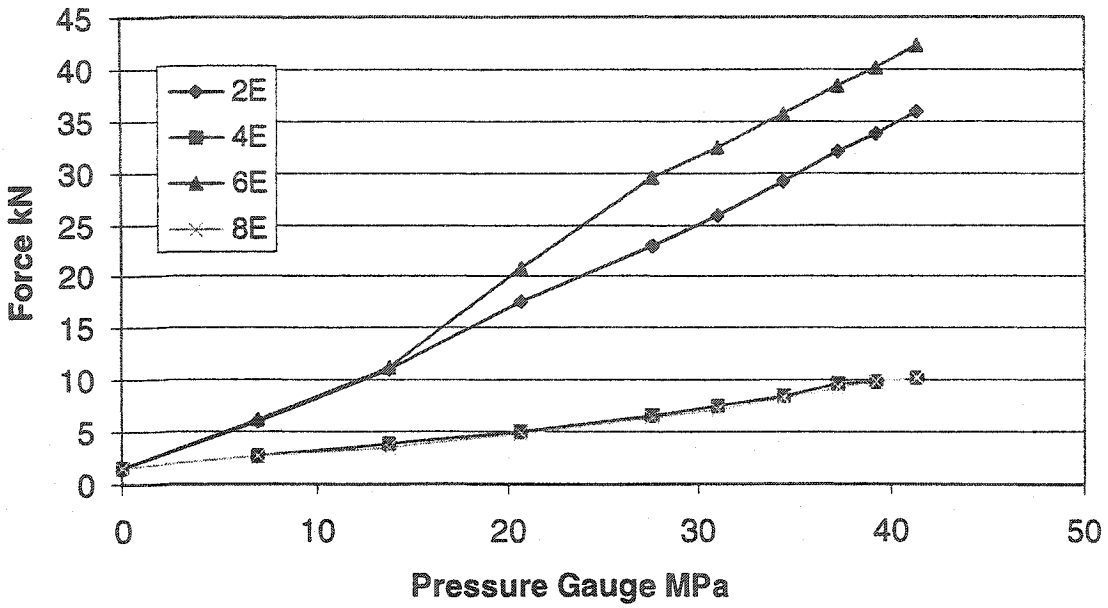

Figure 4.7 Forces of tension rods versus pressure gauge at edge columns.

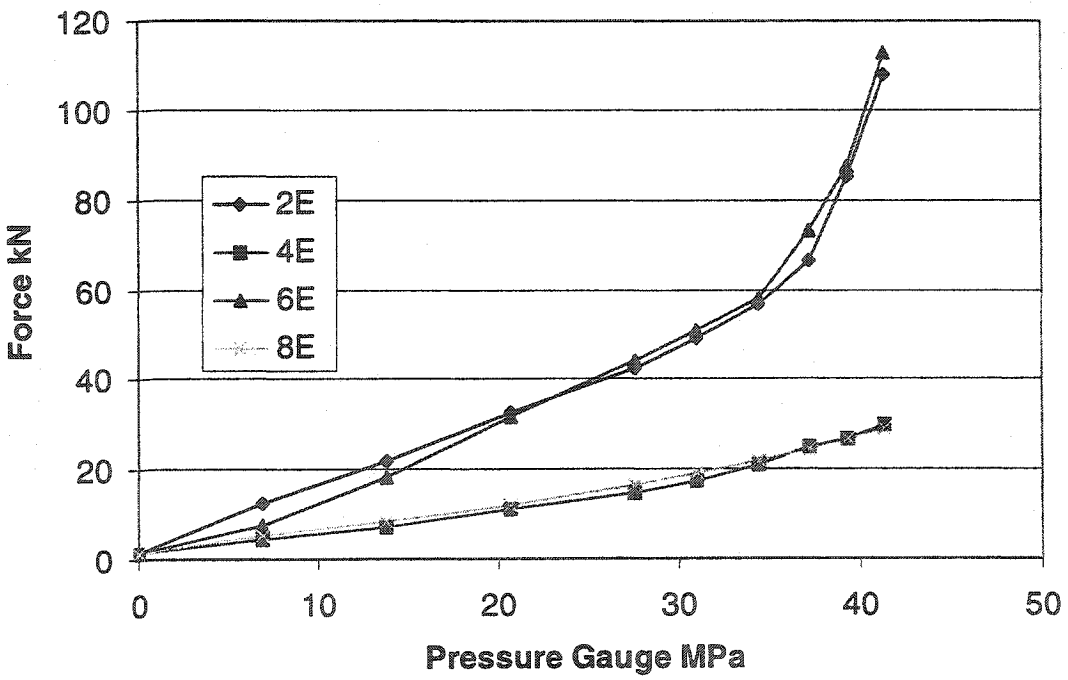

Figure 4.8: Forces of compression rod versus pressure gauge at edge columns.

It can be observed that in Figure 4.8 the measured forces in the rods are close to each other. Forces increased linearly with load until the compression rods at columns 2E and 6E started to buckle. This can be clearly seen in the changes of slope in the curves for rods 2E and 6E.

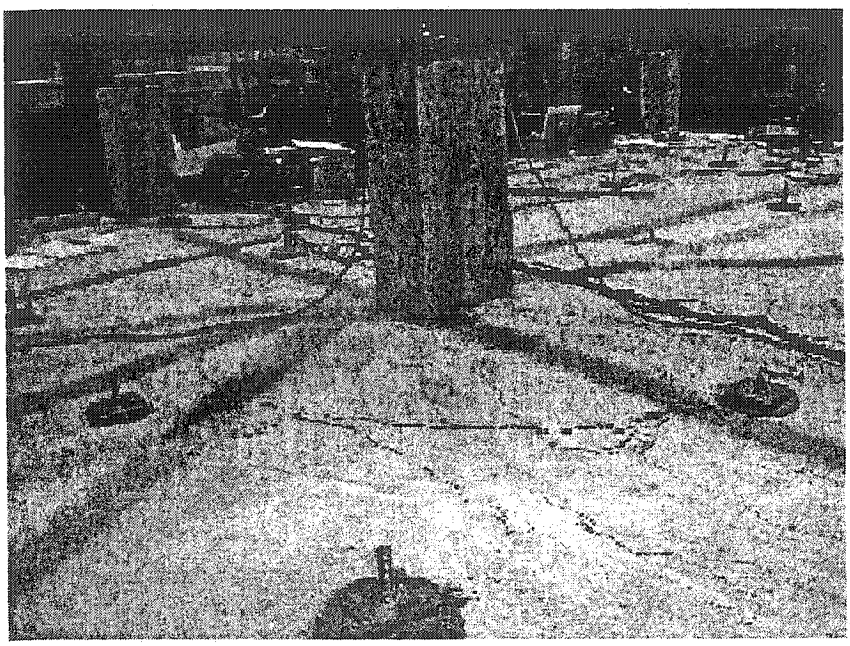

Figure 4.9: Collapse of the middle column

Figure 4.9 shows the collapse pattern at the 9M interior slab column connection. The crack pattern around the middle column was almost a 1400 mm diameter circle with many radial cracks. After the cracked concrete was removed, it was observed that the shape of the collapsed area was the expected cone shape.

Horizontal load cells showed, for every edge and corner connection, the compression forces in horizontal rods were more than the tension forces in horizontal rods.

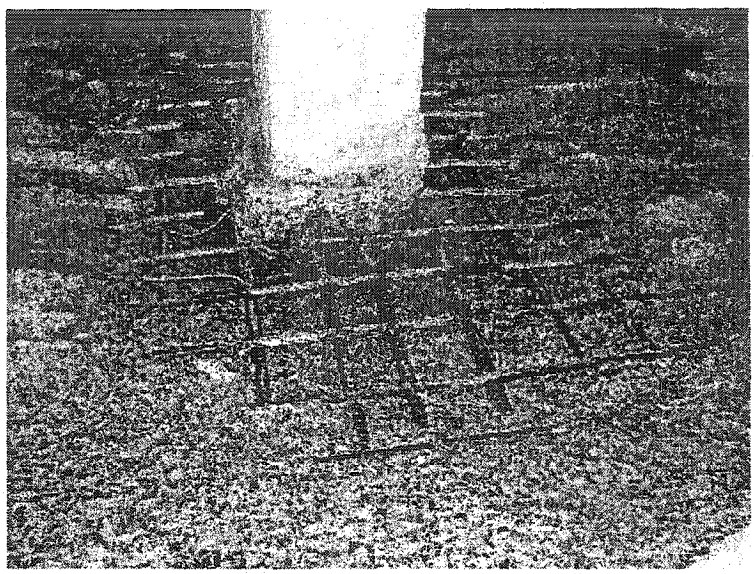

Figure 4.10: Cracked concrete removed at column 9M connection.

In Figure 4.10 it can be seen that the slab had displaced vertically bending the negative moment reinforcements.

Figures 4.11 and 4.12 show the strains in the negative reinforcement versus the interior column shear force for the short and long directions respectively.

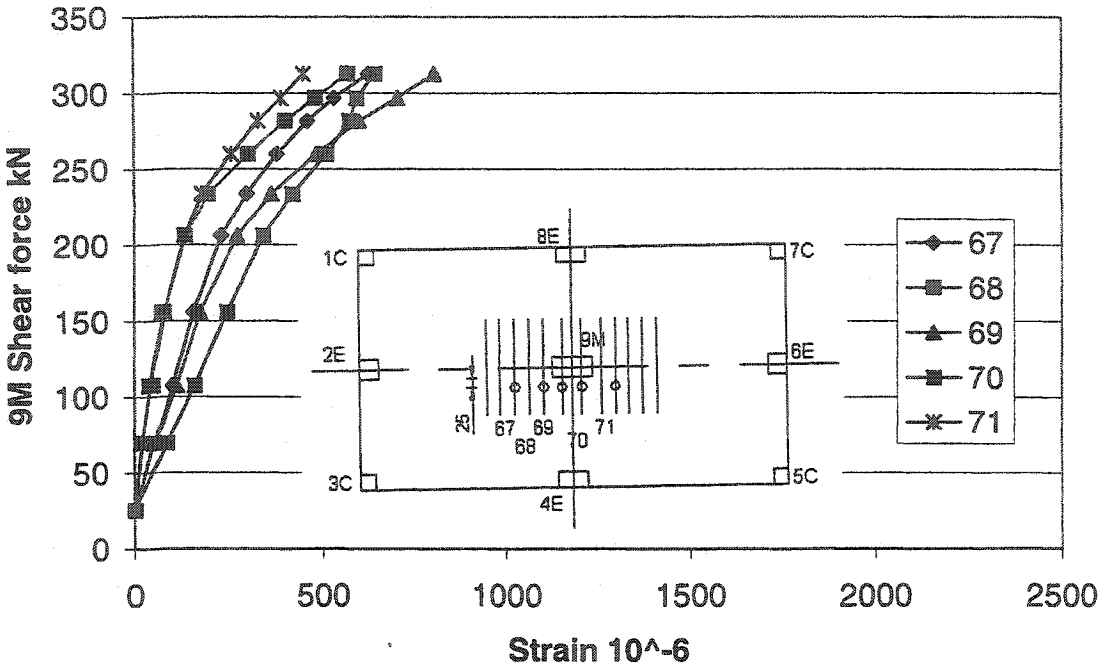

Figure 4.11: Strain vs shear force in middle column (9M) in short direction.

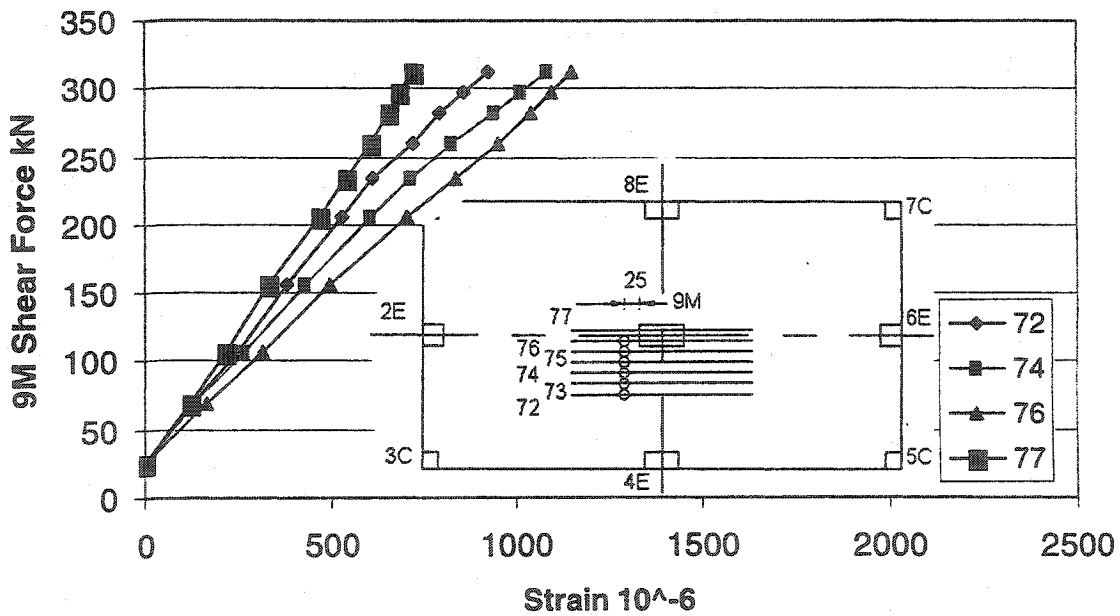

Figure 4.12: Strain vs shear force in middle column (9M) in long direction

Comparing graphs, Fig 4.11 and Fig 4.12 with respect to Figures 3.23, 3.25, shows that larger strains occurred in long direction than the short direction, though the

flexural reinforcement was proportional to the moments. None of the reinforcements yielded.

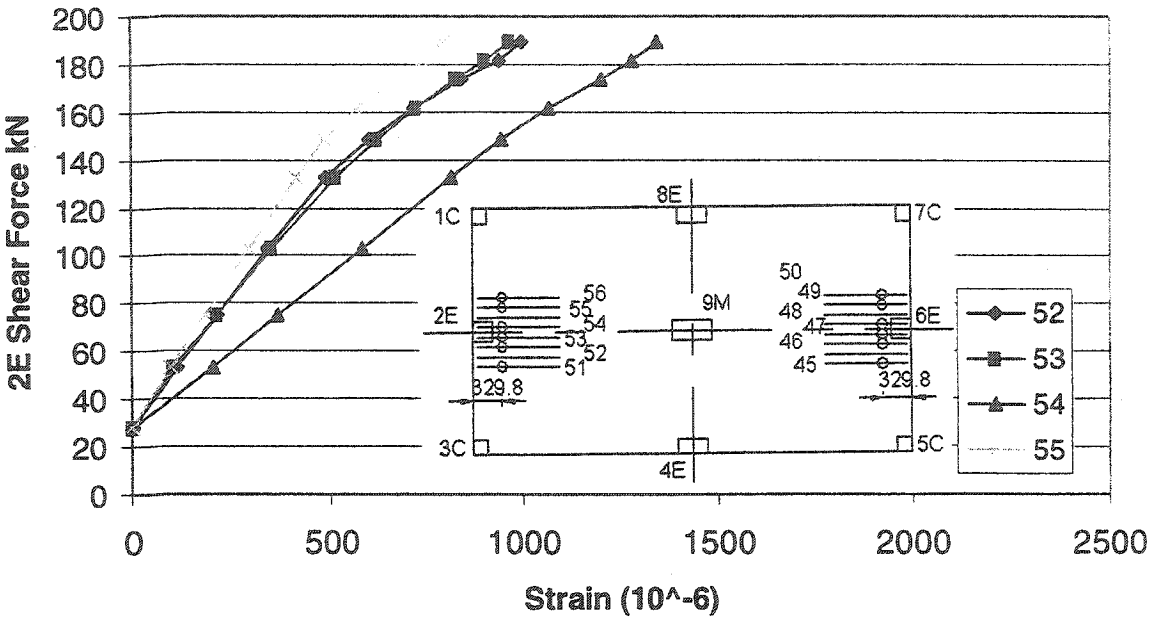

Figure 4.13: Strain vs shear force in edge column 2E in long direction

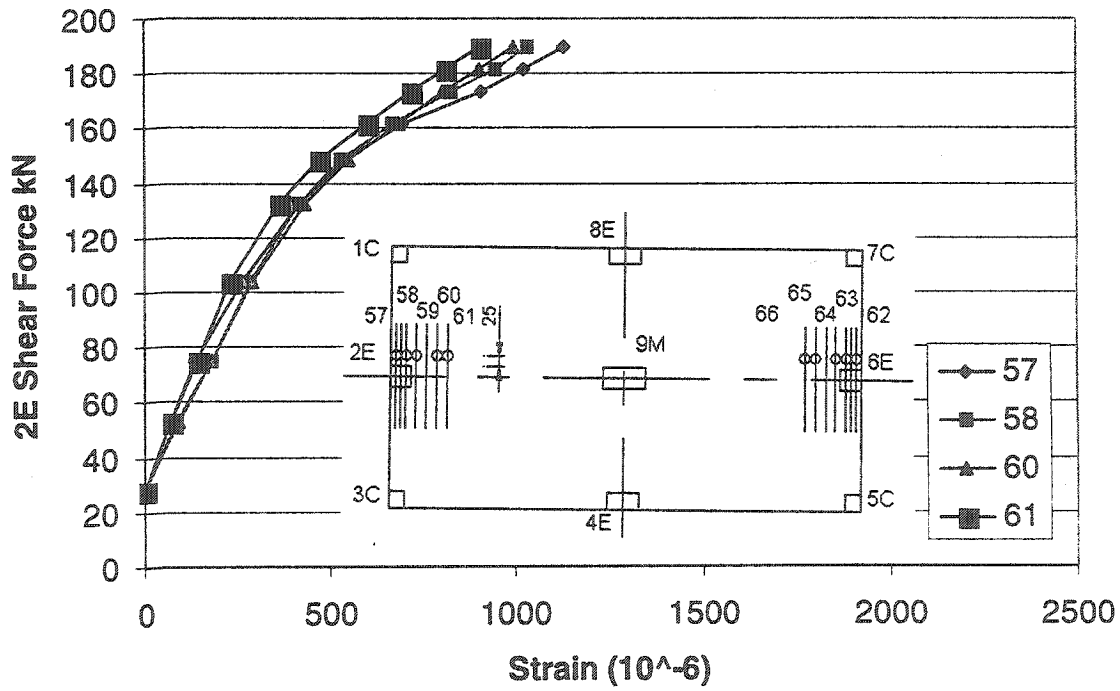

Figure 4.14: Strain vs shear force in edge column 2E in short direction

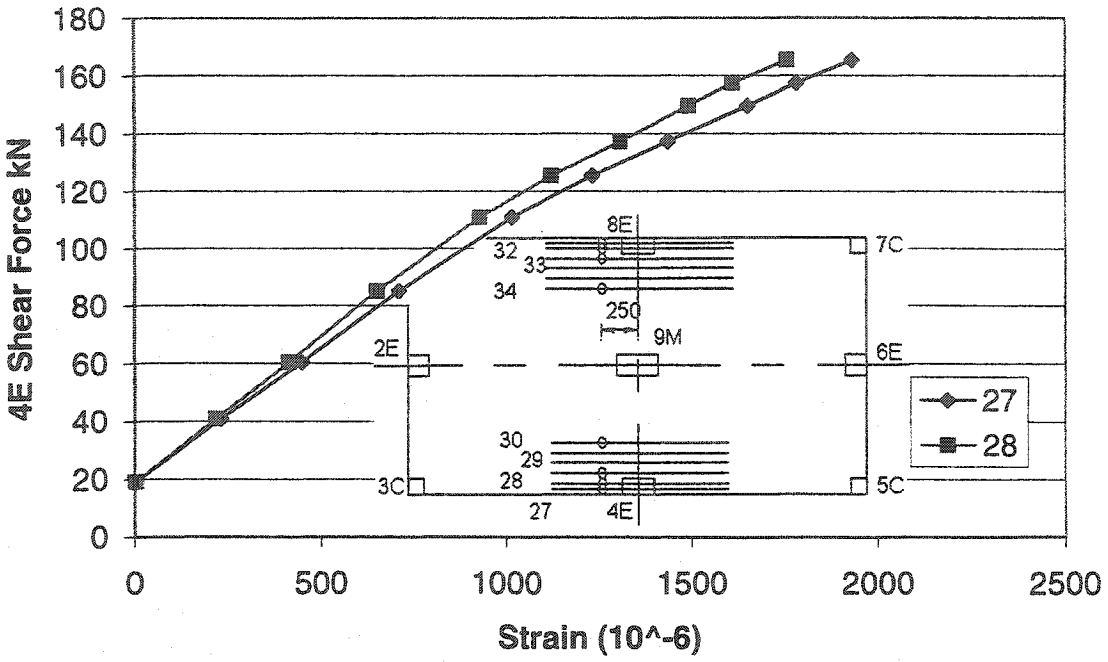

Figure 4.15: Strain vs shear force in edge column 4E in long direction

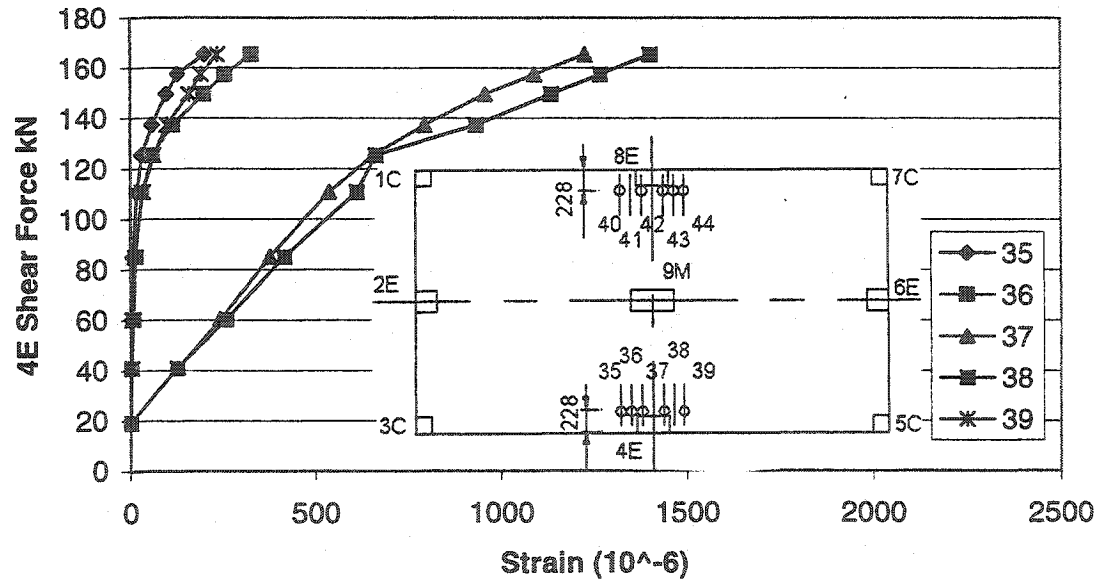

Figure 4.16: Strain vs shear force in edge column 4E in short direction

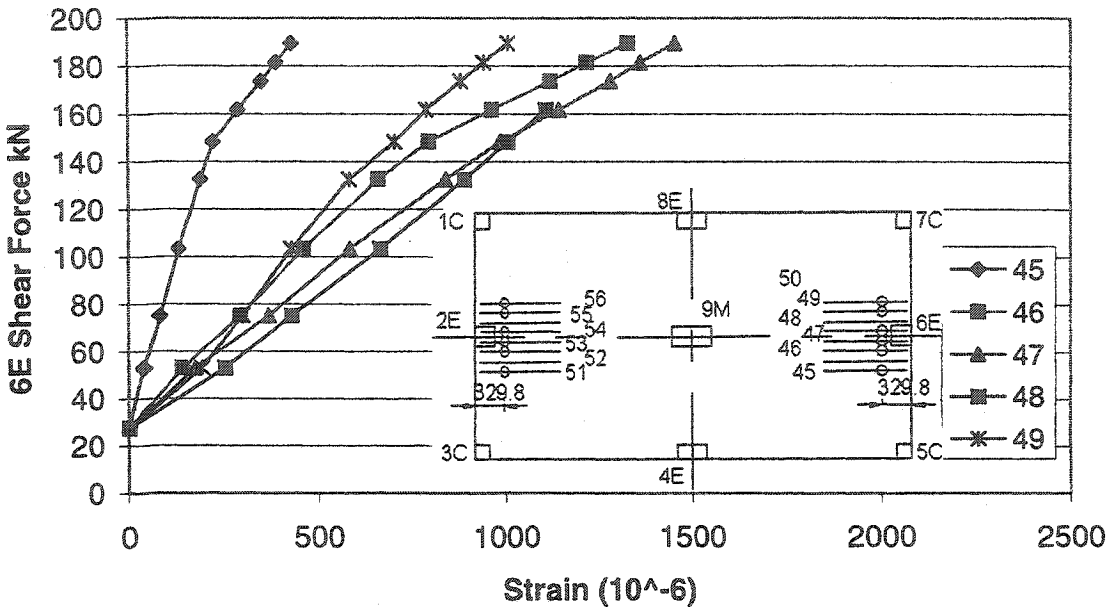

Figure 4.17: Strain vs shear force in edge column 6E in long direction

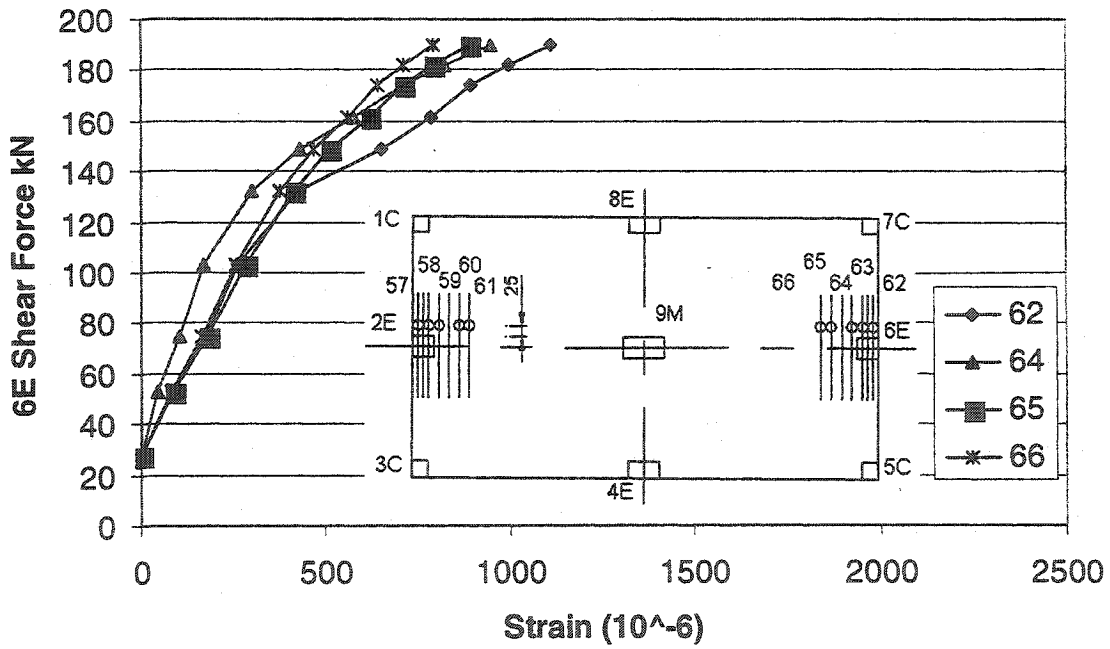

Figure 4.18: Strain vs shear force in edge column 6E in short direction

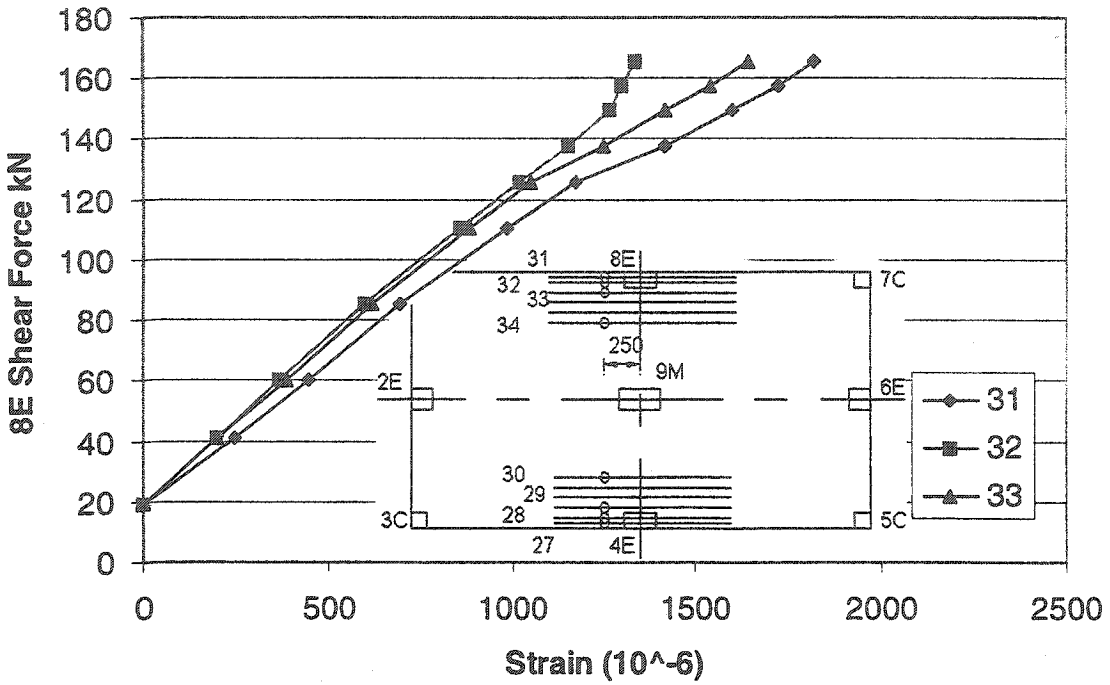

Figure 4.19: Strain vs shear force in edge column 8E in long direction

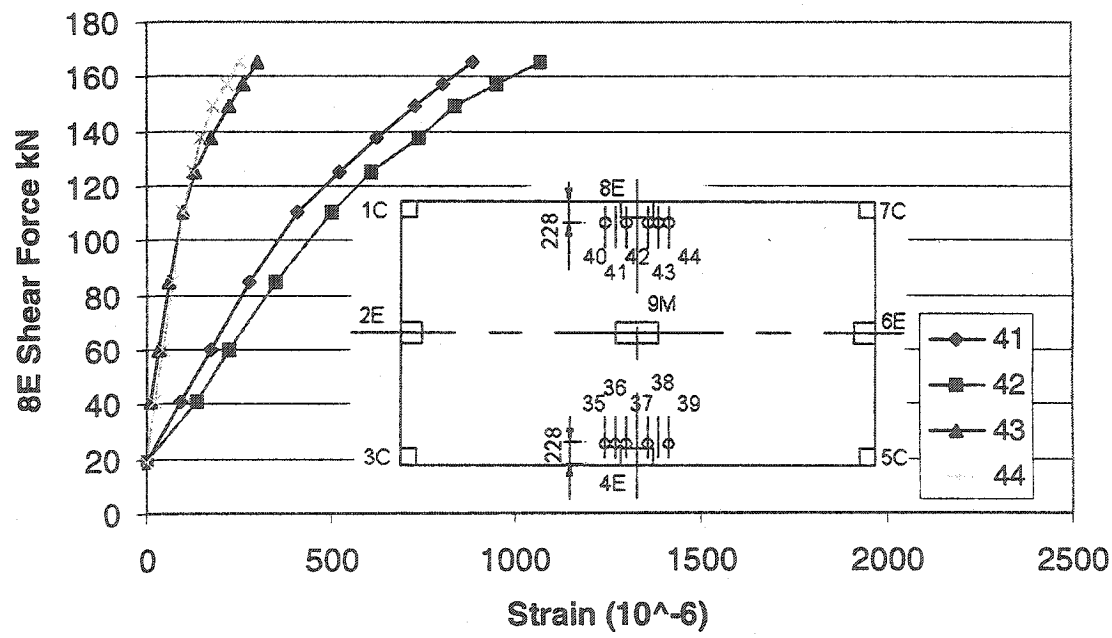

Figure 4.20: Strain vs shear force in edge column 8E in short direction

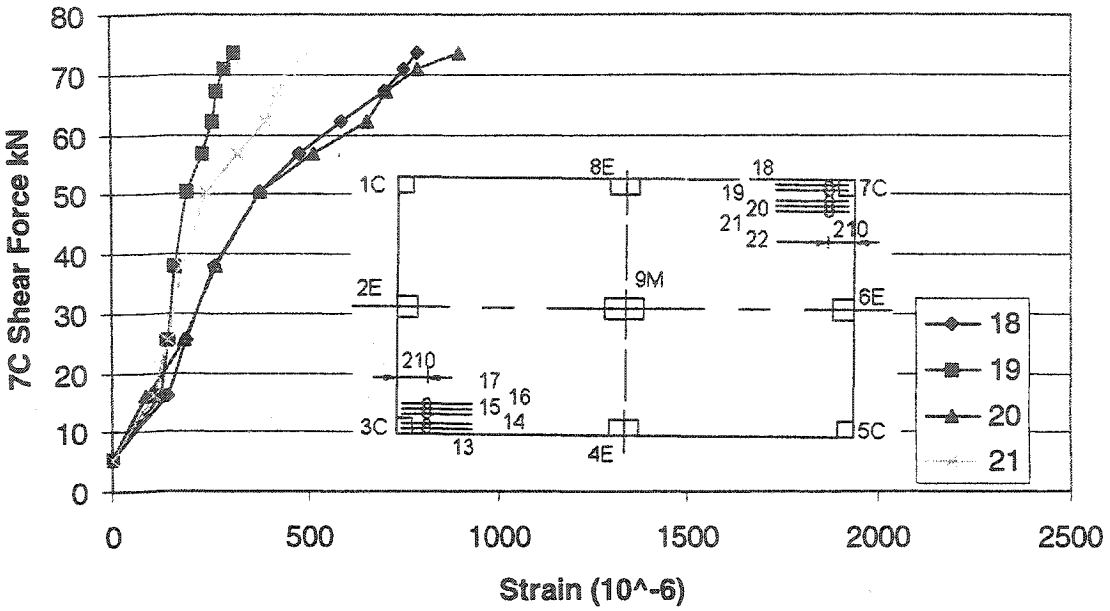

Figure 4.21 Shear force vs strain for corner column connection 7C

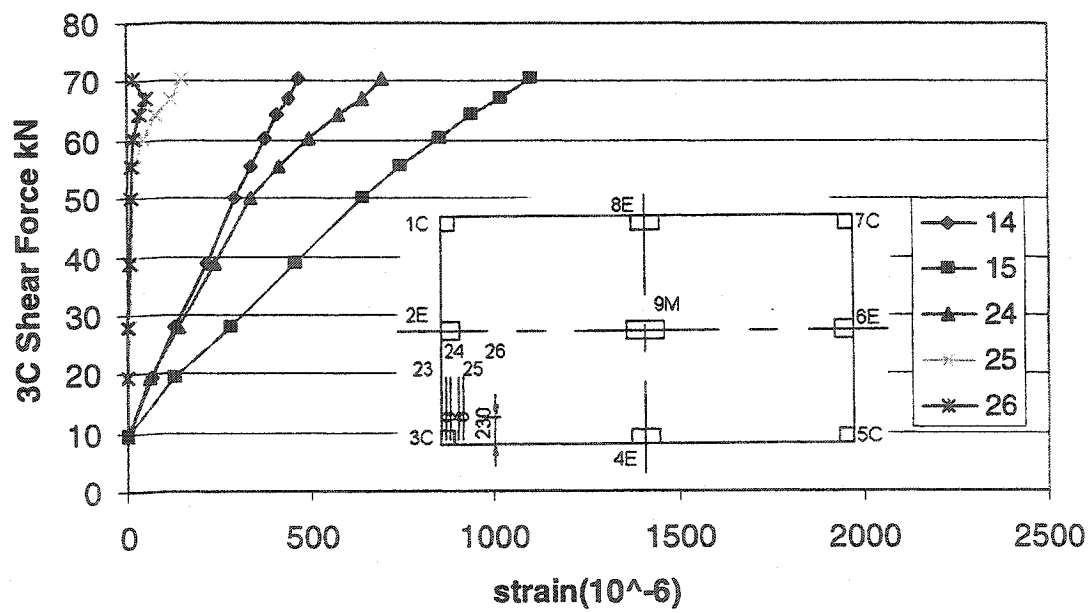

Figure 4.22: Shear force vs strain for corner column connection 3C

4.2.1 Repair of connection 9M

The failed concrete around column connection 9M was removed, the area was vacuum cleaned and washed. The connection was repaired using high early strength concrete. The slab was shored using 6 screw jacks.

4.3 Edge column connections

After repairing the middle column connection with high early strength concrete the connection was shored to ensure the middle column connection did not fail again. By shoring the middle column the perimeter of critical area became larger increasing the resistance of the connection to enable the edge connections to fail. All the compression-threaded rods restraining the edge and corner columns were replaced with tubes. The size of the tubes, 26.62 mm outside diameter and 18.80 mm inside diameter, was chosen to provide an increased second moment of area without increasing the area of the cross section.

4.3.1 Failure of Edge column 8E

The load was increased in 6.89 MPa (1000 psi) pressure gauge increments and data were recorded from the strain indicators. At each increase of 6.89 MPa (1000 psi), the data were recorded until 34.470 MPa (5000 psi). Then the load was increased in 3.44 MPa (500 psi) increments and data were recorded. After the 41.34 MPa (6000 psi) load range, data were recorded each 1.37 MPa (200 psi).

Connection 8E failed at 45.47 MPa (6600 psi). After failure, the oil gauge pressure dropped to 44 MPa (6400 psi) because of the displacement of the slab after failure.

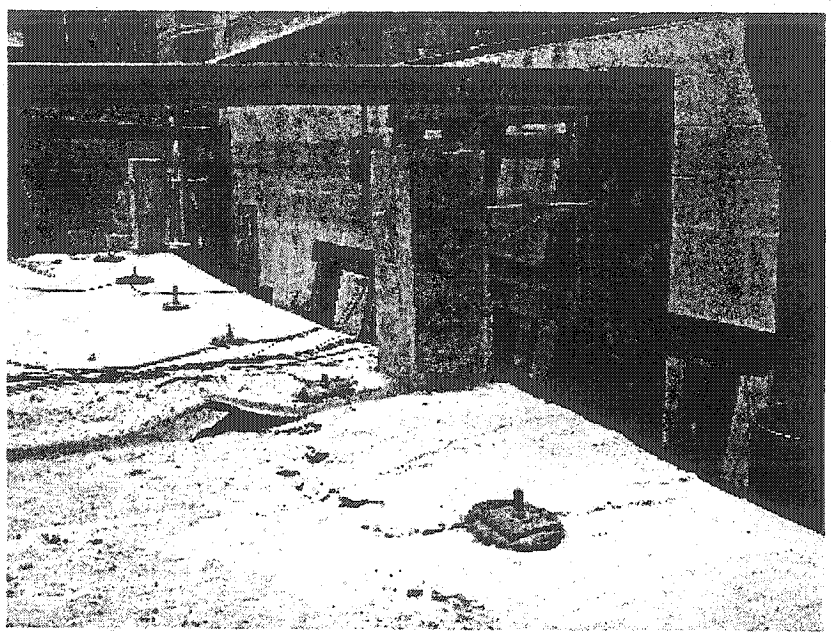

Figure 4.23: Failure of column connection 8E

Fig 4.23 shows the failure of connection 8E. The cracks were elliptic in the long direction. The unbalanced moment in the short direction caused torsion cracks in column connection 8E, which are clearly shown in Figure 4.24.

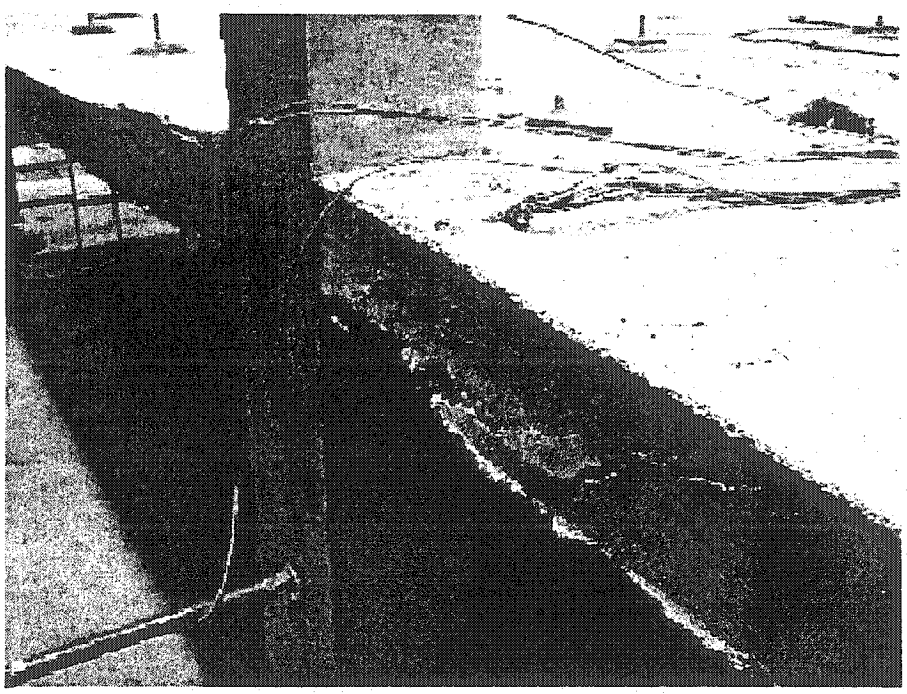

Fig 4.24: Torsion cracks in column connection 8E

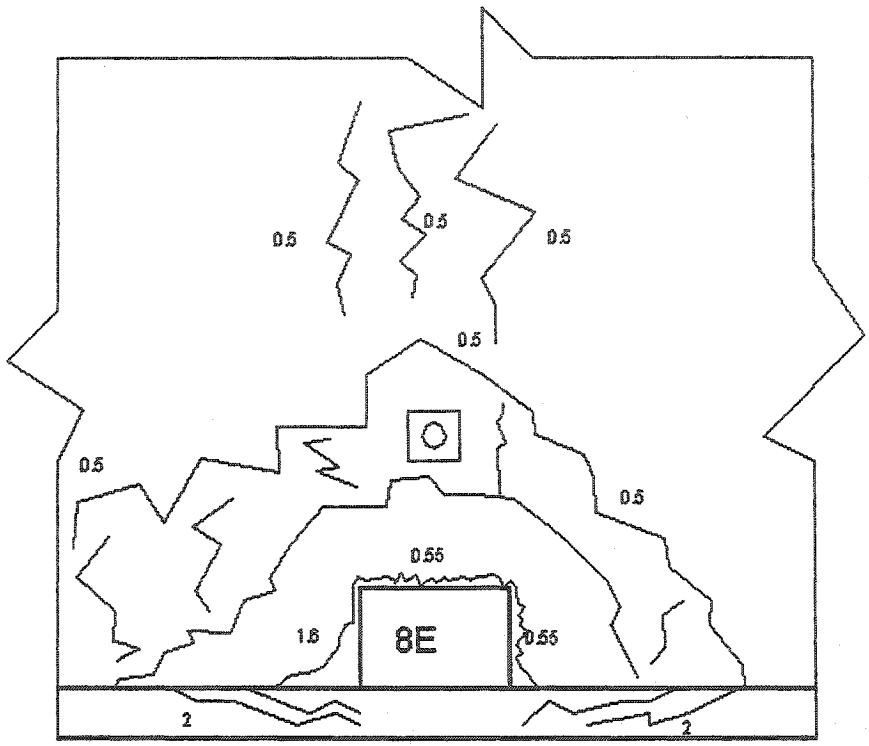

Fig 4.25: Crack pattern of column 8E connection, all the size of the cracks are in mm

The crack pattern was sketched and is shown in Fig 4.25. The failure surface included both flexural and torsional cracks.

In Figures 4.26 through 4.29 the strain of bending reinforcement vs shear force at connection 8E and 4E are shown.

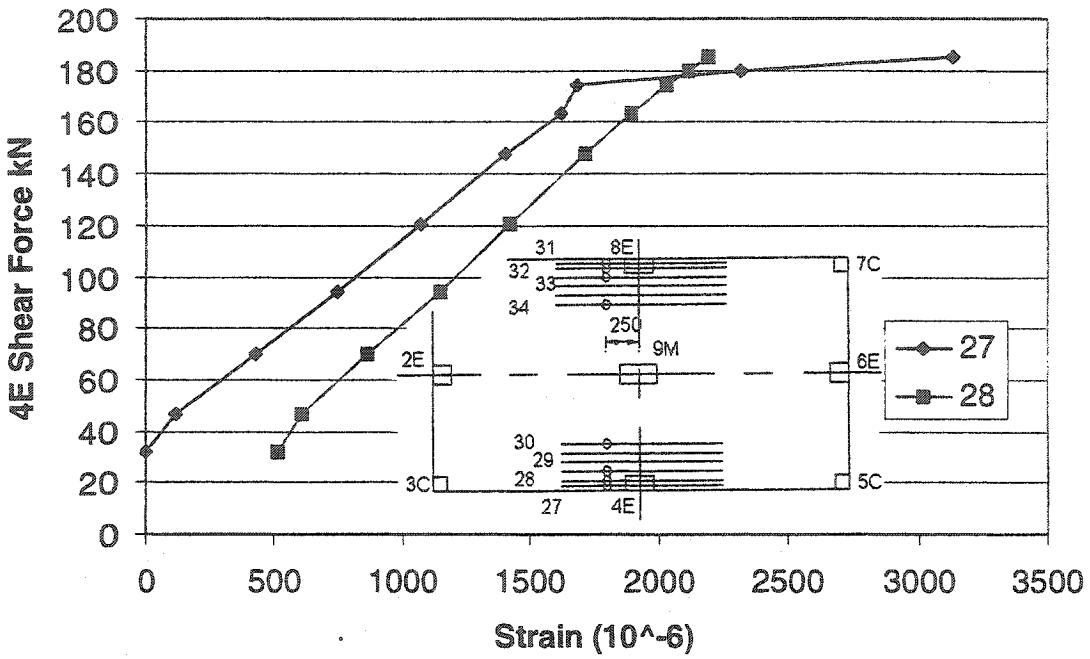

Fig 4.26: Strain vs shear force in connections 4E (long direction)

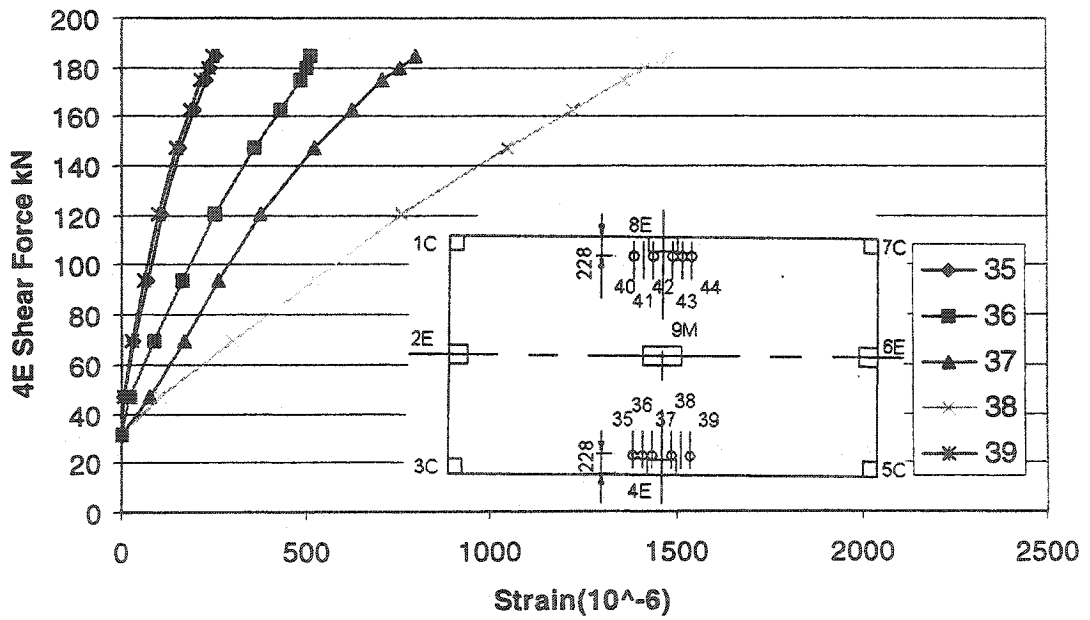

Fig 4.27: Strain vs shear force in connection 4E (short direction)

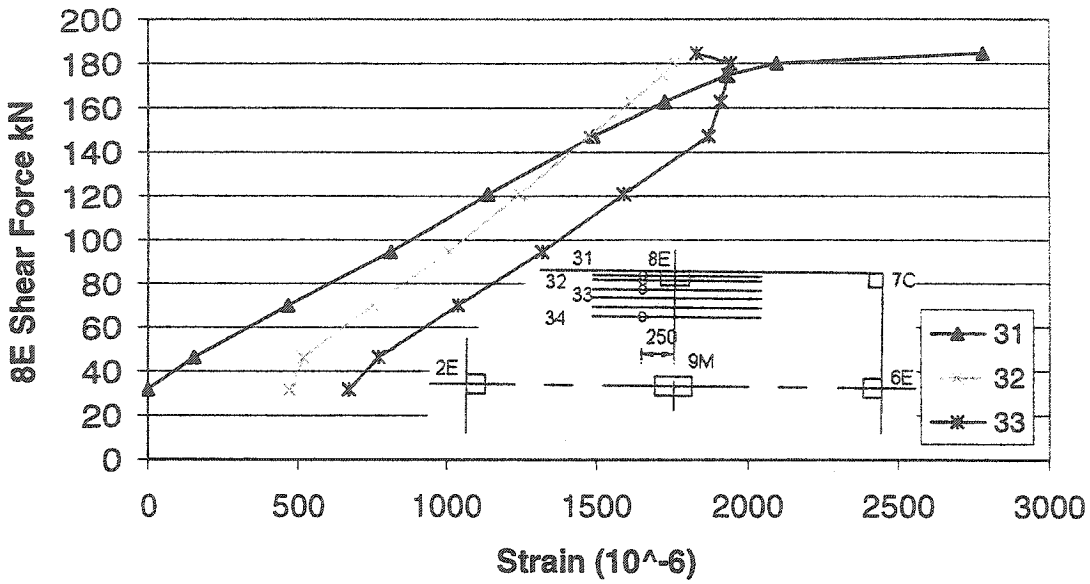

Fig 4.28: Strain vs shear force in connections 8E (long direction)

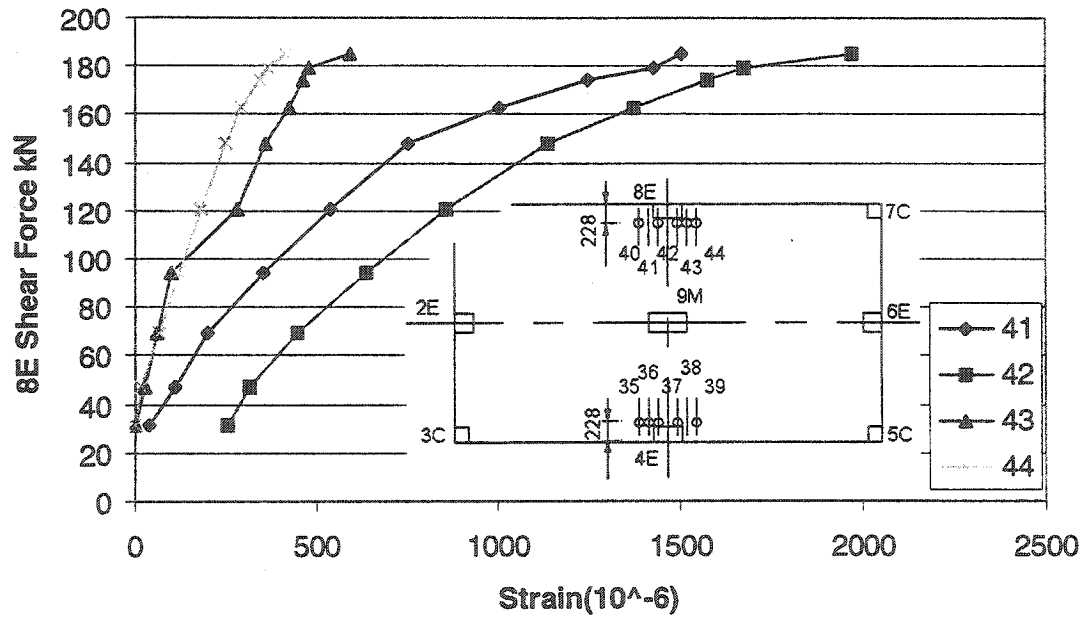

Fig 4.29: Strain vs shear force in connection 8E (short direction)

As shown in the two diagrams 4.27 and 4.29 the negative reinforcements, (37, 38, 42, 41), passing through the column had more strain than the other reinforcements out side the column.

As shown in Figures 4.26 and 4.28 gauges 31 and 27 show more strain than the other reinforcement. Rebar 31 and 27 were closer to edge and influenced by torsion.

Moments at the connections were calculated at the lower surface of the slab. The moment was calculated as the tension force times 0.57 m plus the compression force times 0.43 m.

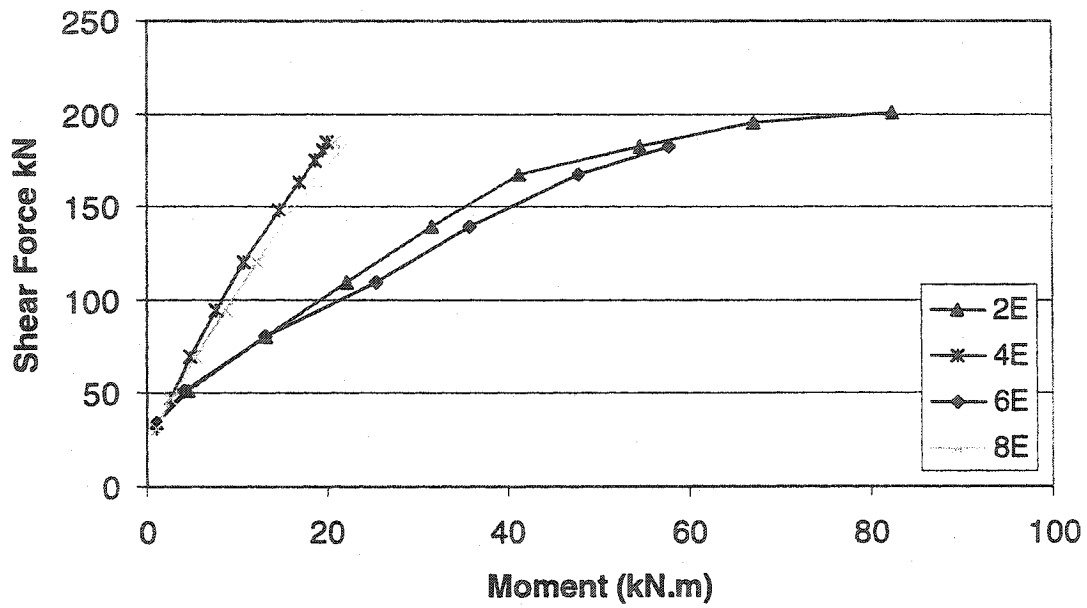

Fig 4.30: Relationship of moment and shear force in edge columns

Comparing the shear forces and moments of the columns leads to the fact that in the long direction there is more moment (2E and 6E) – but a short direction connection failed. As failure occurred at the 8E connection, the moment decreased during the failure (the last point in diagram for 8E connection in Figure 4.30)

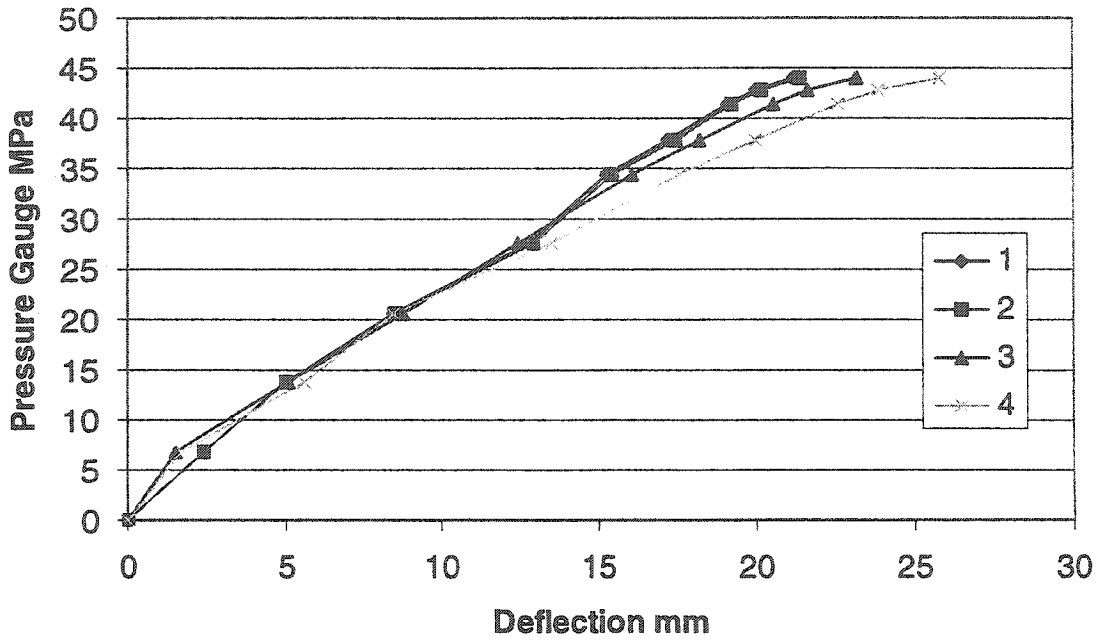

Fig 4.31: Pressure gauge vs deflections in four panels

4.3.2. Failure of the column 2E connection

After unloading the slab, connection 8E was shored and 4E (the other long side connection in the short direction) was shored to avoid its collapse, and the slab was reloaded. Ninety-millimeter square timber was used to shore connections 8E and 4E. Because the lower tube of connection 6E buckled again, the tube was changed with a bigger size tube with out attaching any strain gauges. Failure of short side connection 2E occurred at 49.64 MPa (7200 psi) of pressure gauge, much higher than the failure load of 8E long side connection 45 MPa (6600 psi). The failure is shown in Figure 4.32.

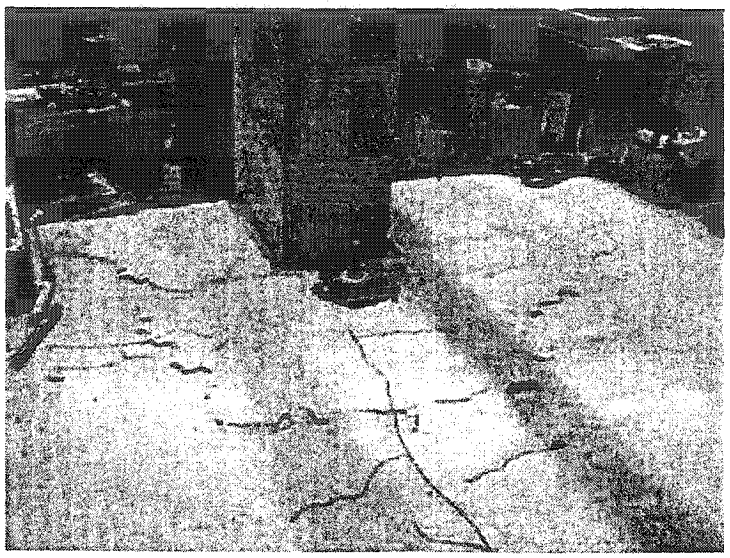

Figure 4.32: Failure of column 2E

As shown in the picture the cracks are both tangential and radial.

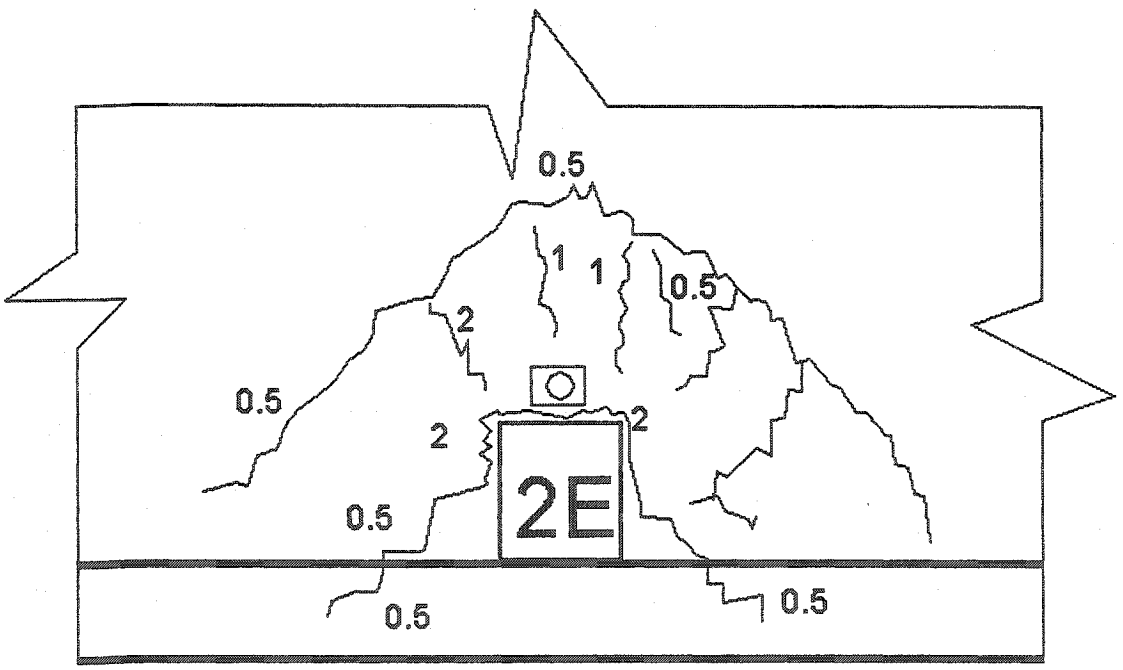

Figure: 4.33 crack pattern of connection 2E. (the size of cracks are in mm)

From figures 4.32 and 4.33 it can be noted fewer torsional cracks occurred atn connection 2E compared to connection 8E.

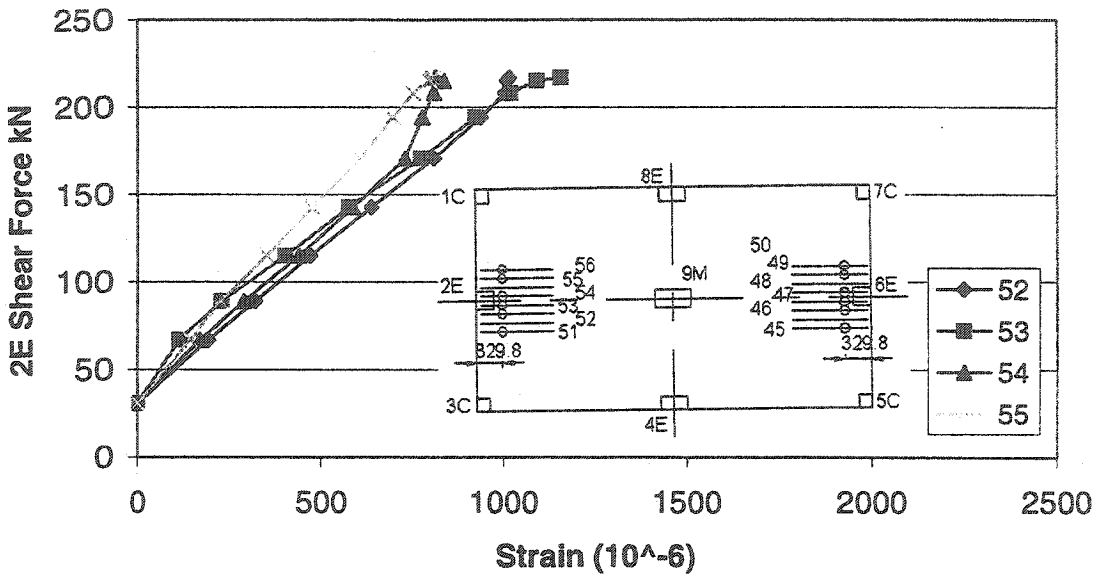

Figure 4.34: Strain of negative reinforcement in long direction 2E connection.

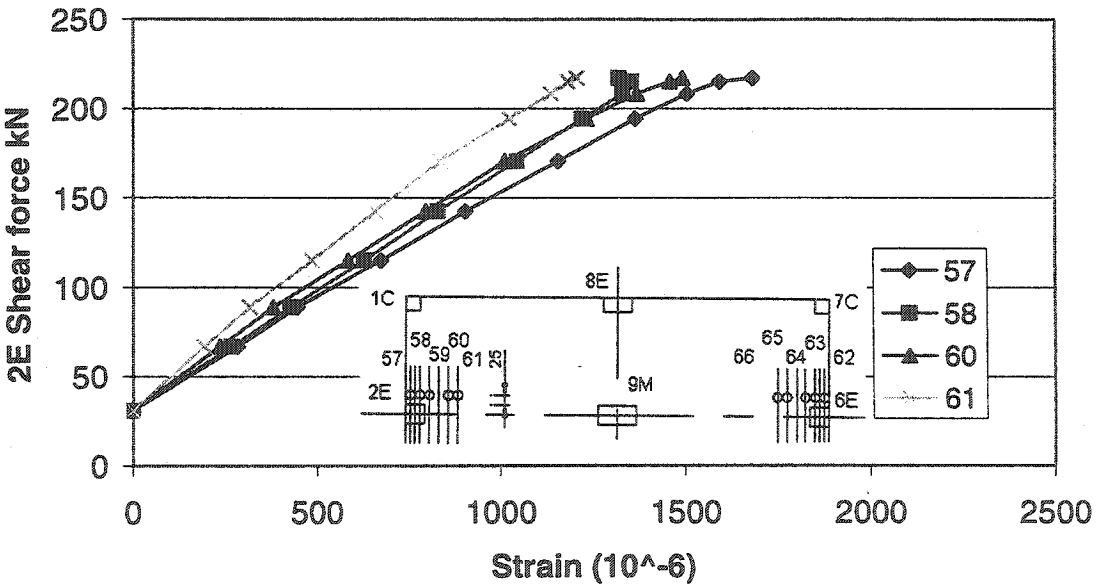

Figure 4.35: Strain of negative reinforcements in short direction 2E connection

By comparing the strain gauges in Figures 4.34 and 4.35, it can be concluded that the reinforcement close to edge of the slab experienced more strain. Comparing strains in long and short directions in connection 2E shows that there is more strain in the short direction than in the long direction.

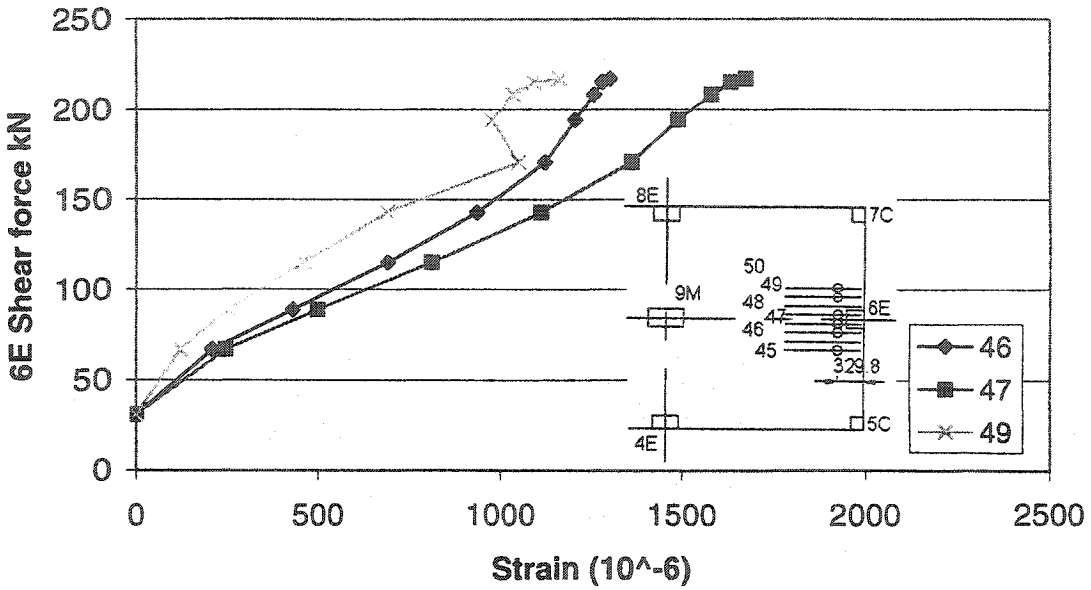

Figure 4.36: Strain of negative reinforcement in long direction connection 6E

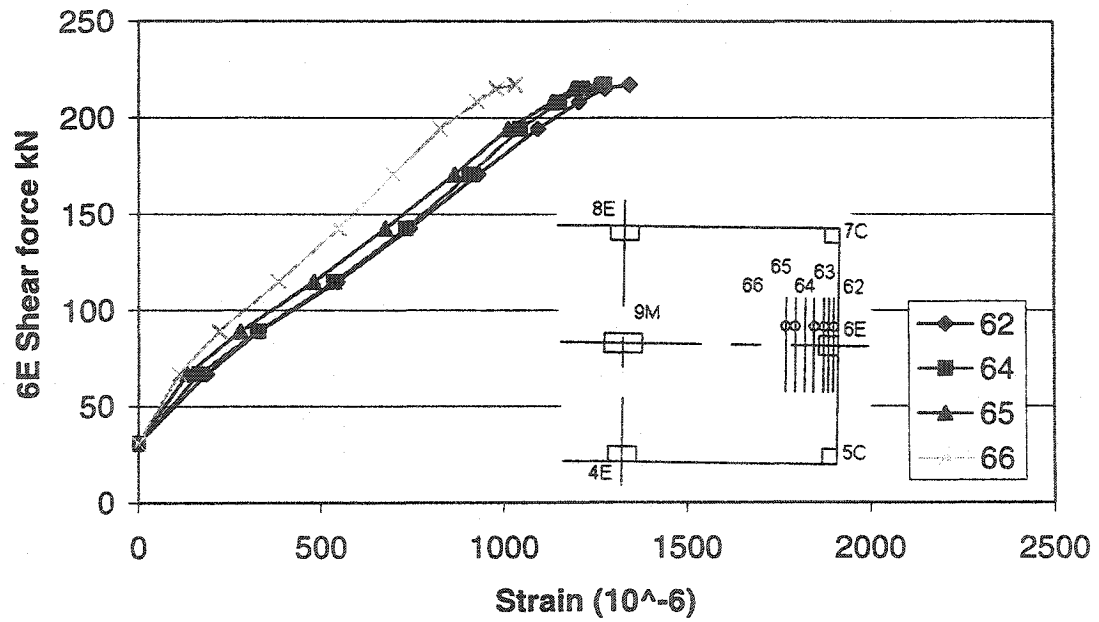

Figure 4.37: Strain of negative reinforcements in short direction 6E connection

Because no load cells were attached to lower tube of connection 6E only the tension forces of connections 6E and 2E are shown in Figures 4.38, 4.43 and 4.46.

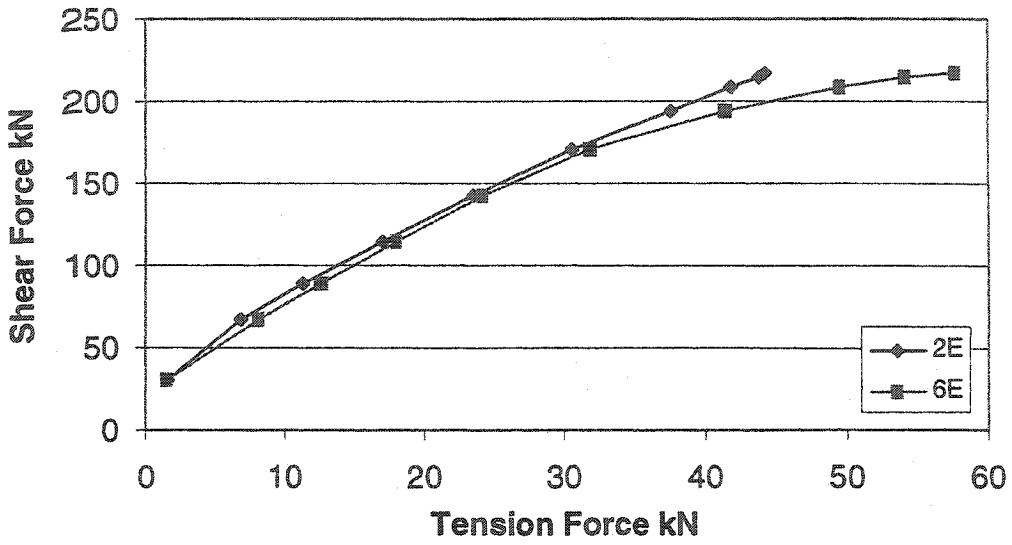

Figure 4.38 Tension force of threaded rods and shear force relation for the short direction connections

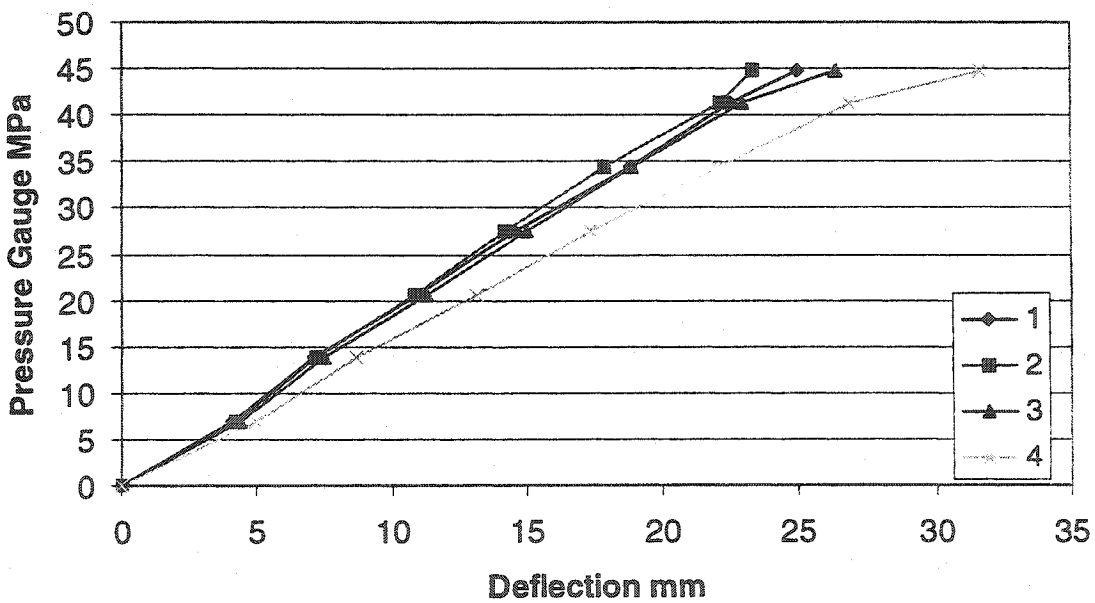

Figure 4.39: Relationship of pressure gauge and deflection of the four panels

As it is shown on Fig.4.39 the deflection of four panels in slab was very close to each other because all of them were symmetric.

4.3.3. Failure of the column 4E connection

After unloading the slab, the collapsed column connection 2E was shored. Because 4E column connection had been shored to avoid its collapse in the previous test, 4E connection was unshored. The slab was subjected to distribute load again. Failure of the 4E connection occurred at 40 MPa (5800 psi) of pressure gauge.

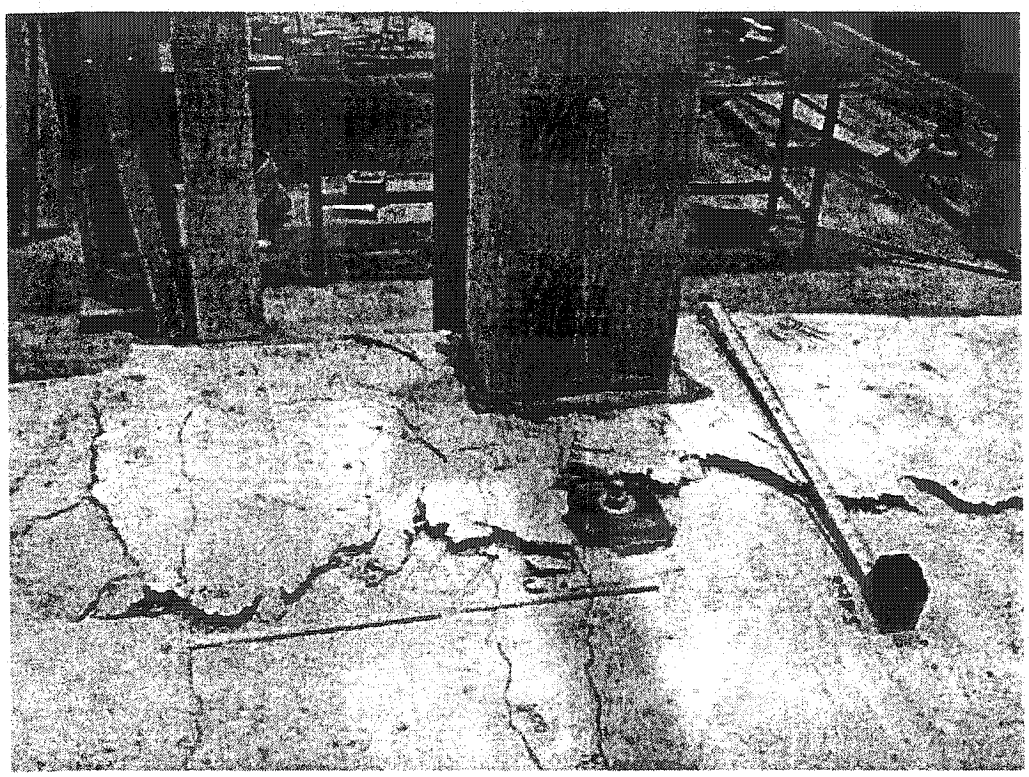

Figure 4.40: failure of the edge column connection 4E

Fig 4.40 shows that the cracks at connection 4E were elliptic in long directions and both radial and tangential cracks occurred in connection 4E.

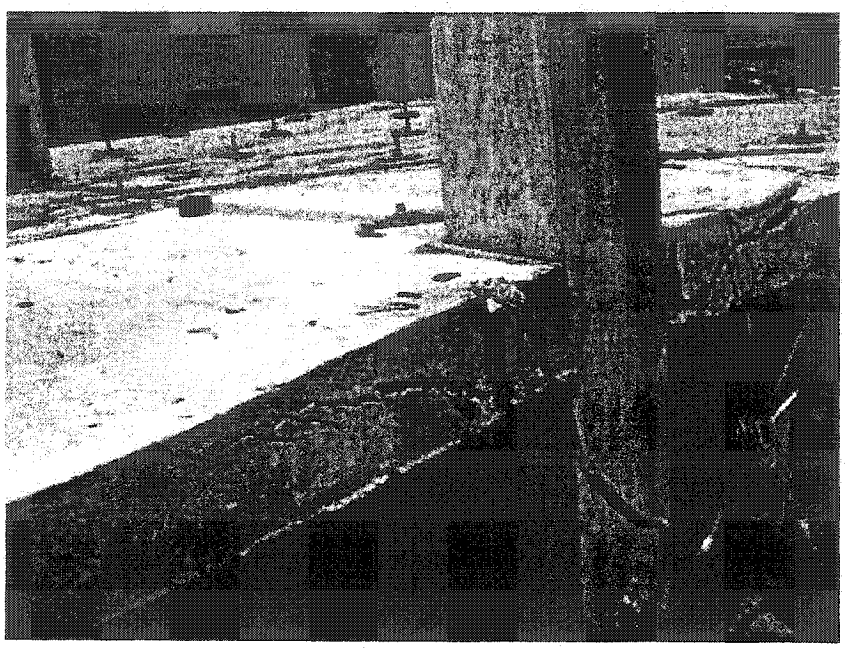

Figure 4.41: Large torsion cracks in connection 4E.

The torsion cracks which were observed in the face of edge connection 4E, were similar to those observed at 8E connection.(Fig 4.41)

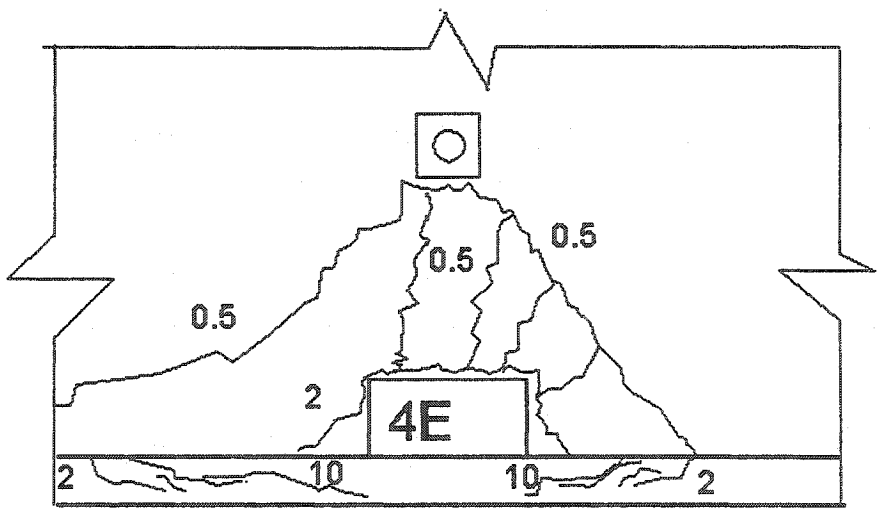

Figure 4.42: Crack pattern of connection 4E.

The crack pattern shows that in the 4E column connection torsional cracks were included with punching shear cracks and bending moment cracks.(Fig 4.42)

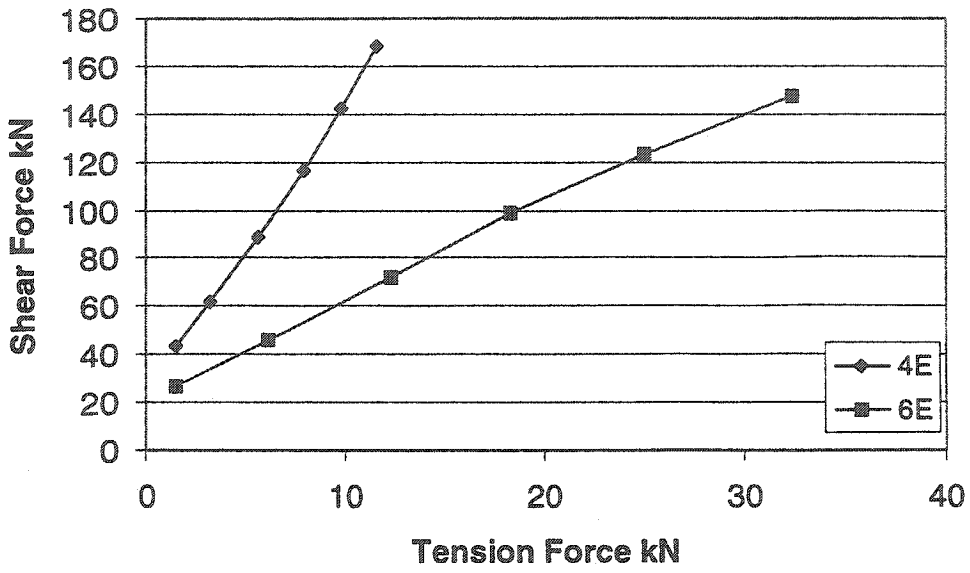

Figure 4.43: Shear force and tension force of threaded rods for edge connections 4E & 6E

4.3.4. Failure of the column 6E connection

After the collapse of connection 4E, the slab was unloaded, connection 4E was shored and then the slab subjected again to distributed load. Connection 6E failed at 49.64 MPa (7200 psi) of the pressure gauge. The failure load of connection 6E was identical to that of 2E, 49.64 MPa (7200 psi), which was high compared to short direction connections 4E, 40 MPa (5800psi) and 8E, 45.5 MPa (6600psi).

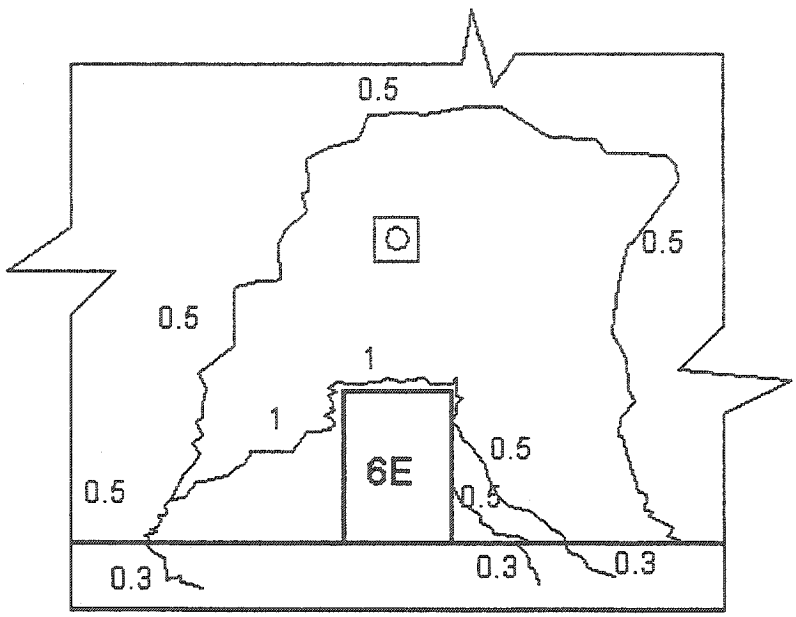

Figure 4.44 Crack pattern of connection 6E (size of cracks in mm)

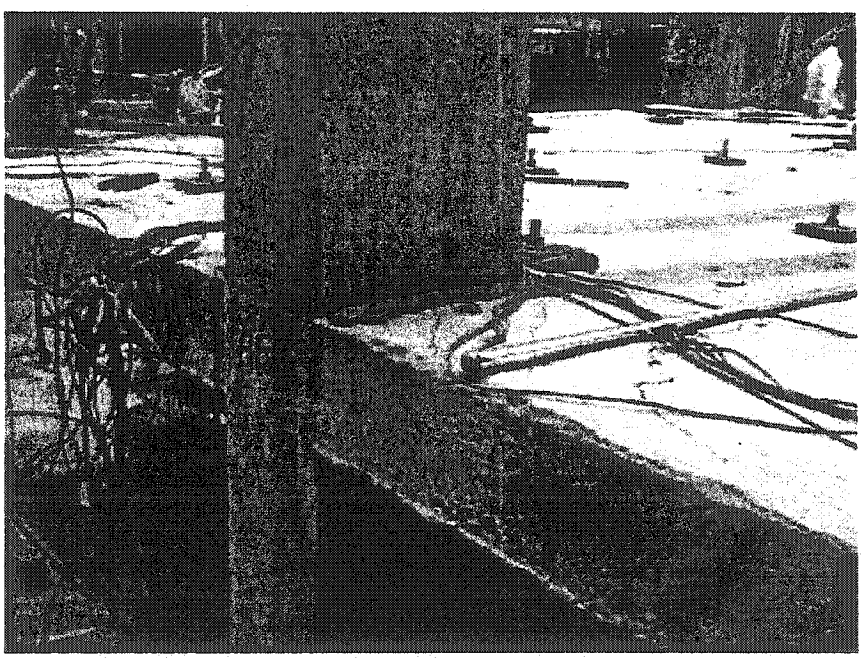

Figure 4.45: Small size torsion cracks in connection 6E

Fig 4.45 shows that less torsion cracks appeared in long direction compared with short direction.

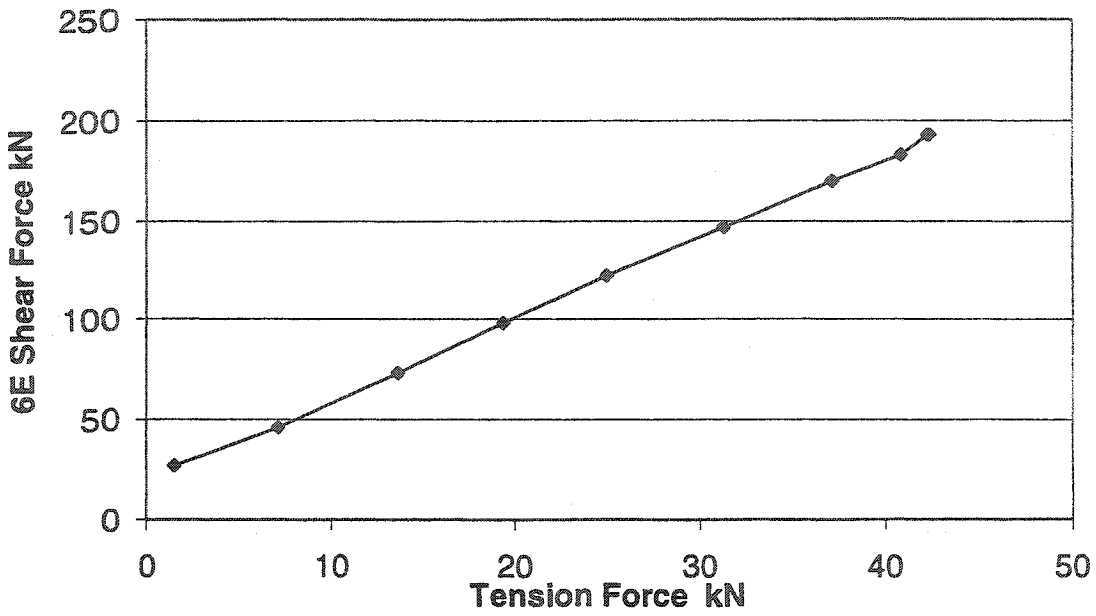

Figure 4.46: Shear force of connection 6E vs tension force of threaded rod

4.4. Failure of the middle repaired column connection

After failure of all the edge columns, it was decided to fail the repaired middle column, so after shoring all the edge columns the slab was subjected to load. At 27.6 MPa (4000 psi) of the pressure gauge the middle column failed again from the same place where it had failed before. Although high early strength concrete was used and the age of the concrete was 10 days on the testing day, and before casting the area of casting was cleaned carefully from cracked and damaged concrete and washed, the failure happened because of bond failure between the new and old concrete.

4.5. Failure of the corner column connections

After shoring the middle column the behavior of the corner column connections was investigated. Because the corner columns were subjected to less shear force and less unbalanced moments, more oil pressure had to be applied to the hydraulic jacks in order to fail corner columns compared to the middle and edge columns. The oil pressure was

increased to 57.9 MPa (8400 psi) but no failure happened in the corner columns although some cracks appeared around the corner column connections Fig (4.47). Because of the limitations of the equipment, it was not possible to further increase the pressure of the oil in the hydraulic jacks so the test was terminated at 57.9 MPa (8400 psi) pressure gauge.

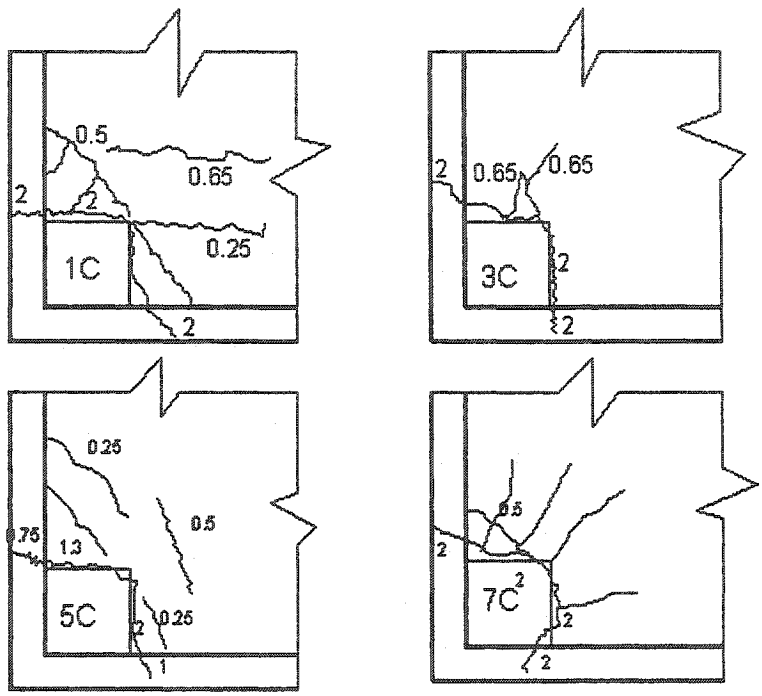

Figure 4.47: Crack patterns of corner column connections

The crack pattern shows that most deep and wide cracks appeared around the column faces and no diagonal cracks were observed at column connections 3C. Because column 7C had crushed during the failure of connection 2E test the moment and shear force of connection 7C is excluded in Figure 4.48.

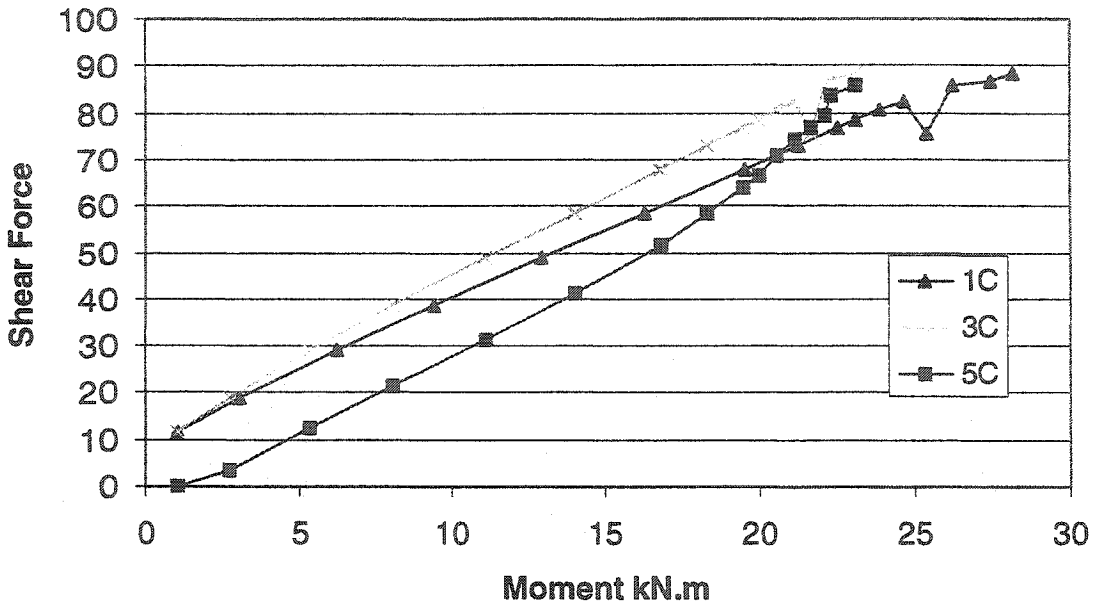

Figure 4.48: Moment vs shear force for corner columns

In Figure 4.48, because just two load cells were located under columns 1C and 5C, it is assumed that the shear force of column3C is equal to column1C.

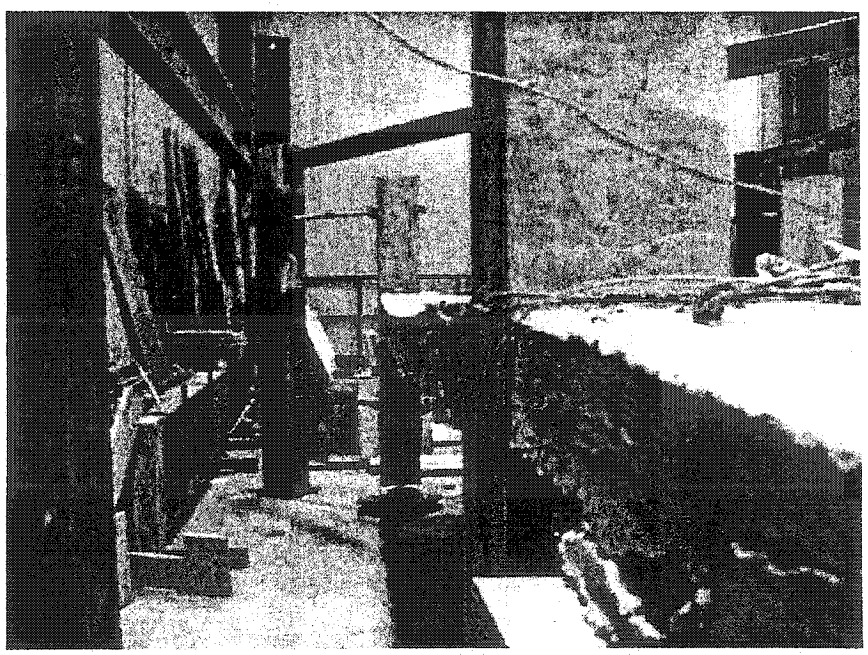

Figure 4.49: Deflection of slab under distributed load

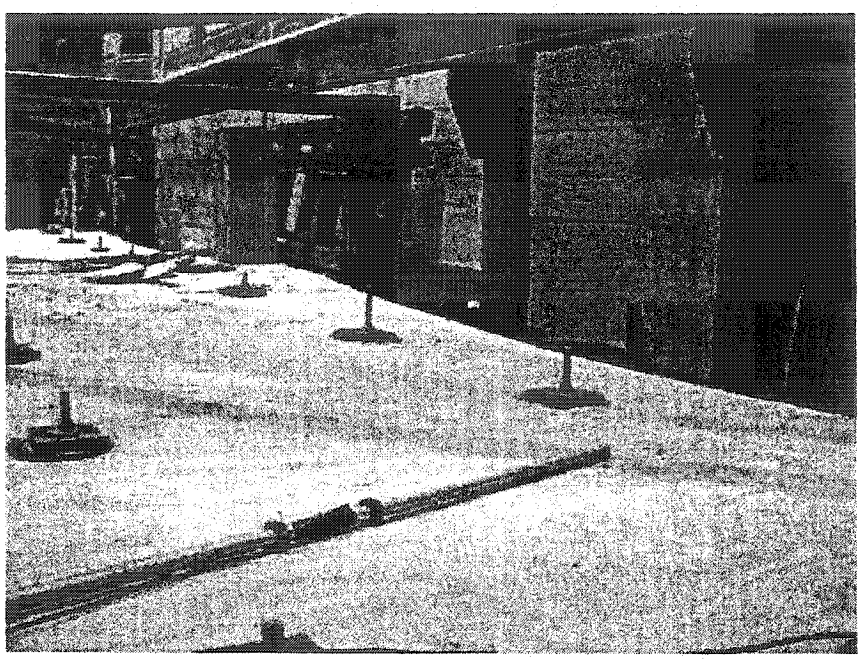

Figure 4.50: Deflection of the flat slab under distributed load

Figures 4.49 and 4.50 show the deflections in the flat slab when is subjected to distributed load.

Chapter 5

Discussion and Analysis

5.1 General

In this chapter the measured results of the tests are compared with results of RDDM and SAP (Structural Analysis Program) Finite Element Method and the measured load capacity at each connection is compared with load capacity of the tests calculated using the code predictions and Gardner's proposed method.

As the loads were controlled by the line pressure to the hydraulic jacks the applied load is denoted by the line pressure. The slab remained elastic till 27.6 MPa (4000 psi) line pressure because after unloading the deformations returned back to zero. The measured deflections shown in Figures 4.3, 4.31 and 4.39 were almost symmetrical except panel 4, which had a little more deflection than the other panels. Other than surface shrinkage cracks, no visible cracks were observed on the surface of the slab during the elastic range of loading. Because the bending moments were larger in the long direction, flexural cracks started to appear in the short directions orthogonal to their causing moments between columns 4E and 8E.

After the load exceeded 27.6 MPa (4000 psi), negative moment flexural cracks appeared at the column connections. The most noticeable cracks appeared around connection 9M. On increasing the applied load, the cracks became visibly deeper and wider. Radial cracks started at the column corners due to high stress concentrations at these locations. The negative moments bending cracks joined together before collapse of column connection 9M. As the slab lost its stiffness, the cracks got deeper and wider.

Some cracks appeared at the corner column connections. Torsion moments caused most of the cracks at the corner column connections.

The next section compares the measured column reactions in the test with those predicted. It is important to note many parameters influence the experimental results that are not included in the analysis.

5.2 Comparison of measured and calculated results

The test that caused failure of connection 9M at 41.36 MPa line pressure was the only test where none of the connections had been previously failed or were shored. Consequently the vertical reactions and reactive moments are calculated for a jack pressure of 41.36 MPa.

The force of 22 jacks, area of 1445 mm ^{2} at 41.36 MPa line pressure distributed over the total area of the slab gives an equivalent uniformly distributed load of 38 kPa.

5.2.1 RDDM

Equivalent distributed load: W_u =38 kPa

Long direction:

$$M_0 = \frac{38 \times 4114^2 \times 2286}{8} = 184 \text{ kN.m}$$

Moment of edge column connection = 0.275 ×184=50.6 kN.m

Moment of corner column connections = 50.6×0.5=25.3 kN.m

Short direction:

$$M_0 = \frac{38 \times 4114 \times 2286^2}{8} = 102 \text{ kN.m}$$

Moment of edge column connection = 0.275 ×102=28 kN.m

Moment of corner column connections in each direction = 28×0.5=14 kN.m

The axial load of the columns was determined using the factors 28% of total four panel load for middle column, 5.5% of total load for the corner column and 12.5% of total load for edge column.

Middle column=28% ×1447=405 kN

Edge columns = 12.5%1447=180 kN

Corner columns =5.5% ×1447=79 kN

5.2.2 FEM (Finite Element Method) results

A linear elastic finite element analysis was done as a check on the magnitude of the column reactions – it was not intended to be an exhaustive study of FEM as applied to flat plates. The accuracy of the answers of the FEM method depends on the mesh size and shape of the mesh. If the chosen mesh size is very small then the risk of round off error will be high. Choosing a large mesh size will reduce accuracy. The slab was modeled by three mesh sizes. All the input files and output files are available in the attached CD. For all the models it was assumed that all the supports were fixed and 44 concentrated loads were applied.

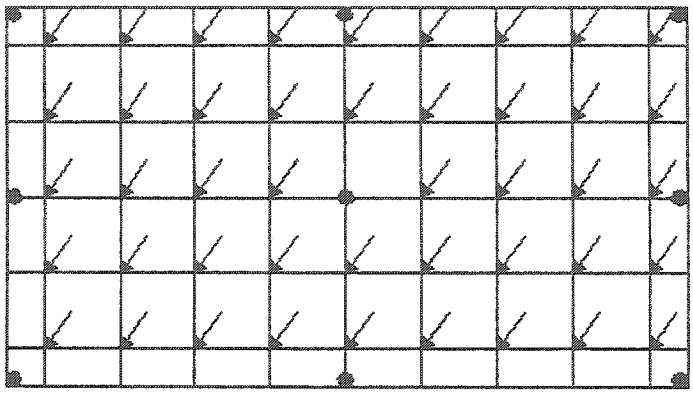

Fig 5.1A: First model that was analyzed by finite element method

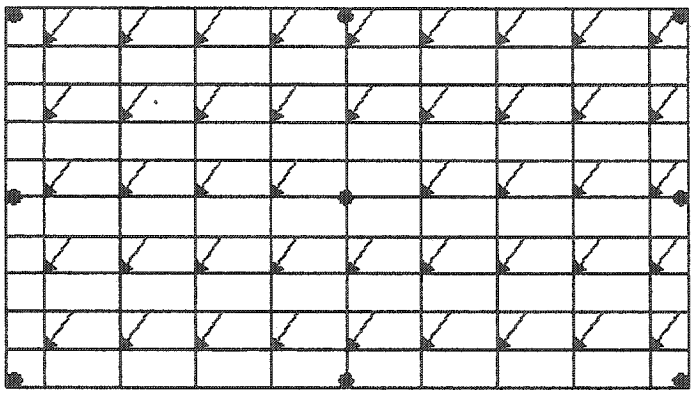

Fig 5.1B: Second model that was analyzed by finite element method

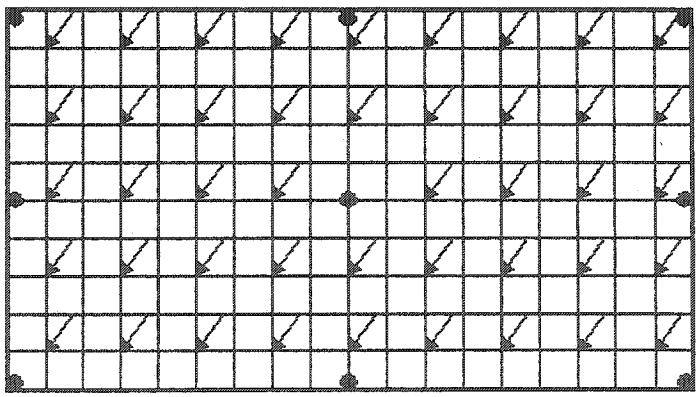

Fig 5.1C: Third model that was analyzed by finite element method

Table 5.1: Measured and calculated column reactions for different mesh sizes

Axial load (kN)	Experimental	FEM (a)	FEM (b)	FEM (c)
2E	189.4	192	180	180
4E	165.4	188	188	178.2
9M	312	396	411	431
3C	70.57	67	69	69
7C	73.64	67	69	69

It can be observed that the interior column measured reaction is significantly less than calculated by any of the FEM calculations or the RRDM. Unfortunately the interior column reaction measurement was the only reaction for which an alternative measurement was not available. This load cell was in place when the slab was constructed which did not permit it to be removed for checking during the tests. No reason can be advanced for this low value and the centre column reaction is omitted from any comparisons.

Table 5.2: FEM method for different mesh sizes and experimental results

	FEM (a)/EXP	FEM (b)/EXP	FEM (c)/EXP
2E	1.014	0.950	0.950
4E	1.137	1.137	1.077
3C	0.949	0.978	0.978
7C	0.910	0.937	0.937
Average	1.00	1.00	0.986
Variance	0.01	0.01	0.004
S.D:	0.10	0.09	0.06
C.V:	0.10	0.09	0.06

Because the coefficient of variation for model c is smaller than the others model c is compared with the RDDM in the next section.

5.2.3 Comparing the results

Table 5.3 compares loads in edge and middle columns in test number 2 (failure of 9M column connection) with the FEM and RDDM results. It can be seen the FEM results are close to the RDDM method.

Table 5.3 RDDM, FEM and Experimental results

Axial load (kN)	Experimental	FEM	RDDM	FEM/Exp	RDDM/Exp
2E	189.4	180	178.4	0.950	0.942
4E	165.4	178	178.4	1.076	1.078
3C	70.57	69	78.5	0.977	1.112
7C	73.64	69	78.5	0.937	1.066
			Average	0.985	1.05
			Variance:	0.004	0.006
			Standard Deviation:	0.063	0.074
			Coefficient of Variation:	0.064	0.071

5.3 Punching shear failure of current flat slab

The punching shear capacity of the edge column connections was the main concern of the current research. Load cells were provided to measure the loads transferred to columns 9M, 2E, 3C, 4E, 5C.The load cells under columns 2E, 3C, 4E, 5C could be switched under others columns if it was necessary. All the unbalanced moments transferred to the edge columns were measured. Because the slab was rectangular in plan, the behavior of the slab was more complicated than a square slab. Most of the available literature was developed on square flat slab.

The interior column connection 9M failed due to punching shear at an applied load of 41.36 MPa (6000psi). Edge column connection 8E failed at 45.5 MPa (6600 psi). Edge column connection 4E failure occurred at 40 MPa (5800psi). Both 2E and 6E connections failed at 49.6 MPa (7200 psi). After each set of the tests the failed column connection was shored. The punching failure of the interior column was completely cone

shape having both tangential and radial cracks. The tangential cracks were almost circular with a little skew in the long direction because of the larger bending moments in the long direction.

The failures of the 4E and 8E column connections were similar to each other. The tangential cracks were elliptic in shape with skew toward the long direction. In both failures torsion cracks occurred on the edge of the slab. The bending reinforcements which passed through the columns deformed more than the reinforcements which did not pass through the columns. The failure mechanism was cone shape in both cases the 4E and 8E column connections. In both cases both tangential and radial cracks appeared and in both cases failure happened suddenly. In both column connections the tension rods were subjected to less force than the compression rods that made understanding the behavior of the slab more complicated. The distance between compression and tension rods were one meter and thickness of the slab was 140 mm. To calculate the moments of each connection, the force of tension rods multiplied by 57 cm and compression rod force by 43 cm.

Larger moments in long directions caused the strains to be larger in the long directions than in the short directions. In the tests to fail the long direction column connections (2E, 6E), the failure mechanism was similar to that of the other edge column connections. The cracks consisted of shear cracks, bending cracks and torsion cracks. The torsion cracks that occurred on the edge of the slab at the 2E and 6E column connections were less than those of the 4E and 8E column connections. Both tangential and radial cracks appeared on the face of the slab around both column connections 2E and 6E. Column connection 2E failed at 49.64 MPa (7200 psi) and column connection 6E also

failed at 49.64 MPa (7200 psi). Column connections 2E and 6E had more punching shear resistance compared to the 4E (40 MPa) and 8E (45.5 MPa) column connections. The crack pattern was again elliptic with skew toward the long direction because of the larger moments in the long direction. The strains in the reinforcements parallel to the free edge were larger than the reinforcement perpendicular to the free edge. The reinforcements that passed through columns experienced more strain than those which did not pass through the columns. The reinforcement close to the free edge were subjected to the larger deformations. Column connections 2E and 6E were subjected to more axial load and moments than column connections 4E and 8E because of the rectangular plan of the flat slab. The forces in the compression rods at the 2E and 6E column connections were almost three times larger than the forces in the tension rods. The size and number of torsion cracks in the 6E and 2E column connections were small and less compared to the 4E and 8E column connections. Negative moment bending cracks occurred between 9M, 8E, 4E column connections (Figure 4.1). In all the column connections 9M, 4E, 8E failures, negative bending moment cracks extended to join the shear cracks.

At column connections 2E and 6E because there were less negative bending cracks to join the punching shear cracks, the punching shear capacity of these column connections was higher than the 8E and 4E column connections.

For corner columns there were unbalanced moments in the two perpendicular directions. The crack patterns, which are shown in Fig 4.47, show that the cracks are not always diagonal as expressed in the Canadian code. Most of the cracks appeared around the faces of the columns rather than diagonally across the corner. The corner column connections had more punching shear resistance than the middle and edge columns.

Figures 4.21 and 4.22 show the flexural reinforcement which was embedded in the columns was subjected to more strain than the others. As all corner columns were the same size, symmetrical loading and boundary conditions, the cracks were similar in all four-corner column connections. In order to fail the corner column connections the applied load was increased to 58 MPa (8400 psi) line pressure, but the corner column connections did not fail. In all the corner column connections, shear cracks, bending moment cracks and torsion cracks appeared.

The slab in the later series of tests had lost some of its stiffness from previous tests which caused larger deformations. By losing stiffness in each round of test the deflections could be higher in later tests, but because shoring the failed column connections in each round of the tests reduced effective span lengths, the slab regained some stiffness.

5.4 Comparing punching shear predictions with experiment results

Previous research (Gardner and Shao 1996) showed that the coefficient of the ACI 318-99 punching shear equation had a mean value of 0.45 with a coefficient of variation of 22%. This would imply that the failure load of the interior 9M connection should have been 420 kN +/- 150 kN for a 90% confidence interval. The measured strength was close to the lower 10% value. Similar comments apply to strengths calculated using BS 8110-85 and Gardner 97. Consequently comparisons of the measured 9M connection with the three prediction methods were not included in any statistics.

Each code has its own definition of the critical area of punching shear capacity as a multiple of d (effective depth) of the slab from face of the column. The American and

Canadian codes suggest that the critical section must be assumed d/2 from the column face. The British code proposes that this distance must be 1.5d instead of 0.5d. The critical sections proposed by the different codes do not necessarily demonstrate the real mechanism of failure. Those numbers are chosen to demonstrate a simple model of the failure mechanism and to approximate the real behavior of the structure.

CSA A23.3 and ACI 318 use the same method to predict the punching shear capacity of flat slab structures. In both codes the critical perimeter assumed for punching shear failure is d/2 from the face of the column. In both codes the same concept is assumed to calculate the punching shear stress in column connections for middle, edge and corner connections. In both codes to calculate stresses that results from transferred moments, a parameter J is used that is a function of the column dimensions.

The British code multiplies the shear stress by a constant factor to consider the effect of unbalanced moments applied to edge and corner connections.

Comparing the experimental results with code predictions show that ACI 318-99 gives more conservative answers than BS 8110-85. Because the British code uses the same factor for different moments, maybe for unusual structures, which have large moments, the predictions will not agree with real behavior of the structures. In the current research, the results show that British code predictions are closer to experimental data than ACI code.

In Gardner's method the critical perimeter is smaller than the ACI and British code methods but for edge columns the answers are closer to the experimental results than the ACI and British code methods.

All three prediction methods were designed to be conservative in predicting punching shear failure of interior flat plate column connections without moment transfer. The comparisons presented are calculated using the recommended equations and the predicted moments and do not allow for the known conservations inherent in calculating the values of v_c.

Because of uncertainty in the moments calculated from the horizontal restraints the moments calculated in section 5.2.1 increased by the ratio of the failure jack pressure to a jack pressure of 41.36 MPa were used in the comparisons with code predictions.

5.4.1 Comparison of experimental results with ACI 318-99

For calculating shear resistance of the column connections, equations 2.9, 2.10, 2.11 were used. Equation 2.11 gave the smallest value. The shear resistance calculated using $f_{cm} = 38$ MPa gives $v_c = 2.03$ MPa.

In Table 5.4 the results are compared with the ACI predictions. For short direction unbalanced moments column connections (8E, 4E) the results are slightly better than long direction unbalanced moments (2E, 6E).

Table 5.4 Comparing the results with ACI 318-99

Column	Test results (MPa)	ACI/Test result
8E	3.49	0.58
2E	3.94	0.52
4E	3.15	0.64
6E	3.72	0.55
Average		0.57
Coefficient of Variation:		0.15

The high calculated stresses resisted by the edge connections are the reason why the design was unsuccessful in provoking the first failure at an edge connection.

Alternatively it can be stated that ACI 318-99 is very conservative for edge column slab connections. However it must be noted that the v_c used in Table 5.4 was not modified for the 45% conservatism in v_c. The calculations of Table 5.4 are based on the section data in Table 5.5.

Table 5.5 Parameters to calculate shear stresses

Column	V_U (N)	M_U (N.mm)	d (mm)	A (mm^2)	e_1 (mm)	J(mm^4)	γ
8E	1.99E+05	3.09E+07	105	91350	75.03	702512505	0.36
2E	2.17E+05	6.12E+07	105	107415	124.93	1590771390	0.42
4E	1.68E+05	3.09E+07	105	91350	75.03	702512505	0.36
6E	1.93E+05	6.12E+07	105	107415	124.93	1590771390	0.42

5.4.2 Comparing experimental results with British code (BS 8110-85)

Because the densities of the reinforcements in short and long directions were different, the average of ρ for short and long directions was used for calculating resistance shear stress. The data used in calculating the BS 8110-85 results are given in Table 5.6.

Table 5.6: Parameters for calculating shear stresses

Column	V_U (N)	V_{eff} (N)	d (mm)	$u(mm)$	ρ
8E	1.99E+05	2.49E+05	105	1290.6	1.40
2E	2.17E+05	2.71E+05	105	1442.8	1.20
4E	1.68E+05	2.10E+05	105	1290.6	1.40
6E	1.93E+05	2.41E+05	105	1442.8	1.20

The calculated and predicted shear stresses at failure using BS 8110-85 are tabulated in Table 5.7. It can be seen in Table 5.7 the British code gives better prediction than the ACI 318-99 despite its simplicity.

Table 5.7: Comparing experimental results with British code

Column	v (MPa)	v_c (MPa)	$\frac{v_c}{v}$
8E	1.84	1.22	0.67
2E	1.79	1.16	0.65
4E	1.55	1.22	0.79
6E	1.59	1.16	0.73
		Average:	0.71
	Coefficient of	Variation:	0.15

5.4.3 Comparing the experimental results with Gardner's method

Gardner (1997) method suggests two methods to calculate the capacity of edge connections – using a simple BS 8110-85 type multiplier or the ACI eccentric shear method on a critical surface at the faces of the columns. Table 5.8 gives the data used to calculate the predictions in Table 5.9. Table 5.9 gives the results calculated using the simple multiplier. It can be seen in Table 5.9 that the coefficient of variation for Gardner's method using a simple multiplier is 18% with a mean value of 0.96.

Table 5.8 Data used for Gardner's method

Column	V_U (N)	V_{eff} (N)	C (mm)	d(mm)	$u(mm)$	ρ
8E	1.99E+05	2.99E+05	227.3	105	660.6	1.28
2E	2.17E+05	3.26E+05	248.8	105	812.8	0.87
4E	1.68E+05	2.52E+05	227.3	105	660.6	1.28
6E	1.93E+05	2.90E+05	248.8	105	812.8	0.87

Table 5.9 Gardner's method (using B.S 8110-85 simple multiplier method)

Column	Test results(MPa)	Prediction(MPa)	Prediction/test result
8E	4.30	3.92	0.91
2E	3.81	3.29	0.86
4E	3.63	3.92	1.08
6E	3.39	3.29	0.97
		Average:	0.96
	Coefficient	Of Variation:	0.18

Using an ACI eccentric shear type method to calculate combined shear and moment results in a lower mean value and a larger coefficient of variation. As mentioned in Chapter 2, the control perimeter is taken at the periphery of the column or loaded area.

Table 5.10 Parameters to calculate shear stresses Gardner's method (using ACI 318-99 method)

Column	V_U (N)	M_U (N.mm)	d (mm)	A (mm^2)	e_1 (mm)	J(mm^4)	γ
8E	1.99E+05	3.08E+07	105	69300	62.44	354580935	0.37
2E	2.17E+05	6.12E+08	105	85365	114.42	927299533	0.45
4E	1.68E+05	3.08E+07	105	69300	62.44	354580935	0.37
6E	1.93E+05	6.12E+08	105	85365	114.42	927299533	0.45

For calculating stresses in Table 5.11, the section parameters of Table 5.10 were used.

Table 5.11 Gardner's method (using ACI 318-99 method)

Column	Test results(MPa)	Prediction(MPa)	Prediction /Test result
8E	5.15	3.92	0.76
2E	5.68	3.29	0.58
4E	4.69	3.92	0.84
6E	5.39	3.29	0.61
		Average:	0.70
		Coefficient of Variation:	0.31

Chapter 6

Conclusion and future work

6.1 Conclusion

Edge column slab connections of continuous flat plate structures, under combined shear and moment transfer, can be susceptible to failure by punching shear. Investigating punching shear experimentally using isolated single column slab connections requires compromises in the boundary conditions of the slab. A 2 bay by 2 bay rectangular flat plate, panel aspect ratio 2:1, was fabricated and loaded to failure under a simulated uniformly distributed load to investigate the punching shear capacity of edge column slab connections under different ratios of shear and moment transfer. Because the slab panel aspect ratio was 2:1 the reinforcement/unit width in the longer direction was approximately twice that in the shorter direction. The edge and corner columns were supported so that the reactions and reactive moments could be measured. All edge columns were rectangular in section. Because the slab was rectangular in plan, the behaviour of the slab was more complicated than a square slab. Most of the available literature has been developed for square flat slabs.

Measuring the column reactive moments was not totally successful. It was expected that the forces in the gauged upper and lower restraining elements would be identical; however the lower, compressive, restraining rods had two or more times the force of the tension rods which make calculating the restraining moments uncertain.

The measured reactions and reactive moments were compared to those calculated by finite element analysis, FEM, and a modified direct design method, RDDM. Comparison of the experimental reactions with those calculated shows that both methods

predict the reactions with acceptable accuracy. Both methods over-estimated the measured interior column reaction. After much manipulation the measured edge and corner column moments were also in agreement with those measured. Consequently it is concluded that the Direct Design Method limitation on a minimum of three spans in each direction can be removed provided the interior column moment is increased.

Because the connection reactions were measured, the prediction equations could be compared directly to the experimental results. Only the ACI 318-99, BS 8110-85 and Gardner 97 prediction equations were considered. The interior column, no moment transfer, punching shear strength was significantly less than inferred from previous research. Based upon the strain gauge results neither the long or short direction flexural reinforcements yielded. The fact that the interior column was rectangular in section was a complication.

The long direction connections, with approximately twice the unbalanced moment of the short direction connections, failed at a larger load. Recognising that the reinforcement ratios provided were appropriate to the expected moments this would indicate that unbalanced moments have only a minor effect.

Using calculated moments the punching shear capacities of the edge column slab connections were conservatively predicted by the ACI 318-99 equations with a mean predicted/experimental value of 0.57 for the edge columns with a coefficient of variation of 15%.

The BS 8110-85 and Gardner 97 punching capacity equations require the reinforcement ratio. However when the reinforcement at a connection is different in the two directions some determination has to be made as to which ratio is appropriate i.e.

which direction is critical. Calculations were made using the simple average of the flexural steel ratio in the two directions. The very simplistic BS 8110-85 expressions also predicted a mean predicted/experimental ratio of 0.71 and a coefficient of variation of 15%. In this research Gardner's method prediction using a simple multiplier was very close to reality for edge column connections with a mean value of 0.96 with a coefficient of variation of 18%. Using Gardner's method with the ACI type eccentric shear expression was less successful with a mean of 0.70 and a coefficient of variation of 31%.

For corner column connections the main cracks, which indicate distress were not always diagonal as assumed in the Canadian code CSA A23.3-94. The current research shows in most cracks occur around the column-slab connection rather than diagonally across the slab.

6.2 Future research

More attempts should be made to measure the edge and corner column moments in flat slab system.

The eccentric shear expression should be examined to determine its appropriateness.

The effects of different reinforcement ratios in the two directions, and none-square column sections on the punching shear capacity of column slab connections require investigation.

REFERENCES

ACI Committee 318, 1999, "Building Code Requirements for Reinforced Concrete (ACI 318-99) and Commentary (ACI 318R-99)", *American Concrete Institute*, Detroit.

ACI Committee 318, 1965, "Commentary on Building Code Requirements for Reinforced Concrete (ACI 318-63)", Publication SP 10, *American Concrete Institute*, Detroit.

ACI-ASCE Committee 352, 1988,"Recommendations for Design of Slab-Column Connections in Monolithic Reinforced Concrete Structures", *ACI Structural Journal*, Vol. 85, November-December, pp. 675-696.

ACI-ASCE Committee 426 on Shear and Diagonal Tension, 1974, "The Shear Strength of Reinforced Concrete Members–Slabs", *Journal of Structural Division, Proceedings of ASCE*, Vol. 100, No. ST8, August, pp. 1543-1591.

British Cement Association, 2001,"Early age strength assessment of concrete on site", Best Practice Guides For In-Situ Concrete Frame Building. www.bca.org.uk

British Cement Association, 2001,"Early striking and improved backpropping for efficient flat slab construction", Best Practice Guides For In-Situ Concrete Frame Building. www.bca.org.uk.

British Cement Association, 2001,"Flat slabs for efficient concrete construction", Best Practice Guides For In-Situ Concrete Frame Building. www.bca.org.uk

British Standard (BS 8110-85), 1985, "Structural Use of Concrete", *British Standard Institution*, London.

CSA-A23.3-M94, 1994, "Design of Concrete Structures for Buildings", *Canadian Standard Association*, December.

David A.Fanella , Javeed A.Munshi and Basile G.Rabbat , 1999, "Notes on ACI 318-99 Building Code Requirements for Structural Concrete with Design Applications". Portland Cement Association.

Dilger, W.H., 2000, "Flat Slab-Column Connections", *Progress in Structural Engineering and Materials*, Vol. 2, issue 3, November, pp. 386-399.

Elgabry, A. and Ghali, A., 1996, "Transfer of Moments between Columns and Slabs: Proposed Code Revisions", *ACI Structural Journal*, Vol. 93, No. 1, January-February, pp. 56-61.

Engineering News Record, 1971, "Building Collapse Blamed on Design Construction", July 15, p.19.

Gardner, N.J., 1990, "Relationship of the Punching Shear Capacity of Reinforced Concrete Slabs with Concrete Strength", *ACI Structural Journal*, Vol. 87, No. 1, January-February, pp. 66-71.

Gardner, N.J., 1995, "Discussion on Punching Shear Provisions for Reinforced and Prestressed Concrete Flat Slabs", *Proceedings, CSCE Annual Conference*, Ottawa, June, pp. 247-256.

Gardner, N.J., 1996, "Punching Shear Provisions for Reinforced and Prestressed Concrete Flat Slabs", *CSCE Journal*, Vol. 23, No. 2, April, pp. 502-210.

Gardner, N.J. and Shao, X.Y., 1996, "Punching Shear of Continuous Flat Reinforced Concrete Slabs", *ACI Structural Journal*, Vol. 93, No. 2, March-April, pp. 218-228.

Gardner, N.J. and Kallage, M.R., 1998, "Punching Shear Strength of Continuous Post-Tensioned Concrete Flat Plates", *ACI Material Journal*, Vol. 95, No. 3, May-June, pp.272-283.

Gardner, N.J., Huh, J., and Chung, Lan, 2000, "What Can We Learn from the Sampoong Department Store Collapse", *International Workshop on Punching Shear Capacity on RC Slabs-Proceedings*, Royal Institute of Technology, Stockholm, June, pp. 225-233.

MacGregor, J.G., 1997, *Reinforced Concrete: Mechanics and Design*, 3rd Edition, Prentice Hall Inc., New Jersey, 939pp.

MacGregor, J.G., and Bartlett, F.M., 2000, *Reinforced Concrete: Mechanics and Design*, 1st Canadian Edition, Prentice Hall Canada Inc., Ontario, Canada, 1042 pp.

Megally, S. and Ghali, A., 2000, "Punching of Concrete Slabs due to Column Moment Transfer", *Journal of Structural Engineering, ASCE*, Vol. 126, No. 2, February, pp. 180-189.

Moehle, J.P., Kreger, M.E. and Leon, R., 1988, "Background to Recommendations for Design of Reinforced Concrete Slab-Column Connections", *ACI Structural Journal*, Vol. 85, November-December, pp. 636-644.

Moehle, J.P., 1988, "Strength of Slab-Column Edge Connections", *ACI Structural Journal*, Vol. 85, January-February, pp. 89-98.

Ross, S.S., 1984, *Construction Disasters: Design Failure, Causes and Prevention, An Engineering News-Record Book*, McGraw Hill Inc., New York, USA, 417 pp.

Sherif, A.G. and Dilger, W.H., 1996, " Critical Review of the CSA A23.3-94 Punching Shear Strength Provision for Interior Columns", *Canadian Journal for Civil Engineering*, Vol. 23, pp. 998-1011.

Sherif, A.G., 1996, *Behaviour of Reinforced Concrete Flat Slabs*, Ph.D. Thesis, Department of Civil Engineering, University of Calgary, Alberta, June.

Sudarsana, Ketut,2001, *Behaviour of Edge Column Flat Slab Connections*, Ph.D. Thesis, Department of Civil Engineering, University of Ottawa, Ontario, December.

Tankut, T., 1969, *The behaviour of Reinforced Concrete Flat Plate Structures Subjected to Various Combinations of Vertical and Horizontal Loads*, Dissertation, University of London, November.

Vanderbilt, M.D., 1972, "Shear Strength of Continuous Plates", *Journal of the Structural Division, ASCE*, Vol. 98, No. ST4, August,